Direction of Arrival Estimation with Coprime Arrays

Xiao Yang

DOCTORAT BRETAGNE LOIRE / MATHSTIC

UNIVERSITÉ DE NANTES

THESE DE DOCTORAT DE

L'UNIVERSITE DE NANTES

ECOLE DOCTORALE N° 601
Mathématiques et Sciences et Technologies de l'Information et de la Communication
Spécialité : Traitement du signal

Par
Xiao YANG

Direction of Arrival Estimation with Coprime Arrays

Thèse présentée et soutenue à Nantes, le 27 Novembre 2020
Unité de recherche : IETR UMR CNRS 6164

Rapporteurs avant soutenance :

Rémy BOYER	Professeur des universités, Université de Lille
Anne FERREOL	Ingénieur de recherche/HDR, Thalès SIX GTS Gennevilliers

Composition du Jury :

Président :	Salah BOURENNANE	Professeur des universités, Ecole centrale de Marseille
Examinateurs :	Rémy BOYER	Professeur des universités, Université de Lille
	Anne FERREOL	Ingénieur de recherche/HDR, Thalès SIX GTS Gennevilliers
Dir. de thèse :	Yide WANG	Professeur des universités, Université de Nantes
Co-dir. de thèse :	Pascal CHARGE	Professeur des universités, Université de Nantes

ACKNOWLEDGEMENT

First of all, I would like to express my deepest gratitude to my supervisors, Professor Yide Wang and Professor Pascal Chargé, for their patience, encouragement and guidance during the three years of my PhD study at Polytech Nantes. They are not only diligent researchers but also excellent advisors and teachers. They taught me how to develop the research of my topic, how to write papers and give presentations, and how to face the difficulties and failures in the researching life. Without their suggestions and help, much of the work in the thesis would not be possible. It is a precious fortune to me to be advised by them.

I would also thank all my colleagues in IETR team Polytech de Nantes for their help and support especially at the beginning of my PhD research. It was because of you that I have past three wonderful and memorable years in Nantes.

Besides, I would like to thank China Scholarship Council (CSC) for giving me the precious opportunity to work on such an interesting topic, and also Chinese Embassy for the care and concern during the three years, especially when we were under the threaten of COVID-19.

Finally, my sincere gratefulness goes to my family, especially my wife, for her unconditional love, support and encouragement in my life, without which the pursuing of my PhD would never go such smoothly.

RÉSUMÉ

Dans les années récentes, grâce à la capacité de capturer spatialement le front d'onde des signaux entrants, les réseaux de capteurs ont été largement utilisés dans de nombreuses applications, telles que le radar, l'astronomie, le sonar et le système de communication sans fil. En tant qu'une base fondamentale des réseaux de capteurs, les techniques de traitement d'antennes permettent l'estimation des paramètres du signal, tels que la fréquence, la puissance et l'emplacement des sources, par l'observation perturbée par le bruit et les interférences, ce qui soutient grandement le développement de systèmes de réseau de capteurs.

La direction d'arrivée (DOA), qui est définie par les angles d'incidence des signaux entrants, est l'un des paramètres des signaux sources les plus significatifs, et l'estimation de DOA est considérée comme un problème crucial dans le radar, sonar et autres systèmes où des réseaux de capteurs sont impliqués. Pendant ces dernières décennies, l'estimation de DOA a été bien étudiée sur la base de réseaux linéaires uniformes (ULAs), dont les capteurs sont uniformément répartis en ligne droite avec un espacement inter-élément égale à une demi-longueur d'onde des signaux entrants pour éviter les ambiguïtés. De nombreux algorithmes ont été proposés pour l'estimation de DOA, y compris des méthodes basées sur la formation de voies comme la formation de voies conventionnelle et Capon, et les méthodes à haute résolution basées sur un sous-espace comme MUSIC et ESPRIT. Cependant, pour la configuration ULA, la longueur du réseau est limitée par son petit espacement inter-éléments, ce qui entraîne des performances d'estimation insatisfaisantes. Par ailleurs, seulement jusqu'à $M-1$ sources peuvent être détectées aves M capteurs. Par conséquent, un nombre important de capteurs est nécessaire lorsque le nombre de signaux entrants est grand, ce qui est irréaliste et difficile à réaliser pour les applications pratiques.

Récemment, les configurations de réseaux lacunaires ont attiré beaucoup d'attention. Étant supérieurs aux ULAs traditionnels, les réseaux lacunaires, avec des capteurs localisés non uniformément, peuvent fournir un réseau de capteurs de longueur importante avec moins de capteurs, améliorant ainsi les performances d'estimation. En effet, en exploitant la difference coarray obtenue par l'observation du réseau de capteurs physiques, un long ULA

virtuel avec l'espacement de demi-longueur d'onde ULA peut être obtenu. Avec beaucoup plus des éléments virtuels que le nombre d'éléments de capteurs physiques, l'ULA virtuel peut être utilisé pour effectuer l'estimation de DOA, et beaucoup plus de sources peuvent être détectées.

Parmi les configurations de réseaux lacunaires, les réseaux linéaires coprimes (CLAs) ont été considérés comme les plus prometteurs grâce à la solution analytique des positions des capteurs et grâce à la réduction du couplage entre les capteurs. La recherche existante pour l'estimation de DOA avec CLAs évolue vers deux orientations, qui sont les méthodes basées sur le difference coarray et les méthodes basées sur les sous-réseaux. Les premières exploitent le CLA du point de vue des difference coarrays, en essayant d'augmenter le nombre maximum de sources détectables ; les dernières traitent le CLA comme deux sous-réseaux linéaires uniformes avec grande distance inter-capteurs, essayant d'obtenir une estimation de DOA avec haute précision et d'éliminer les ambiguïtés causées par le grand espacement inter-éléments. Cependant, pour les méthodes basées sur le difference coarray, le nombre d'éléments virtuels effectifs dans le difference coarray est limité par l'existence de trous, de sorte que le nombre de signaux détectables n'est pas aussi élevé que prévu ; pour les méthodes basées sur les sous-réseaux, à cause du grand espacement inter-éléments de chaque sous-réseau, certains problèmes ont été ignorés par les études existantes, affaiblissant leur robustesse et limitant le développement des réseaux coprimes dans des applications réelles.

Dans cette thèse, nous nous concentrons sur l'estimation de DOA par des méthodes basées sur le difference coarray et des méthodes basées sur les sous-réseaux, en essayant d'augmenter le nombre de sources détectables et d'améliorer la robustesse. Le travail principal est résumé comme suit.

1. Pour fournir les bases théoriques de toute la thèse, nous introduisons tout d'abord les bases des techniques de traitement d'antenne, y compris le modèle mathématique des signaux reçus par un réseau de capteurs, plusieurs configurations de réseaux de capteurs uniformes traditionnels, et certains algorithmes d'estimation de DOA conventionnels. Ensuite, l'estimation de DOA avec CLAs est présentée, impliquant les deux orientations de recherche, , notamment, les méthodes basées sur le difference coarray et les méthodes basées sur les sous-réseaux, avec leurs modèles de signaux reçus, les principes d'estimation de DOA et les principaux défis de recherche.

2. Du point de vue des méthodes basées sur le difference coarray, pour augmenter le nombre d'éléments virtuels effectifs dans le difference coarray ainsi que le nombre de sources détectables, les CLAs basés sur d'une plate-forme mobile ont été étudiés, et il a été montré que le nombre de sources détectables peut être augmenté en décalant le CLA d'une demi-longueur d'onde des signaux. Dans cette thèse, le difference coarray du CLA après le mouvement est analysé, et une configuration de CLAs améliorée pour la plate-forme mobile est proposée. En redéfinissant judicieusement les positions des capteurs, le mouvement du CLA peut être exploité plus efficacement, de sorte que beaucoup plus de signaux entrants peuvent être détectés avec le même nombre de capteurs physiques et la même longueur de mouvement de réseau.

3. La structure des difference coarrays des CLA a été bien étudiée, mais les réseaux planaires coprimes (CPAs) sont plus pertinentes pour les applications pratiques que les CLAs. Cependant, contrairement aux CLAs, les travaux de recherche sur les difference coarrays des CPAs n'ont pas été aussi développés. Afin d'apporter une meilleure compréhension des CPAs et de faciliter la recherche future dans ce domaine, dans cette thèse, les CPAs sont étudiés du point de vue des difference coarrays. Plusieurs propriétés des difference coarrays des CPAs sont dérivées, sur la base desquelles une méthode efficace est proposée pour augmenter le nombre d'éléments virtuels effectifs dans les difference coarrays ainsi que le nombre de signaux détectables.

4. Du point de vue des méthodes basées sur les sous-réseaux, plusieurs problèmes potentiels associés à cette classe de méthodes sont discutés, et nous montrons que les méthodes existantes ne peuvent pas fonctionner correctement lorsque les signaux provenant de certaines directions particulières ou souffrent d'une faible précision d'estimation et d'une grande complexité de calcul. Dans cette thèse, une méthode fiable et efficace d'estimation de DOA est proposée, dans laquelle le modèle de système avec des sous-réseaux uniformes avec grand espacement inter-éléments est transformé en ULAs virtuels traditionnels avec espacement de demi-longueur d'onde, et les vrais DOA sont traités comme leurs angles équivalents associés aux ULAs virtuels pour éviter les problèmes potentiels. Par rapport à d'autres méthodes existantes basées sur des sous-réseaux, la méthode proposée est capable d'obtenir une meilleure performance d'estimation dans toutes les situations, en termes de précision

et de complexité.

5. Dans les méthodes basées sur les sous-réseaux, le traitement séparé des deux sous-réseaux pose des problèmes tels que le faible nombre de sources détectables et des performances d'estimation sous-optimales. Pour résoudre ces problèmes, une configuration de réseaux de capteurs nommée réseau linéair coprime déplié (UCLA) est proposée, et il a été admis que les ambiguïtés provoquées par le grand espacement inter-éléments peuvent être supprimées automatiquement grâce à la propriété de coprime, et aucun autre processus n'est nécessaire pour les éliminer. Cependant, ce n'est pas toujours vrai. Il y aurait encore des ambiguïtés lorsque les signaux proviendraient des directions particulières. Dans cette thèse, la raison du problème d'ambiguïté ignorée est mise en évidence, et une méthode d'estimation de DOA modifiée avec l'élimination de l'ambiguïté est proposée, par laquelle le problème d'ambiguïté peut être résolu avec succès.

L'efficacité de toutes les propositions de cette thèse est soutenue par des résultats des simulations et par la publication de trois articles dans des revues [ii—iv], et quelques suggestions des recherches futures dans ce domaine sont fournies à la fin de cette thèse.

ABSTRACT

In recent years, being able to spatially capture the wavefront of incoming signals, sensor arrays, composed of multiple sensor elements, have been widely applied in practical applications, such as radar, astronomy, sonar and wireless communication system. As a critical basis of sensor arrays, array signal processing technique focuses on the estimation of signal parameters, such as frequency, power and source location, from the observation contaminated by noise and interference, greatly supporting the development of sensor array systems.

Direction of arrival (DOA), defined by the incident angles of incoming signals, is one of the most significant array signal parameters, and DOA estimation has been considered as a crucial issue in radar, sonar and other systems where sensor arrays are involved. In the last decades, DOA estimation has been well studied based on uniform linear arrays (ULAs), of which the sensor elements are uniformly distributed in a straight line with inter-element spacing equaling to a half-wavelength of incoming signals to avoid ambiguities. Many algorithms have been proposed for DOA estimation, including beamforming based methods like classical beamforming method and Capon method, and high resolution subspace based methods like MUSIC and ESPRIT. However, for ULA configuration, the array aperture is limited by its small inter-element spacing, resulting in unsatisfying estimation performance. On the other hand, only up to $M - 1$ sources can be detected with M sensor elements, therefore numerous sensor elements will be required when the number of incoming signals is large, which is unrealistic and hard to be accomplished in terms of practical applications.

Recently, sparse array configurations have attracted lots of attention. Being superior to traditional ULAs, sparse arrays, with sparsely located sensor elements, can achieve a larger array aperture with fewer sensors, improving estimation performance. Besides, by exploiting the difference coarray obtained from the observation of the physical sensor array, a long virtual half-wavelength spacing ULA can be obtained. With more distinct lags than the number of physical sensor elements, the virtual ULA can be used to perform the DOA estimation, and much more sources can be detected.

Among sparse array configurations, coprime linear arrays (CLAs) have been conside-

red as the most promising one thanks to their closed-formed expressions of sensor locations and limited mutual coupling effect. The existing research for DOA estimation with CLAs develops towards two orientations, which are difference coarray-based methods and subarray-based methods. The former exploits the CLA from the perspective of difference coarrays, trying to increase the maximum number of detectable sources ; the latter treats the CLA as two sparse uniform linear subarrays with large array aperture, trying to obtain high precision DOA estimation and eliminating the ambiguities caused by the large inter-element spacing. However, for the difference coarray-based methods, the number of effective lags in the difference coarray is limited by the existence of holes, such that the number of detectable signals is not as high as expected ; for the subarray-based methods, because of the large inter-element spacing of each subarray, some problems have been ignored by the existing studies, weakening their robustness and limiting the development of coprime arrays in real applications.

In this dissertation, we focus on the DOA estimation with coprime arrays from the perspectives of both the difference coarray-based methods and subarray-based methods, trying to increase the number of detectable sources and enhance the robustness. The main work is summarized as follows.

1. To provide the theoretical foundation for the whole dissertation, firstly, we introduce the basic of array signal processing techniques, including the mathematical model of received signals of sensor arrays, several traditional uniform sensor array configurations, and some conventional DOA estimation algorithms. Then, the DOA estimation with CLAs is presented, involving the two research orientations of difference coarray-based methods and subarray-based methods respectively, with their corresponding received signal models, DOA estimation principles, and main research challenges.

2. From the perspective of difference coarray-based methods, to increase the number of effective lags in the difference coarray as well as the number of detectable sources, moving platform based CLAs have been studied, and it has been shown that the number of detectable sources can be increased by shifting the CLA a half wavelength of incoming signals. In this thesis, the resulting difference coarray of the CLA after array motion is analyzed, and an improved CLA configuration for moving platform is proposed. By judiciously redesigning the sensor element positions, the shift of the

CLA can be exploited more efficiently, such that much more incoming signals can be detected with the same number of physical sensor elements and the same length of array motion.

3. The difference coarray structure of CLAs has been well studied, whereas coprime planar arrays (CPAs) are more relevant to practical applications compared with CLAs. However, unlike CLAs, the research of the difference coarrays of CPAs is not such developed that the high number of detected signals offered by the coprime geometry has not been fully exploited. In order to offer a better understanding of CPAs and facilitate the future research in this field, in this dissertation, CPAs are investigated from the perspective of difference coarrays. Several properties of the difference coarrays of CPAs are derived, based on which an efficient method is proposed to further increase the number of effective lags in the difference coarray as well as the number of detectable signals of CPAs.

4. From the perspective of subarray-based methods, several potential problems associated with such class of methods are discussed, and we show that the existing methods cannot work correctly when the signals coming from some particular directions or suffer from low estimation accuracy and high computational complexity. In this thesis, a reliable and efficient DOA estimation method is proposed, in which the system model with large inter-element spacing uniform subarrays is mapped into virtual traditional half-wavelength spacing ULAs, and the true DOAs are treated as their equivalent angles associated with the virtual ULAs to avoid the potential problems. Compared with other existing subarray-based methods, the proposed method is able to achieve better estimation performance in all situations, in terms of accuracy and complexity.

5. In subarray-based methods, separately handling the two subarrays causes problems such as the small number of detectable sources and sub-optimal estimation performance. To address this issue, a sensor array configuration named unfolded coprime linear array (UCLA) is proposed, and it has been admitted that the ambiguities caused by the large inter-element spacing can be suppressed automatically thanks to the coprime property, and no further process is required to eliminate the ambiguities. However, it is not always true. There would still exist ambiguities when the signals impinge from particular directions. In this thesis, the principle of the igno-

red ambiguity problem is investigated, and a modified DOA estimation method with ambiguity-eliminating is proposed, by which such ambiguity problem can be successfully solved.

The efficiency of all propositions in this dissertation are supported by adequate simulation results and three published journal articles [ii—iv], and some suggestions of the future research in this domain are provided at the end of this dissertation.

LIST OF PUBLICATIONS

i. X. Yang, Y. Wang, and P. Chargé, "Improved coprime linear array configuration for moving platform in DOA estimation," *IEEE Communication letters*, 2020 (Early access).

ii. X. Yang, Y. Wang, and P. Chargé, "Hole locations and a filling method for coprime planar arrays for DOA estimation," *IEEE Communication letters*, 2020 (Early access).

iii. X. Yang, Y. Wang, P. Chargé, and Y. Ding, "An efficient DOA estimation method for co-prime linear arrays," *IEEE Access*, vol. 7, pp. 90874-90881, 2019.

iv. X. Yang, Y. Wang, and P. Chargé, "Modified DOA estimation with an unfolded co-prime linear arrays," *IEEE Communication letters*, vol. 23, no.5, pp, 859-862, 2019.

v. W. He, X. Yang, and Y. Wang, "A high-resolution and low-complexity DOA estimation method with unfolded coprime linear arrays," *Sensors*, vol. 20, no. 218, 2020.

TABLE OF CONTENTS

LIST OF FIGURES

LIST OF TABLES

INTRODUCTION

Research Background and Motivation

In the last decades, sensor arrays have been widespreadly used in communications, biomedical engineering, remote sensing and other applications [1–10]. Being superior to single sensor systems, sensor arrays, composed of multiple sensor elements, can spatially capture the wavefront of incoming signals and extract the information of interest from the observation in the presence of noise and interference. Supporting the development of sensor array systems, array signal processing techniques focus on the estimation of signal parameters, such as frequency, power and source location, by exploiting the temporal and spatial characteristics of the signal received by regularly distributed sensor elements, and have become an active research topic in the field of wireless signal processing [11–15].

Direction of arrival (DOA), defined by the incident angles of signals impinging on a array of sensors, is one of the most significant array signal parameters, and DOA estimation is an important research branch of array signal processing techniques, playing a crucial role in many fields of real applications [11]. In multiple-input and multiple-output (MIMO) radar systems, an excellent bearing resolution is highly demanded, and a radar with an effective DOA estimation capacity can detect and track targets accurately [16, 17]. In sonar systems, because of the complexity of underwater environment, a robust DOA estimation is a critical issue for ships navigation [18, 19]. In wireless communication systems, in order to improve the signal transmission efficiency, adaptive beamforming technique, which is able to focalize the transmission energy to the wanted users and efficiently eliminate interferences, has been proved as a promising technology to increase the channel capacity [20, 21]. DOA estimation is highly required by the adaptive beamforming technique, providing signal direction information for the latter, such that the antenna array can capture the signals impinging from certain directions to obtain useful information and minimize the interference from others [22–24].

Motivated by the obvious importance, a variety of algorithms have been proposed for DOA estimation. Classical beamforming (CBF) method steers the main beam to all possible directions and calculates the corresponding output powers, and the source directions

are determined when the power gets maximal [11]. Taking the presence of other sources or interferences into consideration, based on the classical beamforming method, Capon method keeps the gain for the signal coming from the current searching direction and minimizes the power contributed by the interfering signals from other directions and additive noise, and the DOAs can be determined by the directions giving the maximal output powers [25]. Although the principle and implementation of the two methods are simple, they suffer from low resolution and lack of robustness. Subspace based methods have attracted lots of attention for several years thanks to their high resolution and accurate estimation performance [26]. Among the most popular algorithms within subspace based methods are the method of multiple signal classification (MUSIC) [27] and the method of estimation of signal parameters via rotational invariance techniques (ESPRIT) [28]. By exploiting the orthogonality between the signal and noise subspaces, and the rotational invariance property of the directional matrices of sensor arrays, both the methods can achieve a DOA estimation with satisfactory accuracy. However, the current research is mostly limited in the scene of uniform linear arrays (ULAs) [29, 30], where the inter-element spacing equals to a half-wavelength of incoming signals to maintain the Vandermonde structure of the directional matrices of sensor arrays to avoid ambiguities, such that the estimation performance is constrained by the limited array aperture. On the other hand, ULAs based MUSIC or ESPRIT can resolve up to $N - 1$ sources with N sensor elements [27, 28], and a high number of degrees of freedom (DOFs), determining the number of detectable sources, is highly required in various applications [31–33].

Sparse array configurations such as minimum redundancy arrays (MRAs) [34, 35] and nested arrays [36–38] have been proposed and drawn lots of attention in recent years. Compared with conventional ULAs, sparse arrays, with larger inter-element spacing, can achieve larger array aperture with the same number of sensor elements. In addition, by exploiting difference coarrays obtained from the covariance matrix of received signals, a long virtual half-wavelength spacing ULA can be generated and used to perform the DOA estimation, such that more sources than the number of physical sensor elements can be detected. However, MRAs do not have closed-form expressions of the array geometries such that the design and performance analysis of MRAs are complicated [39]. Besides, with several sensors densely distributed in the physical configurations, nested arrays face the problems of mutual coupling and lack of robustness [40–42] in practical applications. Recently, the configuration of coprime linear arrays (CLAs) has been developed [43–45]. Unlike the MRAs, CLAs have closed-form expressions of the sensor locations such that it

is easy to be constructed. Furthermore, because most of the sensor elements are distributed sparsely, the mutual coupling effect becomes not significant in coprime array systems. Although since there exist holes in the difference coarray of the CLAs and only the consecutive part can be directly used by subspace based methods, the number of detectable sources are not as high as the MRAs and nested arrays, the CLAs reach a balance point among different performance needs, being promising to the real applications.

There exist two main research orientations for the DOA estimation with CLAs, which are difference coarray-based methods and subarray-based methods. The difference coarray-based methods try to increase the number of the consecutive segments in the difference coarray such that the effective DOFs can be greatly increased [33, 44, 46–55]. The subarray-based methods treat the coprime linear array as two sparse uniform linear subarrays with large inter-element spacing ; from each of them, high precision but ambiguous DOA estimation can be obtained, and the ambiguities are eliminated according to the coprime property [56–64].

Main Contributions

In this thesis, we focus on the DOA estimation with coprime arrays from the perspectives of both the difference coarray-based methods and subarray-based methods. The main contributions are summarized as follows.

- For the difference coarray-based methods

  Moving platform based CLAs have been studied, and it is shown that by shifting a CLA a half wavelength, the majority or all holes in the original difference coarray can be filled, generating a difference coarray with more consecutive lags and increasing the effective DOFs [65–68]. After analyzing the final difference coarray resulted from the array motion, an improved CLA configuration for moving platform is proposed [i]. By judiciously redesigning the sensor element positions, a difference coarray with more consecutive lags has been obtained after the same length of array motion, such that much higher DOFs are obtained.

  Compared with linear arrays, two dimensional (2D) planar arrays are more relevant to real applications, especially in massive MIMO systems [69–72]. However, coprime planar arrays (CPAs) have not been well studied from the perspective of difference coarray to exploit the high DOFs offered by the coprime geometry [73–78]. To offer a better understanding of CPAs and facilitate the future research in this

field, the structure of the difference coarrays of CPAs is investigated [ii]. Closed-form expressions of the exact hole locations are derived, and a holes-filling method is proposed, such that the most critical holes in the difference coarray can be filled, generating a difference coarray with more consecutive lags and higher effective DOFs.

- For the subarray-based methods

  Although the principle of subarray-based methods is simple, the existing methods suffer from the insufficient reliability and high computational complexity [58–60]. Based on the discussion of the potential problems associated with such methods, an efficient DOA estimation method is proposed [iii]. Compared with other existing methods, the proposed method is able to work correctly in all situations with better estimation performance in terms of accuracy and complexity.

  To tackle the problems of subarray-based methods such as insufficient DOFs and sub-optimal estimation performance, an array geometry named unfolded coprime linear array (UCLA) is proposed, enjoying the advantages of full DOFs and better estimation performance [79–83]. However, an ambiguity problem has been ignored by the existing works. The problem is discussed in the thesis, and an appropriate solution is proposed [iv], by which such problem can be solved successfully and efficiently.

Thesis Organization

The organization of the thesis is as follows.

Chapter 1 introduces the basic theory of array signal processing, which is used throughout the thesis, including the signal model and several conventional sensor array geometries. Besides, some popular DOA estimation methods including beamforming based methods and subspace based methods are also presented in this chapter.

Chapter 2 provides an overview of the DOA estimation with CLAs from the perspectives of both the difference coarray-based methods and subarray-based methods. For the difference coarray-based methods, we present the concept of difference coarray and the coarray based MUSIC method ; for the subarray-based methods, three potential problems including ambiguities, pair matching errors and grating angles problem are discussed.

Chapter 3 discusses the moving platform based CLAs. The difference coarray resulted from the array motion is analyzed, and the improved array configuration with higher DOFs

is presented. Simulation results are provided to show the performance.

Chapter 4 explores the 2D CPAs from the perspective of difference coarray. The characteristics of the difference coarray of CPA configuration are deduced, and the closed-form expressions of the holes locations are provided with a detailed proof. Then, the proposed holes-filling method is introduced, of which the effectiveness is illustrated by simulation results.

Chapter 5 considers the DOA estimation with CLAs in the subarray-based methods perspective. Taking the potential existence of the grating angles problem into consideration, an equivalent signal model is constructed, based on which, the proposed efficient DOA estimation method is presented with simulations results.

Chapter 6 analyzes the DOA estimation with UCLAs. The ignored ambiguity problem is discussed with mathematical proof and specific examples, and the proposed methods of determining the existence of the problem and eliminating the ambiguity are presented. Simulation results are given to show the efficiency.

Chapter 7 concludes the thesis by highlighting the main contributions and discusses the possibilities of the future work on this subject.

CHAPITRE 1

BASIC OF ARRAY SIGNAL PROCESSING

This chapter presents the basic of array signal processing techniques, providing the foundation of the whole thesis. The chapter is composed of three parts. The first part presents the mathematical model of received signals for DOA estimation, and the second part introduces the geometries of several traditional uniform sensor arrays. Based on the former two parts, the third part discusses some conventional DOA estimation algorithms with the corresponding simulation results.

1.1 Received Signal Model

As shown in FIGURE 1.1, consider that a sensor array consists of M isotropic sensor elements located at positions $\mathbf{p}_m = (x_m, y_m, z_m)^T$, with $m = 0, 1, \cdots, M-1$. An incoming signal impinges on the array from the direction (θ, φ), with θ and φ denoting the elevation angle and azimuth angle respectively. For simplicity, the incoming signal is supposed to be far-field such that it could be regarded as a plane wave.

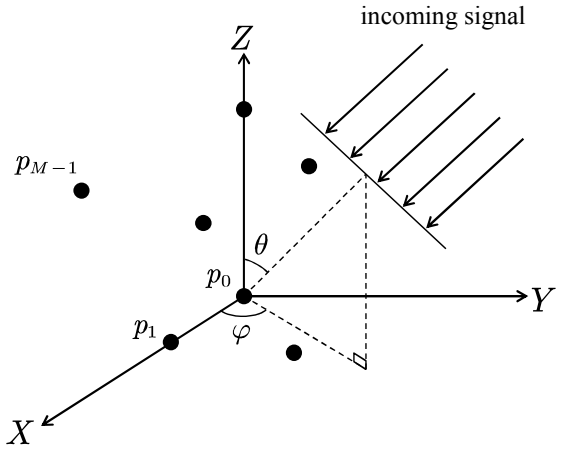

FIGURE 1.1 – Signal receiving model

Let $s(t)$ be the signal observed at the origin of the coordinate system, then the received signals at the sensor array can be given as

$$\mathbf{x}(t) = \begin{bmatrix} s(t-\tau_0) \\ s(t-\tau_1) \\ \vdots \\ s(t-\tau_{M-1}) \end{bmatrix} \tag{1.1}$$

where $s(t-\tau_m)$ denotes the signal received by the sensor element located at position $\mathbf{p}_m$, with τ_m the time delay of the received signal at that sensor element with respect to the signal observed by the origin of the coordinate system, which can be expressed as

$$\tau_m = \frac{\mathbf{d}^T \mathbf{p}_m}{c} \tag{1.2}$$

where c is the velocity of propagation and $\mathbf{d}$ the unit directional vector with

$$\mathbf{d} = -\begin{bmatrix} \sin\theta\cos\varphi \\ \sin\theta\sin\varphi \\ \cos\theta \end{bmatrix} \tag{1.3}$$

In most of the practical applications, the signals are often modulated, such that the signal observed at the origin of the coordinate can be written as

$$s(t) = m(t)\, e^{j2\pi f_0 t} \tag{1.4}$$

where $m(t)$ is the modulation message or the complex envelop of $s(t)$, and f_0 is the carrier frequency.

Then the received signal vector can be written as

$$\mathbf{x}(t) = \begin{bmatrix} s(t-\tau_0) \\ s(t-\tau_1) \\ \vdots \\ s(t-\tau_{M-1}) \end{bmatrix} = \begin{bmatrix} m(t-\tau_0)\, e^{-j2\pi f_0 \tau_0} \\ m(t-\tau_1)\, e^{-j2\pi f_0 \tau_1} \\ \vdots \\ m(t-\tau_{M-1})\, e^{-j2\pi f_0 \tau_{M-1}} \end{bmatrix} e^{j2\pi f_0 t} \tag{1.5}$$

In many cases of interest, the bandwidth of the complex envelop $m(t)$ is narrowband

and is much smaller than the carrier frequency, which means

$$m(t) \simeq m(t-\tau_0) \simeq m(t-\tau_1) \simeq \cdots \simeq m(t-\tau_{M-1}) \tag{1.6}$$

and the received signal vector can be re-written as

$$\mathbf{x}(t) = \begin{bmatrix} s(t-\tau_0) \\ s(t-\tau_1) \\ \vdots \\ s(t-\tau_{M-1}) \end{bmatrix} = m(t)\, e^{j2\pi f_0 t} \begin{bmatrix} e^{-j2\pi f_0 \tau_0} \\ e^{-j2\pi f_0 \tau_1} \\ \vdots \\ e^{-j2\pi f_0 \tau_{M-1}} \end{bmatrix} = s(t)\, \mathbf{a}(\theta, \varphi) \tag{1.7}$$

with

$$\mathbf{a}(\theta, \varphi) = \begin{bmatrix} e^{-j2\pi f_0 \tau_0} \\ e^{-j2\pi f_0 \tau_1} \\ \vdots \\ e^{-j2\pi f_0 \tau_{M-1}} \end{bmatrix} \tag{1.8}$$

which is called the array directional vector or the array manifold vector.

In general, the number of source signals is more than one and there exists noise in the propagation environment. Supposing that the number of incoming signals is K, the signal received by the sensor array can be given as

$$\mathbf{x}(t) = \begin{bmatrix} e^{-j2\pi f_0 \tau_{1,0}} & \cdots & e^{-j2\pi f_0 \tau_{K,0}} \\ e^{-j2\pi f_0 \tau_{1,1}} & \cdots & e^{-j2\pi f_0 \tau_{K,1}} \\ \vdots & \ddots & \vdots \\ e^{-j2\pi f_0 \tau_{1,M-1}} & \cdots & e^{-j2\pi f_0 \tau_{K,M-1}} \end{bmatrix} \begin{bmatrix} s_1(t) \\ s_2(t) \\ \vdots \\ s_K(t) \end{bmatrix} + \begin{bmatrix} n_0(t) \\ n_1(t) \\ \vdots \\ n_{M-1}(t) \end{bmatrix} \tag{1.9}$$

where $s_k(t)$ stands for the signal transmitted by the k^{th} source and observed at the origin of the coordinate system with $k = 1, 2, \cdots, K$, and $n_m(t)$ denotes the noise collected by the sensor element located at position $\mathbf{p}_m$. $\tau_{k,m}$ represents the time delay of the observation of $s_k(t)$ at the sensor element at $\mathbf{p}_m$ with respect to the observation at the origin of the coordinate system.

In the form of matrix, Equation (1.9) becomes

$$\mathbf{x}(t) = \mathbf{A}\mathbf{s}(t) + \mathbf{n}(t) \tag{1.10}$$

where

$$\mathbf{A} = \begin{bmatrix} \mathbf{a}(\theta_1, \varphi_1) & \mathbf{a}(\theta_2, \varphi_2) & \cdots & \mathbf{a}(\theta_K, \varphi_K) \end{bmatrix} \tag{1.11}$$

denotes the directional matrix of the sensor array, with $\mathbf{a}(\theta_k, \varphi_k)$ the directional vector associated with the k^{th} source, and

$$\mathbf{s}(t) = \begin{bmatrix} s_1(t) & s_2(t) & \cdots & s_K(t) \end{bmatrix}^T \tag{1.12}$$

denotes the incoming signal vector, and

$$\mathbf{n}(t) = \begin{bmatrix} n_0(t) & n_1(t) & \cdots & n_{M-1}(t) \end{bmatrix}^T \tag{1.13}$$

denotes the noise vector. In general, the noise is assumed to be Gaussian white temporally and spatially, which means

$$E\left\{\mathbf{n}(t)\,\mathbf{n}^H(t)\right\} = \begin{bmatrix} \sigma^2 & & & \\ & \sigma^2 & & \\ & & \ddots & \\ & & & \sigma^2 \end{bmatrix} \tag{1.14}$$

with σ^2 the power of the noise, and independent from the source signals.

According to the above analysis, the model of the signals observed by the sensor array consists of the directional matrix $\mathbf{A}$, the incoming signal vector $\mathbf{s}(t)$, and the noise vector $\mathbf{n}(t)$. Containing the information of directions of arrivals, the directional matrix $\mathbf{A}$ is the most important component of the received signal model and the basic element of DOA estimation. For a given sensor array, the corresponding directional matrix $\mathbf{A}$ is determined by the array geometry, and in the following, several traditional uniform array geometries will be introduced.

1.2 Traditional sensor array geometries

1.2.1 Uniform linear array

A uniform linear array (ULA) consists of several sensor elements linearly located with a uniform inter-element spacing. FIGURE 1.2 shows a ULA with M sensors located along the X-axis with an inter-element spacing equaling to d. For the purpose of mathematical

simplicity, the first element of the array is set as the origin of the coordinate system.

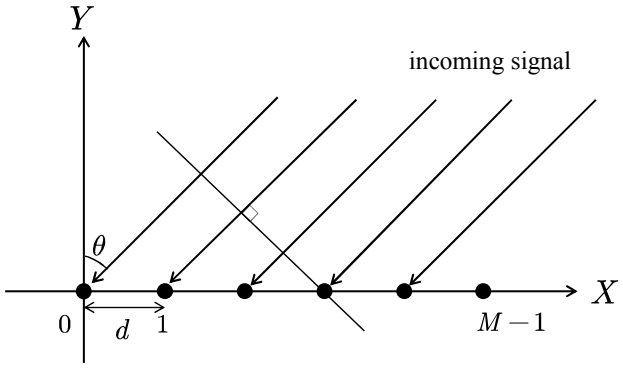

FIGURE 1.2 – Uniform linear array

The positions of the sensor elements can be written as

$$\mathbf{p}_m = (md, 0, 0)^T \qquad m = 0, 1, 2, ..., M-1 \tag{1.15}$$

Suppose that an incoming signal impinges on the ULA from direction θ, and according to Equation (1.2), the delay of the received signal at the sensor element located at $\mathbf{p}_m$ with respect to the signal observed at the origin of the coordinate system can be expressed as

$$\tau_m = -\frac{md\sin\theta}{c} \tag{1.16}$$

Therefore the directional vector associated with the incoming signal is given by

$$\mathbf{a}_{ULA}(\theta) = \begin{bmatrix} 1 \\ e^{j2\pi f_0 \frac{d\sin\theta}{c}} \\ \vdots \\ e^{j2\pi f_0 \frac{(M-1)d\sin\theta}{c}} \end{bmatrix} \tag{1.17}$$

For K source signals coming from $\{\theta_1, \theta_2, \cdots, \theta_K\}$, the signal received by the ULA is

$$\mathbf{x}_{ULA}(t) = \mathbf{A}_{ULA}\mathbf{s}(t) + \mathbf{n}(t) \tag{1.18}$$

with the following directional matrix of the ULA

$$\mathbf{A}_{ULA} = \begin{bmatrix} \mathbf{a}_{ULA}(\theta_1) & \mathbf{a}_{ULA}(\theta_2) & \cdots & \mathbf{a}_{ULA}(\theta_K) \end{bmatrix} \tag{1.19}$$

In general, the inter-element spacing d of ULAs is set as $d = \frac{\lambda}{2}$, where λ is the wavelength of incoming signals, to avoid the aliasing of the exponential function. Then $\mathbf{A}_{ULA}$ can be re-written as

$$\mathbf{A}_{ULA} = \begin{bmatrix} 1 & 1 & \cdots & 1 \\ e^{j\pi \sin\theta_1} & e^{j\pi \sin\theta_2} & \cdots & e^{j\pi \sin\theta_K} \\ \vdots & \vdots & \ddots & \vdots \\ e^{j(M-1)\pi \sin\theta_1} & e^{j(M-1)\pi \sin\theta_2} & \cdots & e^{j(M-1)\pi \sin\theta_K} \end{bmatrix} \tag{1.20}$$

1.2.2 Uniform planar array

A uniform planar array (UPA) consists of several parallel ULAs. Being able to resolve both the elevation and azimuth angles, UPAs are more relevant to real applications. Besides, containing much more sensor elements, UPAs have a bright prospect in massive MIMO systems. FIGURE 1.3 shows a UPA lying in the $X - Z$ plane, with M sensor elements in each column and N sensor elements in each row. The inter-element spacing between adjacent elements is d, and the element in the first column and the first row is set as the origin of the coordinate system.

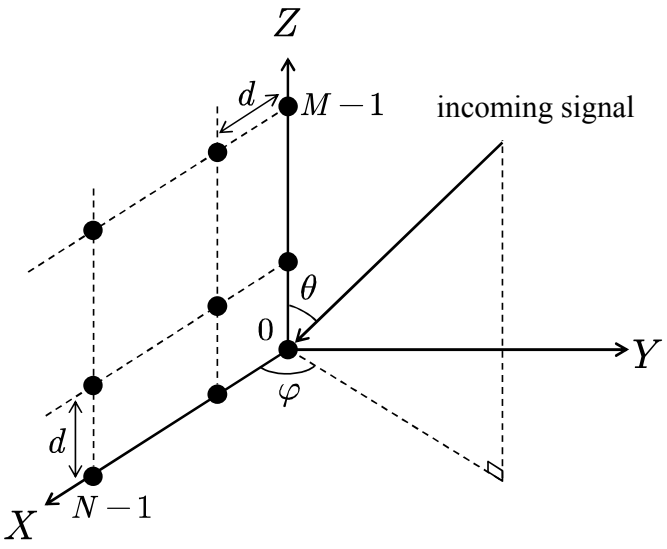

FIGURE 1.3 – Uniform planar array

The position of the sensor elements can be given by

$$\mathbf{p}_{n,m} = (nd, 0, md)^T \tag{1.21}$$

with $n = 0, 1, 2, ..., N-1$ and $m = 0, 1, 2, ..., M-1$.

Suppose that an incoming signal impinges on the UPA from direction (θ, φ), with θ and φ denoting the elevation and azimuth angles respectively. For the ULA lying along Z-axis, the time delay of the received signal at the sensor element located at $\mathbf{p}_{0,m}$ with respect to the received signal at the origin of the coordinate system can be expressed as

$$\tau_{0,m} = -\frac{md\cos\theta}{c} \tag{1.22}$$

and the directional vector of the ULA associated with the incoming signal is

$$\mathbf{a}_{ULA,Z}(\theta, \varphi) = \begin{bmatrix} 1 \\ e^{j2\pi f_0 \frac{d\cos\theta}{c}} \\ \vdots \\ e^{j2\pi f_0 \frac{(M-1)d\cos\theta}{c}} \end{bmatrix} \tag{1.23}$$

For the ULA lying along X-axis, the time delay of the received signal at the sensor element located at $\mathbf{p}_{n,0}$ with respect to the received signal at the origin of the coordinate system can be expressed as

$$\tau_{n,0} = -\frac{nd\sin\theta\cos\varphi}{c} \tag{1.24}$$

and the directional vector of the ULA associated with the incoming signal is

$$\mathbf{a}_{ULA,X}(\theta, \varphi) = \begin{bmatrix} 1 \\ e^{j2\pi f_0 \frac{d\sin\theta\cos\varphi}{c}} \\ \vdots \\ e^{j2\pi f_0 \frac{(N-1)d\sin\theta\cos\varphi}{c}} \end{bmatrix} \tag{1.25}$$

Then the directional vector of the UPA associated with the incoming signal can be given by

$$\mathbf{a}_{UPA}(\theta, \varphi) = \mathbf{a}_{ULA,X}(\theta, \varphi) \otimes \mathbf{a}_{ULA,Z}(\theta, \varphi) \tag{1.26}$$

For K source singals coming from $\Big\{(\theta_1, \varphi_1) \quad (\theta_2, \varphi_2) \quad \cdots \quad (\theta_K, \varphi_K)\Big\}$, the signal re-

ceived by the UPA can be written as

$$\mathbf{x}_{UPA}(t) = \mathbf{A}_{UPA}\mathbf{s}(t) + \mathbf{n}(t) \tag{1.27}$$

with the directional matrix of the UPA

$$\mathbf{A}_{UPA} = \begin{bmatrix} \mathbf{a}_{UPA}(\theta_1, \varphi_1) & \mathbf{a}_{UPA}(\theta_2, \varphi_2) & \cdots & \mathbf{a}_{UPA}(\theta_K, \varphi_K) \end{bmatrix} \tag{1.28}$$

Setting the inter-element spacing d as $\frac{\lambda}{2}$, $\mathbf{A}_{UPA}$ can be re-written as

$$\mathbf{A}_{UPA} = \begin{bmatrix} 1 & \cdots & 1 \\ e^{j\pi\cos\theta_1} & \cdots & e^{j\pi\cos\theta_K} \\ \vdots & \ddots & \vdots \\ e^{j(M-1)\pi\cos\theta_1} & \cdots & e^{j(M-1)\pi\cos\theta_K} \\ e^{j\pi\sin\theta_1\cos\varphi_1} & \cdots & e^{j\pi\sin\theta_K\cos\varphi_K} \\ e^{j\pi(\sin\theta_1\cos\varphi_1+\cos\theta_1)} & \cdots & e^{j\pi(\sin\theta_K\cos\varphi_K+\cos\theta_K)} \\ \vdots & \ddots & \vdots \\ e^{j\pi(\sin\theta_1\cos\varphi_1+(M-1)\cos\theta_1)} & \cdots & e^{j\pi(\sin\theta_K\cos\varphi_K+(M-1)\cos\theta_K)} \\ \vdots & \ddots & \vdots \\ e^{j(N-1)\pi\sin\theta_1\cos\varphi_1} & \cdots & e^{j(N-1)\pi\sin\theta_K\cos\varphi_K} \\ e^{j\pi((N-1)\sin\theta_1\cos\varphi_1+\cos\theta_1)} & \cdots & e^{j\pi((N-1)\sin\theta_K\cos\varphi_K+\cos\theta_K)} \\ \vdots & \ddots & \vdots \\ e^{j\pi((N-1)\sin\theta_1\cos\varphi_1+(M-1)\cos\theta_1)} & \cdots & e^{j\pi((N-1)\sin\theta_K\cos\varphi_K+(M-1)\cos\theta_K)} \end{bmatrix} \tag{1.29}$$

1.3 Conventional DOA estimation algorithms

In this section, several conventional DOA estimation methods, including beamforming based methods like classical beamforming method and Capon method, and the subspace based methods like MUSIC and ESPRIT, are introduced with their corresponding numerical simulations. The geometry of ULAs in FIGURE 1.2 and the received signal model in Equation (1.18) are used for simplicity.

1.3.1 Classical beamforming method

Classical beamforming (CBF) method [11] is a basic array signal processing technique for signal source localization. The main idea behind the classical beamforming method is to steer the main beam of the sensor array to all the possible wave coming directions with appropriate weighting vectors. For each direction in the search range, the power of the array response is calculated, and the steering directions with maximum powers determine the DOA estimations.

By multiplying the weighting vector to the received signal, the response of the array is given by

$$y\left(t\right)=\mathbf{w}^{H}\mathbf{x}\left(t\right) \tag{1.30}$$

where the weighting vector $\mathbf{w}$ is set as the following equation for a particular steering direction θ_c

$$\mathbf{w}=\frac{\mathbf{a}\left(\theta_c\right)}{M} \tag{1.31}$$

Then the power of the output is calculated by

$$\begin{aligned} P_{CBF}\left(\theta_c\right) &= \frac{1}{L}\sum_{t=1}^{L}\left|y\left(t\right)\right|^{2} \\ &= \frac{1}{L}\sum_{t=1}^{L}\mathbf{w}^{H}\mathbf{x}\left(t\right)\mathbf{x}^{H}\left(t\right)\mathbf{w} \\ &= \frac{\mathbf{a}^{H}\left(\theta_c\right)\hat{\mathbf{R}}\mathbf{a}\left(\theta_c\right)}{M^{2}} \end{aligned} \tag{1.32}$$

where $\hat{\mathbf{R}}$ denotes the estimate of the covariance matrix of received signals with

$$\hat{\mathbf{R}}=\frac{1}{L}\sum_{t=1}^{L}\mathbf{x}\left(t\right)\mathbf{x}^{H}\left(t\right) \tag{1.33}$$

and L is the number of snapshots.

The DOA estimation performance of the classical beamforming method is shown in FIGURE 1.4, in which two uncorrelated, far-field and narrowband incoming signal are assumed to impinge on a ULA with 10 sensor elements from directions $\{10^{\circ},30^{\circ}\}$. The number of snapshots and the signal to noise ratio (SNR) are set to 200 and 10dB respectively.

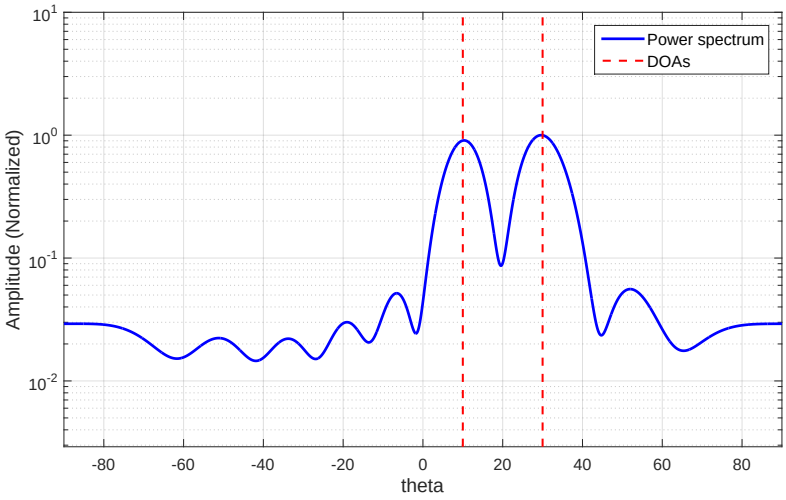

FIGURE 1.4 – DOA estimation by classical beamforming method

1.3.2 Capon method

The classical beamforming method shows disappointing estimation performance when other sources exist expect for the desired one, especially when they are located closer than the width of a beam. Taking the presence of other sources into account, Capon method [25] is proposed to solve this problem.

The principle of the Capon method is to minimize the power contributed by the signals coming from other directions and noise than the current searching one θ_c by

$$\begin{aligned} &\min_{\mathbf{w}} \; P\left(\theta_c\right) \\ &\text{subject to} \quad \mathbf{w}^H \mathbf{a}\left(\theta_c\right) = 1 \end{aligned} \tag{1.34}$$

of which the solution is

$$\mathbf{w} = \frac{\hat{\mathbf{R}}^{-1}\mathbf{a}\left(\theta_c\right)}{\mathbf{a}^H\left(\theta_c\right)\hat{\mathbf{R}}^{-1}\mathbf{a}\left(\theta_c\right)} \tag{1.35}$$

Then the power of the output is given by

$$P_{Capon}\left(\theta_c\right) = \frac{1}{\mathbf{a}^H\left(\theta_c\right)\hat{\mathbf{R}}^{-1}\mathbf{a}\left(\theta_c\right)} \tag{1.36}$$

With the same simulation conditions as FIGURE 1.4, the DOA estimation performance of the Capon method is shown in FIGURE 1.5.

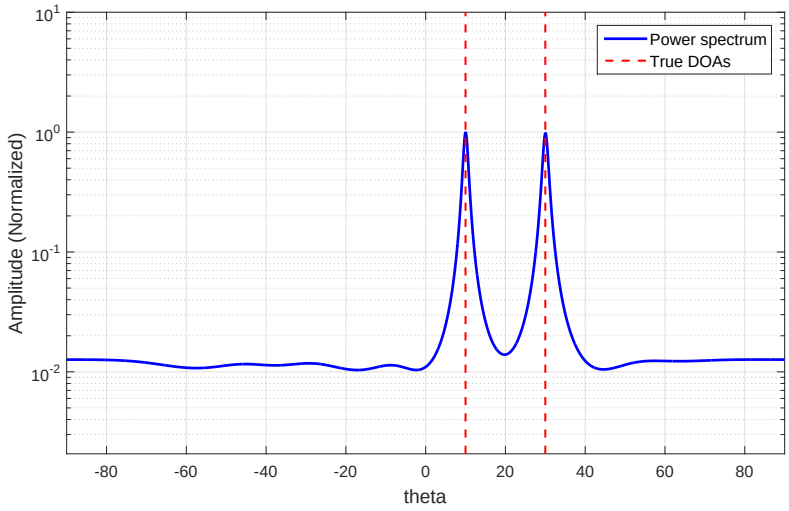

FIGURE 1.5 – DOA estimation by Capon method

1.3.3 Multiple signal classification method

Based on the eigenvalue decomposition of the covariance matrix of received signals, subspace based methods are very popular in the domain of DOA estimation because of their high resolution. Among them, multiple signal classification (MUSIC) method [27] is the most representative one which exploits the orthogonality between the signal and noise subspaces.

The covariance matrix of received signals can be given by

$$\begin{aligned} \mathbf{R} &= \mathbf{A}\mathbf{R}_s\mathbf{A}^H + \sigma^2\mathbf{I}_M \\ &= \mathbf{R}_y + \sigma^2\mathbf{I}_M \end{aligned} \tag{1.37}$$

where $\mathbf{R}_s$ denotes the covariance matrix of the source signals, given by

$$\mathbf{R}_s = E\{\mathbf{s}(t)\mathbf{s}^H(t)\} \tag{1.38}$$

and $\mathbf{R}_y$ denotes the covariance matrix of received signals only contributed by the source signals, and it is clear that $rank\,(\mathbf{R}_y) = K$.

In general, the covariance matrix of received signals $\mathbf{R}$ is full rank with $rank\,(\mathbf{R}) = M$. Therefore among the M eigenvalues of $\mathbf{R}$, K of them are larger than the other $(M - K)$, which are equal to the noise power σ^2.

Then $\mathbf{R}$ can be written as in the terms of its eigenvalues and eigenvectors as

$$\mathbf{R} = \mathbf{U}\mathbf{\Lambda}\mathbf{U}^H \tag{1.39}$$

where $\mathbf{U} = \begin{bmatrix}\mathbf{u}_1 & \mathbf{u}_2 & \cdots & \mathbf{u}_M\end{bmatrix}$ denotes the matrix of eigenvectors associated with $\mathbf{\Lambda} = \operatorname{diag}\begin{Bmatrix}\lambda_1 & \lambda_2 & \cdots & \lambda_M\end{Bmatrix}$ the matrix of eigenvalues, which are sorted in decreasing order as

$$\lambda_1 \geqslant \lambda_2 \geqslant \cdots \geqslant \lambda_K \geqslant \lambda_{K+1} = \lambda_{K+2} = \cdots = \lambda_M = \sigma^2 \tag{1.40}$$

We define

$$\mathbf{\Lambda}_s = \operatorname{diag}\begin{Bmatrix}\lambda_1 & \lambda_2 & \cdots & \lambda_K\end{Bmatrix} \tag{1.41}$$

$$\mathbf{\Lambda}_n = \operatorname{diag}\begin{Bmatrix}\lambda_{K+1} & \lambda_{K+2} & \cdots & \lambda_M\end{Bmatrix} \tag{1.42}$$

$$\mathbf{U}_s = \begin{bmatrix}\mathbf{u}_1 & \mathbf{u}_2 & \cdots & \mathbf{u}_K\end{bmatrix} \tag{1.43}$$

$$\mathbf{U}_n = \begin{bmatrix}\mathbf{u}_{K+1} & \mathbf{u}_{K+2} & \cdots & \mathbf{u}_M\end{bmatrix} \tag{1.44}$$

Then $\mathbf{R}$ can be rewritten by

$$\mathbf{R} = \mathbf{U}_s\mathbf{\Lambda}_s\mathbf{U}_s^H + \mathbf{U}_n\mathbf{\Lambda}_n\mathbf{U}_n^H \tag{1.45}$$

The eigenvectors associated with the smallest eigenvalues $\mathbf{U}_n$ span the noise subspace and are orthogonal to the actual source directional vectors. Therefore, for each direction in the searching range, project the corresponding directional vector on $\mathbf{U}_n$, and the estimation of the DOAs is determined when the projection is zero.

For the current searching direction θ_c, the corresponding pseudo-spectrum of MUSIC is expressed by

$$P_{MUSIC}\left(\theta_c\right) = \frac{1}{\|\mathbf{U}_n^H\mathbf{a}\left(\theta_c\right)\|^2} = \frac{1}{\mathbf{a}^H\left(\theta_c\right)\mathbf{U}_n\mathbf{U}_n^H\mathbf{a}\left(\theta_c\right)} \tag{1.46}$$

and the DOAs can be found by peak-searching of $P_{MUSIC}\left(\theta_c\right)$.

With the same simulation conditions introduced above, the DOA estimation performance of the MUSIC method is shown in FIGURE 1.6, which is significantly better than the beamforming-based methods.

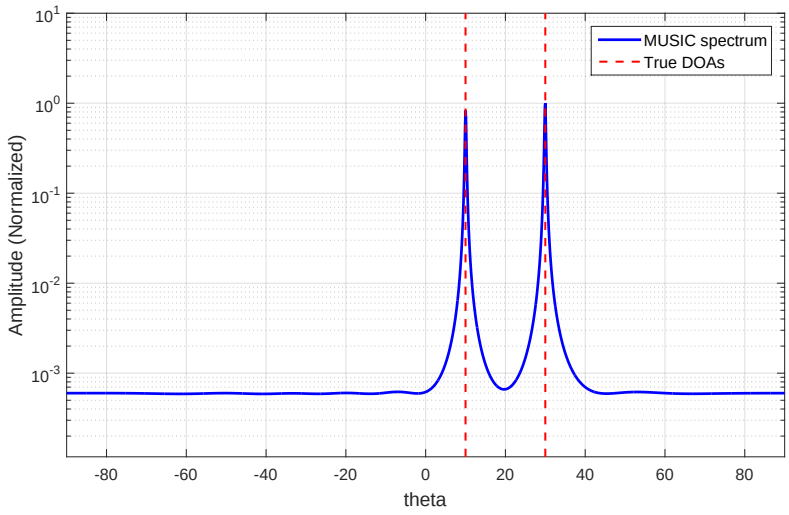

FIGURE 1.6 – DOA estimation by MUSIC method

1.3.4 Estimation of signal parameter via rotational invariance technique

Estimation of signal parameter via rotational invariance technique (ESPRIT) [28] is another efficient subspace based DOA estimation method. By exploiting the rotational invariance property of the directional matrix, high resolution and accurate estimation performance can be achieved without the step of spectral peak searching.

Recall the eigenvalue decomposition of the covariance matrix of received signals

$$\mathbf{R} = \mathbf{U}_s \mathbf{\Lambda}_s \mathbf{U}_s^H + \mathbf{U}_n \mathbf{\Lambda}_n \mathbf{U}_n^H \tag{1.47}$$

the K eigenvectors associated with the K bigger eigenvalues and the source directional vectors span the same signal subspace. Then there is

$$\mathbf{A} = \mathbf{U}_s \mathbf{T} \tag{1.48}$$

where T is a nonsingular matrix.

Define $\mathbf{A}_1$ and $\mathbf{A}_2$ as the first and last $(M-1)$ rows of the directional matrix $\mathbf{A}$ respec-

tively

$$\mathbf{A}_1 = \begin{bmatrix} 1 & 1 & \cdots & 1 \\ e^{j\pi \sin\theta_1} & e^{j\pi \sin\theta_2} & \cdots & e^{j\pi \sin\theta_K} \\ \vdots & \vdots & \ddots & \vdots \\ e^{j(M-2)\pi \sin\theta_1} & e^{j(M-2)\pi \sin\theta_2} & \cdots & e^{j(M-2)\pi \sin\theta_K} \end{bmatrix} \tag{1.49}$$

$$\mathbf{A}_2 = \begin{bmatrix} e^{j\pi \sin\theta_1} & e^{j\pi \sin\theta_2} & \cdots & e^{j\pi \sin\theta_K} \\ e^{j2\pi \sin\theta_1} & e^{j2\pi \sin\theta_2} & \cdots & e^{j2\pi \sin\theta_K} \\ \vdots & \vdots & \ddots & \vdots \\ e^{j(M-1)\pi \sin\theta_1} & e^{j(M-1)\pi \sin\theta_2} & \cdots & e^{j(M-1)\pi \sin\theta_K} \end{bmatrix} \tag{1.50}$$

We have

$$\mathbf{A}_2 = \mathbf{A}_1 \mathbf{\Phi} \tag{1.51}$$

with

$$\mathbf{\Phi} = \mathrm{diag}\left\{ e^{j\pi \sin\theta_1} \quad e^{j\pi \sin\theta_2} \quad \cdots \quad e^{j\pi \sin\theta_K} \right\} \tag{1.52}$$

Similarly, define $\mathbf{U}_{s1}$ and $\mathbf{U}_{s2}$ as the first and last $(M-1)$ rows of $\mathbf{U}_s$. Then according to Equation (1.48), there are

$$\mathbf{A}_1 = \mathbf{U}_{s1}\mathbf{T} \tag{1.53}$$

$$\mathbf{A}_2 = \mathbf{U}_{s2}\mathbf{T} \tag{1.54}$$

Then it can be deduced that

$$\mathbf{A}_2 = \mathbf{A}_1\mathbf{\Phi} = \mathbf{U}_{s1}\mathbf{T}\mathbf{\Phi} = \mathbf{U}_{s2}\mathbf{T} \tag{1.55}$$

and

$$\mathbf{U}_{s2} = \mathbf{U}_{s1}\mathbf{T}\mathbf{\Phi}\mathbf{T}^{-1} = \mathbf{U}_{s1}\mathbf{\Delta} \tag{1.56}$$

with

$$\mathbf{\Delta} = \mathbf{T}\mathbf{\Phi}\mathbf{T}^{-1} = \mathbf{U}_{s1}^{+}\mathbf{U}_{s2} = \left(\mathbf{U}_{s1}^{H}\mathbf{U}_{s1}\right)^{-1}\mathbf{U}_{s1}^{H}\mathbf{U}_{s2} \tag{1.57}$$

where $(\cdot)^{+}$ denotes the pseudo-inverse operation, and the diagonal matrix $\mathbf{\Phi}$ is composed of the eigenvalues of the matrix $\mathbf{\Delta}$.

Therefore, after the eigenvalues decomposition of $\mathbf{\Delta}$, the DOAs can be obtained by

$$\theta_k = \arcsin\left(\frac{\text{angle}\left(\mathbf{\Phi}\left(k,k\right)\right)}{\pi}\right) \tag{1.58}$$

Without the spectrum, the DOA estimation performance of the ESPRIT method is shown in FIGURE 1.7 with the results of 20 independent simulations with the same simulation conditions introduced above.

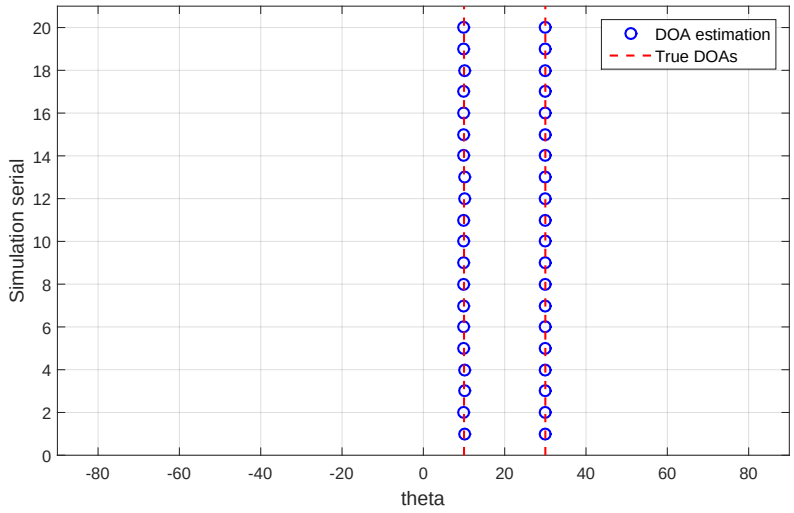

FIGURE 1.7 – DOA estimation by ESPRTI method

1.4 Conclusion

In this chapter, the basic of array signal processing techniques including the received signal model and several conventional algorithms for DOA estimation is introduced based on uniform arrays. However, the inter-element spacing of ULAs is limited to half-wavelength of incoming signals to avoid aliasing, therefore the estimation performance is constrained by the small array aperture. On the other hand, although the methods of MUSIC and ESPRIT can achieve high resolution and accurate estimation performance, based on ULAs, they can only resolve up to $M-1$ sources with M sensor elements due to the limited system DOFs. In the next chapter, the geometry of coprime arrays is introduced, which exhibits larger aperture length and higher DOFs.

CHAPITRE 2

DOA ESTIMATION WITH COPRIME LINEAR ARRAYS

Being superior to the conventional half-wavelength spaced ULAs, coprime linear arrays (CLAs), exhibiting higher DOFs and larger aperture length, have been considered as a promising array configuration. In this chapter, the prototype of CLAs structure is introduced and the DOA estimation with CLAs is presented, involving the two research orientations of difference coarray-based methods and subarray-based methods respectively. For the difference coarray-based methods, the difference coarray, of which the observation can be obtained from the covariance matrix of received signals, exhibits more distinct lags than the number of physical sensor elements, offering much higher DOFs, and then the MUSIC method with the spatial smoothing technique is implemented in the coarray domain to perform the DOA estimation. For the subarray-based methods, a CLA is treated as two ULAs with large aperture length and inter-element spacing. With the simplified system model, DOA estimation is performed on the two subarrays individually. The ambiguities caused by the large inter-element spacing are eliminated by the coprime property.

2.1 Prototype of coprime linear arrays

As illustrated in FIGURE 2.1, a prototype of CLAs consists of two sparse ULAs, having N and M sensor elements, with inter-element spacing $d_1 = Md$ and $d_2 = Nd$ respectively, where M and N are two coprime integers, and $d = \frac{\lambda}{2}$. Without loss of generality, it is assumed that $M < N$. The position of the u^{th} sensor element is given as $p_u d$ with $u = 1, 2, \cdots, L$, where L denotes the total number of sensor elements, and because the first sensor is shared by the two subarrays and set as the reference point, there are $L = M+N-1$ and $p_1 = 0$.

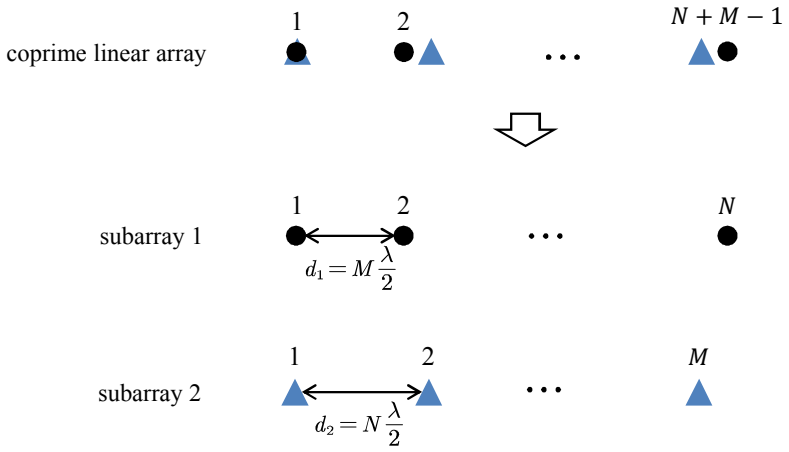

FIGURE 2.1 – Prototype coprime linear array

Suppose that K uncorrelated, far-field and narrowband signals impinge on the CLA from directions $\{\theta_1, \theta_2, \cdots, \theta_K\}$ respectively. The signal vector received at the CLA can be expressed as

$$\begin{aligned} \mathbf{x}(t) &= \sum_{k=1}^{K} \mathbf{a}(\theta_k) s_k(t) + \mathbf{n}(t) \\ &= \mathbf{A}\mathbf{s}(t) + \mathbf{n}(t) \end{aligned} \tag{2.1}$$

where

$$\mathbf{A} = \begin{bmatrix} \mathbf{a}(\theta_1) & \mathbf{a}(\theta_2) & \cdots & \mathbf{a}(\theta_K) \end{bmatrix} \tag{2.2}$$

denotes the directional matrix of the CLA with

$$\mathbf{a}(\theta_k) = \begin{bmatrix} 1 & e^{jp_2\pi\sin\theta_k} & \cdots & e^{jp_{N+M-1}\pi\sin\theta_k} \end{bmatrix}^T \tag{2.3}$$

denoting the directional vector associated with the incoming signal from θ_k.

$$\mathbf{s}(t) = \begin{bmatrix} s_1(t) & s_2(t) & \cdots & s_K(t) \end{bmatrix}^T \tag{2.4}$$

is the incoming signal vector with $s_k(t)$ the signal coming from θ_k and received at the reference sensor. $\mathbf{n}(t)$ is the white Gaussian noise vector with zero-mean and covariance matrix $\sigma^2\mathbf{I}_{M+N-1}$, and it is assumed to be independent from the incoming signals.

From the perspective of subarrays, the signal vectors received by the two sparse uniform

subarrays can be given by

$$\mathbf{x}_1(t) = \sum_{k=1}^{K} \mathbf{a}_1(\theta_k) s_k(t) + \mathbf{n}_1(t) = \mathbf{A}_1 \mathbf{s}(t) + \mathbf{n}_1(t) \tag{2.5}$$

$$\mathbf{x}_2(t) = \sum_{k=1}^{K} \mathbf{a}_2(\theta_k) s_k(t) + \mathbf{n}_2(t) = \mathbf{A}_2 \mathbf{s}(t) + \mathbf{n}_2(t) \tag{2.6}$$

where

$$\mathbf{A}_1 = \begin{bmatrix} \mathbf{a}_1(\theta_1) & \mathbf{a}_1(\theta_2) & \cdots & \mathbf{a}_1(\theta_K) \end{bmatrix} \tag{2.7}$$

$$\mathbf{A}_2 = \begin{bmatrix} \mathbf{a}_2(\theta_1) & \mathbf{a}_2(\theta_2) & \cdots & \mathbf{a}_2(\theta_K) \end{bmatrix} \tag{2.8}$$

are the directional matrices of the two subarrays respectively, with the corresponding directional vectors associated with the incoming signal from θ_k denoted by

$$\mathbf{a}_1(\theta_k) = \begin{bmatrix} 1 & e^{jM\pi \sin\theta_k} & \cdots & e^{j(N-1)M\pi \sin\theta_k} \end{bmatrix}^T \tag{2.9}$$

$$\mathbf{a}_2(\theta_k) = \begin{bmatrix} 1 & e^{jN\pi \sin\theta_k} & \cdots & e^{j(M-1)N\pi \sin\theta_k} \end{bmatrix}^T \tag{2.10}$$

$\mathbf{n}_1(t)$ and $\mathbf{n}_2(t)$ denote the white Gaussian noise vectors observed by the two subarrays with dimensions of $(N \times 1)$ and $(M \times 1)$ respectively.

2.2 Difference coarray-based methods

2.2.1 Difference coarray

Difference coarray is a virtual array usually applied in the difference coarray-based methods instead of the original physical array to obtain higher DOFs with fewer sensor elements. Taking d as unit, the sensor element positions of a CLA can be given as

$$\mathbb{P} = \begin{Bmatrix} p_1 & p_2 & \cdots & p_L \end{Bmatrix} \tag{2.11}$$

and the difference coarray of the CLA is defined as

$$\mathbb{D} = \{ p_u - p_v \mid p_u, p_v \in \mathbb{P} \} \tag{2.12}$$

of which the elements are known as lags which are generated by all pairs of sensor elements in the CLA.

Based on the coprimality of M and N, it has been shown that the difference coarray $\mathbb{D}$ consists of at least MN distinct lags located in the range $[-(N-1)M, (N-1)M]$ [44,46], which is more than the number of sensor elements in the physical CLA, and can be exploited to achieve higher DOFs. The positions in the range $[-(N-1)M, (N-1)M]$ but not being an element of $\mathbb{D}$ are known as holes. The first hole locates at $\pm(M+N)$, and $\mathbb{D}$ exhibits a consecutive ULA segment without holes in the range $[(-M-N+1), (M+N-1)]$ [51]. FIGURE 2.2 shows a CLA with $N=5$ and $M=4$, and the corresponding difference coarray is shown in Figure 2.3, with blue dots and red rhombuses representing the lags and holes respectively.

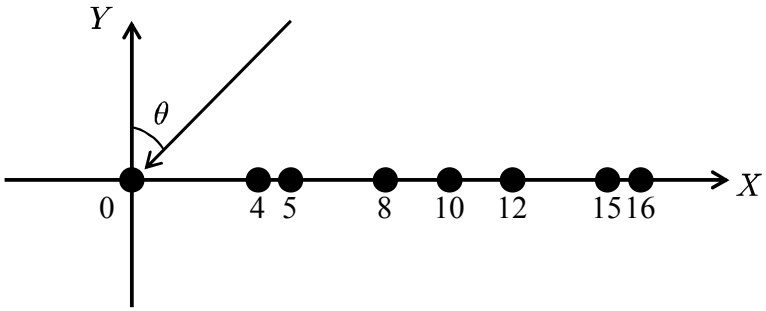

FIGURE 2.2 – Coprime linear array with $N=5$ and $M=4$

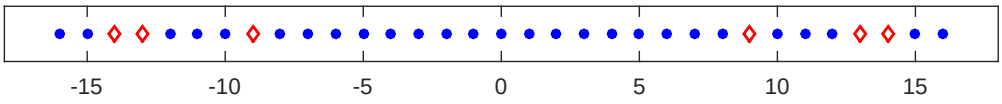

FIGURE 2.3 – Difference coarray with $N=5$ and $M=4$

The observation of the difference coarray can be obtained from the covariance matrix of the received signals, which is calculated by

$$\mathbf{R} = E\left\{\mathbf{x}(t)\,\mathbf{x}^H(t)\right\} = \mathbf{A}\mathbf{R}_s\mathbf{A}^H + \sigma^2\mathbf{I}_{M+N-1} \tag{2.13}$$

where

$$\mathbf{R}_s = E\left\{\mathbf{s}(t)\,\mathbf{s}^H(t)\right\} = \mathrm{diag}\left\{\sigma_1^2 \quad \sigma_2^2 \quad \cdots \quad \sigma_K^2\right\} \tag{2.14}$$

is the covariance matrix of the incoming signals with σ_k^2 denoting the power of the signals coming from θ_k.

Then Equation (2.13) can be re-written as

$$\mathbf{R} = \sum_{k=1}^{K} \sigma_k^2 \mathbf{a}\left(\theta_k\right) \mathbf{a}^H\left(\theta_k\right) + \sigma^2 \mathbf{I}_{M+N-1} \tag{2.15}$$

where $\mathbf{R}$ is an $L \times L$ matrix, of which the element at the u^{th} row and v^{th} column has the form of $\sum_{k=1}^{K} \sigma_k^2 e^{j\pi(p_u - p_v)\sin\theta_k}$. The difference coarray elements $(p_u - p_v)$ appear in the exponents of the correlation terms, which behave like the signals observed by the corresponding lags in the difference coarray, and can be used to perform DOA estimation.

By vectorizing $\mathbf{R}$, we can get

$$\mathbf{z} = \operatorname{vec}\left(\mathbf{R}\right) = \mathbf{B}\mathbf{p} + \sigma^2 \tilde{\mathbf{I}} \tag{2.16}$$

where

$$\mathbf{B} = \begin{bmatrix} \mathbf{a}^*\left(\theta_1\right) \otimes \mathbf{a}\left(\theta_1\right) & \mathbf{a}^*\left(\theta_2\right) \otimes \mathbf{a}\left(\theta_2\right) & \cdots & \mathbf{a}^*\left(\theta_K\right) \otimes \mathbf{a}\left(\theta_K\right) \end{bmatrix} \tag{2.17}$$

$$\mathbf{p} = \begin{bmatrix} \sigma_1^2 & \sigma_2^2 & \cdots & \sigma_K^2 \end{bmatrix}^T \tag{2.18}$$

and

$$\tilde{\mathbf{I}} = \begin{bmatrix} \mathbf{e}_1^T & \mathbf{e}_2^T & \cdots & \mathbf{e}_L^T \end{bmatrix}^T \tag{2.19}$$

with $\mathbf{e}_u$ a column vector with dimension $(L \times 1)$, of which the u^{th} element is '1' and the others are '0'.

Let $\mathbf{B}_{\mathbb{D}}$ denote the distinct rows of $\mathbf{B}$, and $\mathbf{z}_{\mathbb{D}}$ and $\tilde{\mathbf{I}}_{\mathbb{D}}$ denote the corresponding rows of $\mathbf{z}$ and $\tilde{\mathbf{I}}$ respectively, then there is

$$\mathbf{z}_{\mathbb{D}} = \mathbf{B}_{\mathbb{D}}\mathbf{p} + \sigma^2 \tilde{\mathbf{I}}_{\mathbb{D}} \tag{2.20}$$

Compared with Equation (2.1), it can be seen that $\mathbf{B}_{\mathbb{D}}$ behaves like the directional matrix of an array whose sensor locations are given by the lags in the difference coarray, and $\mathbf{z}_{\mathbb{D}}$ can be regarded as the signal vector received by such an array. $\mathbf{p}$ and $\sigma^2 \tilde{\mathbf{I}}_{\mathbb{D}}$ denote the equivalent source signal and noise vectors respectively. Then $\mathbf{z}_{\mathbb{D}}$ can be seen as the signal received by the difference coarray and can be applied to perform DOA estimation instead of the signal received by the physical CLA. The conversion from $\mathbf{R}$ to $\mathbf{z}_{\mathbb{D}}$ is shown in FIGURE 2.4

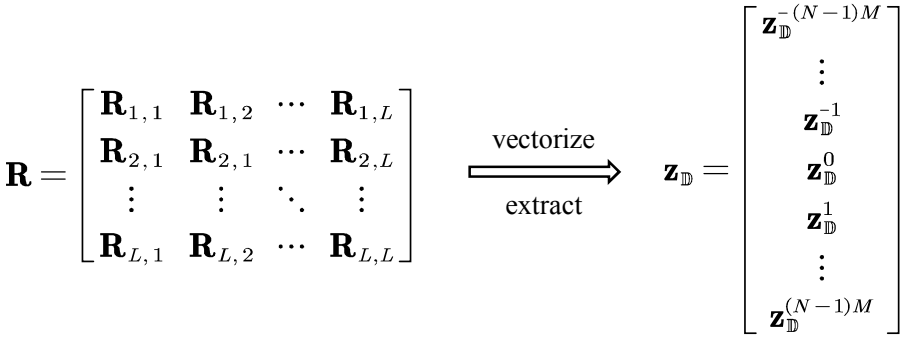

FIGURE 2.4 – The conversion from $\mathbf{R}$ to $\mathbf{z}_{\mathbb{D}}$

in which $\mathbf{z}_{\mathbb{D}}^{m}$ can be calculated by

$$\mathbf{z}_{\mathbb{D}}^{m} = \frac{1}{w\left(m\right)} \sum_{p_u - p_v = m} \mathbf{R}_{u,v} \tag{2.21}$$

with $m \in \mathbb{D}$, and $w(m)$ is the weight function, which is defined by the number of sensor pairs generating the lag m as

$$w\left(m\right) = \left|\left\{\left(p_u, p_v\right) \mid p_u - p_v = m\right\}\right| \tag{2.22}$$

Note that due to the existence of holes in the difference coarray, the superscript m is not continuous in the range $[-(N-1)M, (N-1)M]$.

2.2.2 MUSIC with spatial smoothing technique

Since the difference coarray of a CLA has more lags than the number of sensor elements in the physical array, the signal model in Equation (2.20) is applied to substitute Equation (2.1) in DOA estimation to achieve higher DOFs. However, because the equivalent source signal vector $\mathbf{p}$ is just a single snapshot, the covariance matrix built by $\mathbf{z}_{\mathbb{D}}$ is rank deficient, and in this case high resolution subspace based DOA estiamtion methods, such as MUSIC, fail to yield reliable estimation results. The problem is similar to handling fully coherent source signals, and spatial smoothing technique [44,84–86] should be applied to restore the rank of the covariance matrix.

Because the spatial smoothing technique works only for a set of consecutive lags such that every smoothing subarray has similar directional vector, we focus on the consecutive

part of $\mathbb{D}$, which is defined by $\mathbb{U}$ and

$$\mathbb{U} = \left\{(-M-N+1) \quad \cdots \quad 0 \quad \cdots \quad (M+N-1)\right\} \tag{2.23}$$

Extract the rows of $\mathbf{z}_{\mathbb{D}}$ corresponding to the consecutive part of the difference coarray $\mathbb{U}$, which can be expressed by

$$\mathbf{z}_{\mathbb{U}} = \mathbf{B}_{\mathbb{U}}\mathbf{p} + \sigma^2\tilde{\mathbf{I}}_{\mathbb{U}} \tag{2.24}$$

where $\mathbf{B}_{\mathbb{U}}$ denotes the directional matrix of the ULA segment in the difference coarray, which can be given by

$$\mathbf{B}_{\mathbb{U}} = \left[\mathbf{b}_{\mathbb{U}}(\theta_1) \quad \mathbf{b}_{\mathbb{U}}(\theta_2) \quad \cdots \quad \mathbf{b}_{\mathbb{U}}(\theta_K)\right] \tag{2.25}$$

with the corresponding directional vector

$$\mathbf{b}_{\mathbb{U}}(\theta_k) = \left[e^{j(-M-N+1)\pi\sin\theta_k} \quad \cdots \quad 1 \quad \cdots \quad e^{j(M+N-1)\pi\sin\theta_k}\right]^T \tag{2.26}$$

And $\tilde{\mathbf{I}}_{\mathbb{U}}$ is a $(2M+2N-1)\times 1$ vector with all '0' except a '1' at the $(M+N)^{\text{th}}$ position.

Then the ULA segments of the difference coarray are divided into $M+N$ overlapping subarrays, denoted by $\mathbb{U}_i$, which contains $M+N$ lags located at

$$\{x \mid x = -i+n\} \tag{2.27}$$

where i denotes the index of the subarrays with $i = 1, 2, \cdots, M+N$, and n denotes the index of the lags in each subarray with $n = 1, 2, \cdots, M+N$.

The equivalent signal vector received by the i^{th} subarray corresponds to the $(M+N+1-i)^{\text{th}}$ to $(2M+2N-i)^{\text{th}}$ rows of $\mathbf{z}_{\mathbb{U}}$, which is denoted as

$$\mathbf{z}_{\mathbb{U},i} = \mathbf{B}_{\mathbb{U},i}\mathbf{p} + \sigma^2\tilde{\mathbf{I}}_{\mathbb{U},i} \tag{2.28}$$

where $\mathbf{B}_{\mathbb{U},i}$ is a $(M+N)\times K$ matrix consisting of the $(M+N+1-i)^{\text{th}}$ to $(2M+2N-i)^{\text{th}}$ rows of $\mathbf{B}_{\mathbb{U}}$, and $\tilde{\mathbf{I}}_{\mathbb{U},i}$ is a $(M+N)\times 1$ vector with all '0' except a '1' at the i^{th} position.

Then we define

$$\mathbf{R}_i = \mathbf{z}_{\mathbb{U},i}\mathbf{z}_{\mathbb{U},i}^H \tag{2.29}$$

and taking the average of $\mathbf{R}_i$ over all i, we can get

$$\mathbf{R}_{ss} = \frac{1}{M+N} \sum_{i=1}^{M+N} \mathbf{R}_i \tag{2.30}$$

$\mathbf{R}_{ss}$ is known as the spatially smoothed covariance matrix which is full-rank, such that MUSIC algorithm can be directly performed on it.

However, it can be noticed that although the difference coarray exhibits more distinct lags than the number of sensor elements in the physical CLA, offering higher DOFs, these lags are not consecutive because of the existence of holes, and only the consecutive part can be directly applied in rank restoration and DOA estimation, the effective DOFs, which roughly equal to the half number of the consecutive lags, is not as high as expected. For example, the difference coarray shown in FIGURE 2.3 has 27 distinct lags but only consecutive in the range $[-8, 8]$. After spatial smoothing, a spatially smoothed covariance matrix with dimension 9×9 is obtained, and since at least one eigenvector spanning the noise subspace is needed such that MUSIC algorithm can be performed, merely 8 effective DOFs can be obtained. To overcome this problem, many methods have been proposed to increase the number of the consecutive lags in the difference coarray, among which the extended coprime linear array [51] is the most popular configuration, which is introduced in the following.

2.2.3 Extended coprime linear arrays

The configuration of extended coprime linear arrays (ECLAs) is shown in FIGURE 2.5. Being different from the prototype CLA shown in FIGURE 2.1, an ECLA has lM sensor elements in the second subarray, where l is an integer and $l \geq 2$. Then the total number of the sensor elements is $L = lM + N - 1$.

The characteristics of the difference coarray of the ECLAs including the number of DOFs and the holes positions have been well studied in [51]. Based on the coprime property of M and N, three general rules can be summarized as follows.

1) The difference coarray $\mathbb{D}$ is located in the range $[(-lMN + N), (lMN - N)]$.

2) The difference coarray exhibits a consecutive part $\mathbb{U}$ located in the range $[(-(l-1)MN - M + 1), ((l-1)MN + M - 1)]$.

3) In the range $[(-lMN + N), (-(l-1)MN - M)]$ and $[((l-1)MN + M), (lMN - N)]$, the position is a hole if it is in the form of $-(k-1)MN - aM - bN$ or $(k-1)MN +$

$aM + bN$, where $a \geq 1$ and $b \geq 0$.

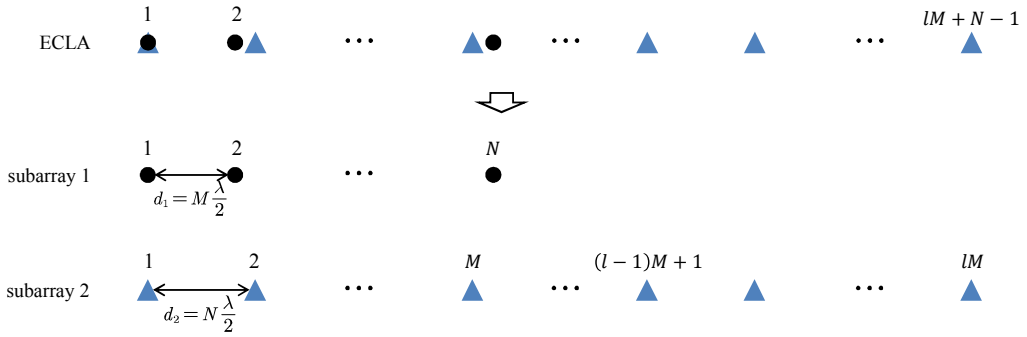

FIGURE 2.5 – Structure of extended coprime linear array

FIGURE 2.6 shows an ECLA with $N = 5$, $M = 4$ and $l = 2$. The corresponding difference coarray is shown in FIGURE 2.7. Compared with the difference coarray of the prototype CLA shown in FIGURE 2.3, it can be seen that by adding few sensor elements to a subarray, the number of consecutive lags in the difference coarray is significantly increased from 17 to 47. After spatial smoothing, a rank restored covariance matrix with dimension 24×24 is obtained, such that up to 23 effective DOFs can be achieved. FIGURE 2.8 depicts the MUISC spectrum of the ECLA with 17 sources uniformly distributed from $-64°$ to $64°$, where the number of snapshots is 2000 and SNR $= 10$dB.

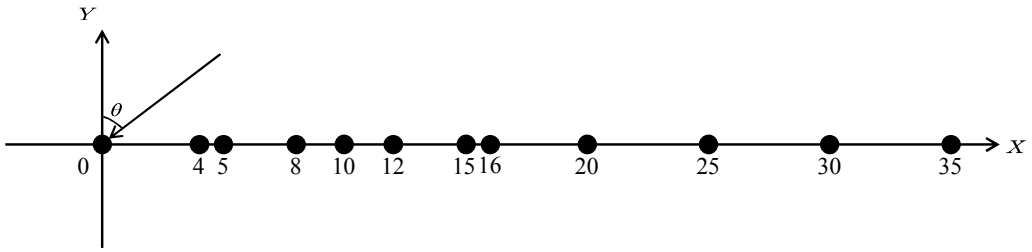

FIGURE 2.6 – Extended coprime linear array with $N = 5$, $M = 4$ and $l = 2$

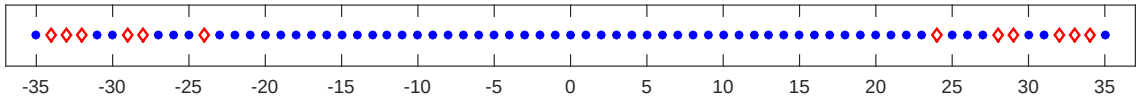

FIGURE 2.7 – Difference coarray with $N = 5$, $M = 4$ and $l = 2$

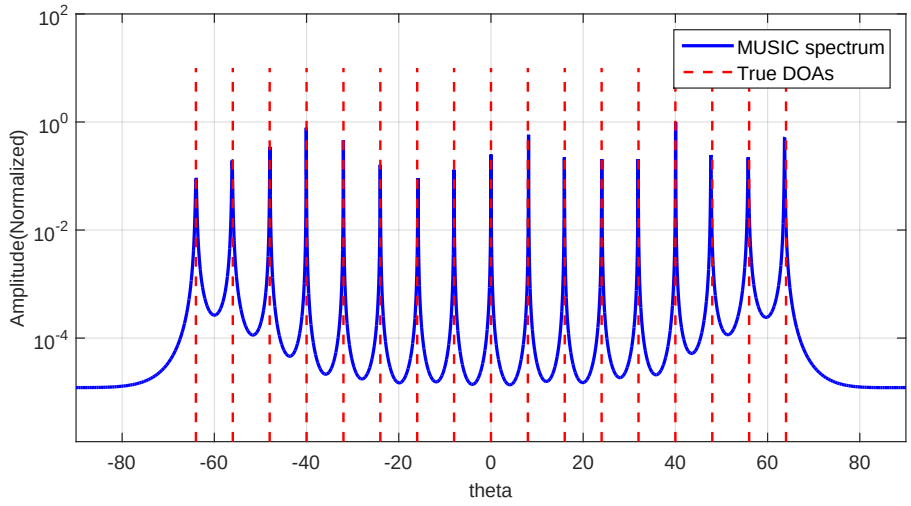

FIGURE 2.8 – MUSIC spectrum of ECLA

Besides, based on the knowledge of the holes positions in the difference coarray, there are some other methods proposed aiming to fill the holes, lengthening the consecutive ULA in the difference coarray and increasing the effective DOFs [47, 49, 87, 88].

2.3 Subarray-based methods

2.3.1 DOA estimation and ambiguity elimination

In the subarray-based methods, instead of exploiting the difference coarray, the CLA is treated as two sparse ULAs and DOA estimation is performed on the two subarrays separately with the signal model shown by Equations (2.5) and (2.6).

Taking MUSIC for example. From the signals observed by the two subarrays $\mathbf{x}_1(t)$ and $\mathbf{x}_2(t)$, two corresponding covariance matrices can be estimated by

$$\hat{\mathbf{R}}_1 = \frac{1}{L}\sum_{t=1}^{L}\mathbf{x}_1(t)\,\mathbf{x}_1^H(t) \tag{2.31}$$

$$\hat{\mathbf{R}}_2 = \frac{1}{L}\sum_{t=1}^{L}\mathbf{x}_2(t)\,\mathbf{x}_2^H(t) \tag{2.32}$$

Applying eigenvalue decomposition on the two covariance matrices yields

$$\hat{\mathbf{R}}_1 = \mathbf{U}_{s,1}\mathbf{\Lambda}_{s,1}\mathbf{U}_{s,1}^H + \mathbf{U}_{n,1}\mathbf{\Lambda}_{n,1}\mathbf{U}_{n,1}^H \tag{2.33}$$

$$\hat{\mathbf{R}}_2 = \mathbf{U}_{s,2}\mathbf{\Lambda}_{s,2}\mathbf{U}_{s,2}^H + \mathbf{U}_{n,2}\mathbf{\Lambda}_{n,2}\mathbf{U}_{n,2}^H \tag{2.34}$$

where $\mathbf{U}_{s,1}$ and $\mathbf{U}_{s,2}$ contain the eigenvectors of $\hat{\mathbf{R}}_1$ and $\hat{\mathbf{R}}_2$ respectively spanning the signal subspace, with the corresponding eigenvalues contained in the two diagonal matrices $\mathbf{\Lambda}_{s,1}$ and $\mathbf{\Lambda}_{s,2}$. Similarly, the $\mathbf{U}_{n,1}$ and $\mathbf{U}_{n,2}$ contain the eigenvectors of $\hat{\mathbf{R}}_1$ and $\hat{\mathbf{R}}_2$ respectively spanning the noise subspace, with the corresponding eigenvalues contained in the two diagonal matrices $\mathbf{\Lambda}_{n,1}$ and $\mathbf{\Lambda}_{n,2}$.

Because of the orthogonality between the signal subspace and the noise subspace, the DOA estimation can be realized by searching for the peaks of the following MUSIC spectrum in the range $(-90^\circ, 90^\circ)$

$$P_{MUSIC,1}(\theta) = \frac{1}{\mathbf{a}_1^H(\theta)\,\mathbf{U}_{n,1}\mathbf{U}_{n,1}^H\mathbf{a}_1(\theta)} \tag{2.35}$$

$$P_{MUSIC,2}(\theta) = \frac{1}{\mathbf{a}_2^H(\theta)\,\mathbf{U}_{n,2}\mathbf{U}_{n,2}^H\mathbf{a}_2(\theta)} \tag{2.36}$$

Noticing that because the adjacent sensor elements in each subarrays are spaced an integer number, M or N, times of half-wavelength, for a given impinging angle θ_k and its exponential $e^{jM\pi\sin\theta_k}$ or $e^{jN\pi\sin\theta_k}$, there exist other angles in the range $(-90^\circ, 90^\circ)$ having the same exponential value and sharing identical directional vector with θ_k. Such angles are denoted ambiguous angles and also exhibit peaks in the MUSIC spectrum.

Taking the 1^{st} subarray with N sensor elements and inter-element spacing $M\frac{\lambda}{2}$ for example, for an impinging signal coming from θ_k, several candidate angles showing peaks $\theta_{1,k}^{cand}$ can be found in the MUSIC spectrum, satisfying the following relationship

$$\sin\theta_k - \sin\theta_{1,k}^{cand} = \frac{2P}{M} \tag{2.37}$$

where P in an integer. When $P = 0$, the candidate angle $\theta_{1,k}^{cand}$ is the true DOA. Otherwise, $\theta_{1,k}^{cand}$ corresponds to an ambiguity of the spectrum.

For any θ_k and $\theta_{1,k}^{cand}$ in the range $(-90^\circ, 90^\circ)$, there is

$$\left|\sin\theta_k - \sin\theta_{1,k}^{cand}\right| = \left|\frac{2P}{M}\right| < 2 \tag{2.38}$$

Except '0', P has another $2(M-1)$ possible values in the range $[-M+1,-1]\cup[1,M-1]$ corresponding to ambiguities. Considering that θ_k and $\theta_{1,k}^{cand}$ are interchangeable, there exist $M-1$ ambiguous angles besides the real DOA. Therefore totally M peaks can be found in the spectrum obtained by the subarray associated with an incoming signal. One of them locates at the true DOA and the other $M-1$ are ambiguities.

Similarly, for the 2nd subarray with M sensor elements and inter-element spacing $N\frac{\lambda}{2}$, for the impinging signal coming from θ_k, the candidate angles exhibiting peaks $\theta_{2,k}^{cand}$ satisfies the relationship

$$\sin\theta_k - \sin\theta_{2,k}^{cand} = \frac{2Q}{N} \tag{2.39}$$

where Q is an integer, and when $Q=0$, the candidate angle $\theta_{2,k}^{cand}$ is the true DOA. Otherwise, $\theta_{2,k}^{cand}$ corresponds to an ambiguity.

For any θ_k and $\theta_{2,k}^{cand}$ in the range $(-90^\circ, 90^\circ)$, there is

$$\left|\sin\theta_k - \sin\theta_{2,k}^{cand}\right| = \left|\frac{2Q}{N}\right| < 2 \tag{2.40}$$

Except '0', Q has another $2(N-1)$ possible values in the range $[-N+1,-1]\cup[1,N-1]$ corresponding to ambiguities. Considering that θ_k and $\theta_{2,k}^{cand}$ are interchangeable, there exist $N-1$ ambiguous angles besides the real DOA. Therefore totally N peaks can be found in the spectrum obtained by the subarray associated with an incoming signal. One of them locates at the true DOA and the other $N-1$ are ambiguities.

According to Equations (2.37) and (2.39), there is a relationship between the candidate angles obtained from the two spectrums, shown by

$$\sin\theta_{1,k}^{cand} - \sin\theta_{2,k}^{cand} = 2\left(\frac{Q}{N} - \frac{P}{M}\right) \tag{2.41}$$

It can be seen that due to the coprimality between M and N, there is $\theta_{1,k}^{cand} = \theta_{2,k}^{cand} = \theta_k$ when and only when $P=Q=0$. For other $P\neq 0$ and $Q\neq 0$, the corresponding candidate angles obtained from the two spectrums always exhibit $\theta_{1,k}^{cand} \neq \theta_{2,k}^{cand}$. Therefore, there exists and uniquely exists an overlapped peak in the spectrums of the two subarrays, which determines the real estimate of DOA [56].

In practical applications with finite number of samples and the existence of noise, we

can search for the closest peaks in the MUSIC spectrums of the two subarrays, i.e.,

$$\min_{\theta_{1,k}^{cand,m},\theta_{2,k}^{cand,n}} \left|\theta_{1,k}^{cand,m} - \theta_{2,k}^{cand,n}\right| \tag{2.42}$$

where $m = 1, 2, \cdots, M$ and $n = 1, 2, \cdots, N$ denote the indexes of the candidate angles. Then the DOA estimation of the coprime array can be obtained by

$$\hat{\theta}_k = \frac{\theta_{1,k}^{cand,m} + \theta_{2,k}^{cand,n}}{2} \tag{2.43}$$

The DOA estimation performance of the coprime subarrays is shown in FIGURE 2.9, in which an incoming signal is assumed to impinge on a CLA with $N = 7$ and $M = 5$ from direction $\theta = 10°$. The number of snapshots is set to 200 with SNR $= 10$dB. It can be seen that there exist $M = 5$ peaks in the spectrum of the 1^{st} subarray with $N = 7$ sensor elements, and $N = 7$ peaks in the spectrum of the 2^{nd} subarray with $M = 5$ sensor elements respectively. The true DOA is determined by the overlapped peaks in the two spectrums.

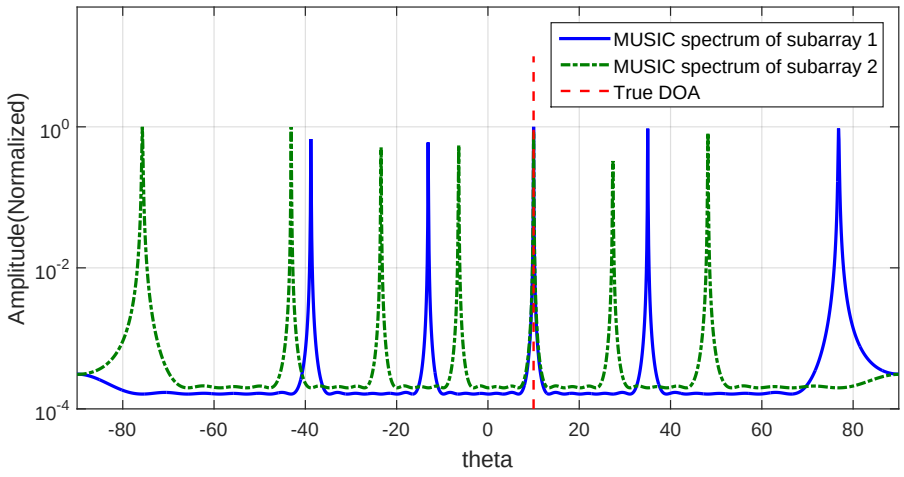

FIGURE 2.9 – MUSIC spectrums of coprime subarrays with $N = 7$ and $M = 5$

2.3.2 Pair matching errors

There exist some potential problems in the subarray-based methods, and the problem of pair matching errors [58, 59] is one of them which we may meet in the step of overlapped peaks searching. Thanks to the coprime property, only one pair of common angles showing overlapped peaks can be found in the two spectrums associated with one incoming signal,

and other angles showing peaks can be eliminated as ambiguities. However, in the situations of multiple incoming signals, besides the common angle pairs in the two spectrums associated with common incoming signals, there may also exist common angle pairs in the two spectrums associated with different incoming signals, resulting in more overlapped peaks than the number of sources, and consequently pair matching errors occur.

Suppose that there are two signals impinging on a CLA from θ_1 and θ_2 respectively. In the spectrum of the 1^{st} subarray, we can find two ambiguous angles $\theta_{1,1}^{amb}$ and $\theta_{1,2}^{amb}$ associated with θ_1 and θ_2 respectively, satisfying

$$\sin\theta_1 - \sin\theta_{1,1}^{amb} = \frac{2P_1}{M} \tag{2.44}$$

$$\sin\theta_2 - \sin\theta_{1,2}^{amb} = \frac{2P_2}{M} \tag{2.45}$$

where P_1 and P_2 are two non-zero integers in the range $[-M+1,-1]\cup[1,M-1]$. In the spectrum of the 2^{nd} subarray, we can also find two ambiguous angles $\theta_{2,1}^{amb}$ and $\theta_{2,2}^{amb}$ associated with θ_1 and θ_2 respectively, satisfying

$$\sin\theta_1 - \sin\theta_{2,1}^{amb} = \frac{2Q_1}{N} \tag{2.46}$$

$$\sin\theta_2 - \sin\theta_{2,2}^{amb} = \frac{2Q_2}{N} \tag{2.47}$$

where Q_1 and Q_2 are two non-zero integers in the range $[-N+1,-1]\cup[1,N-1]$.

It can be seen that for different impinging angles $\theta_1 \neq \theta_2$, we may have the following relationships

$$\sin\theta_1 - \sin\theta_2 = \frac{2Q_1}{N} - \frac{2P_2}{M} \tag{2.48}$$

or

$$\sin\theta_1 - \sin\theta_2 = \frac{2P_1}{M} - \frac{2Q_2}{N} \tag{2.49}$$

With subtraction Equation (2.46)-Equation (2.45) and Equation (2.48), we can deduce that

$$\sin\theta_{1,2}^{amb} = \sin\theta_{2,1}^{amb} \tag{2.50}$$

and with subtraction Equation (2.44)-Equation (2.47) and Equation (2.49), we can deduce that

$$\sin\theta_{1,1}^{amb} = \sin\theta_{2,2}^{amb} \tag{2.51}$$

exhibiting other overlapped peaks or pair matching errors in the two spectrums.

FIGURE 2.10 shows the DOA estimation simulation with coprime subarrays when pair matching errors exist, in which there are $N = 7$ and $M = 5$ sensor elements placed in the two coprime subarrays, and two signals impinging from $\theta_1 = 10.00°$ and $\theta_2 = 39.11°$ respectively. The number of snapshots is set to 200 and SNR $= 10$dB. It can be seen that besides the two real DOAs, there exist two other common angles, $-13.09°$ and $-75.75°$, exhibiting overlapped peaks but associated with different sources. To be more clear, a diagram illustrating the generation of pair matching errors in such situation is given in FIGURE 2.11.

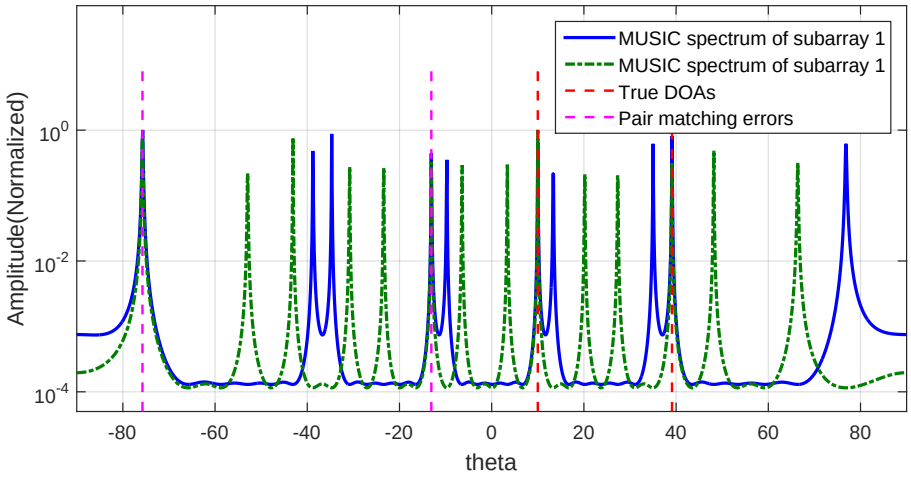

FIGURE 2.10 – MUSIC spectrums of coprime subarrays in pair matching errors situation

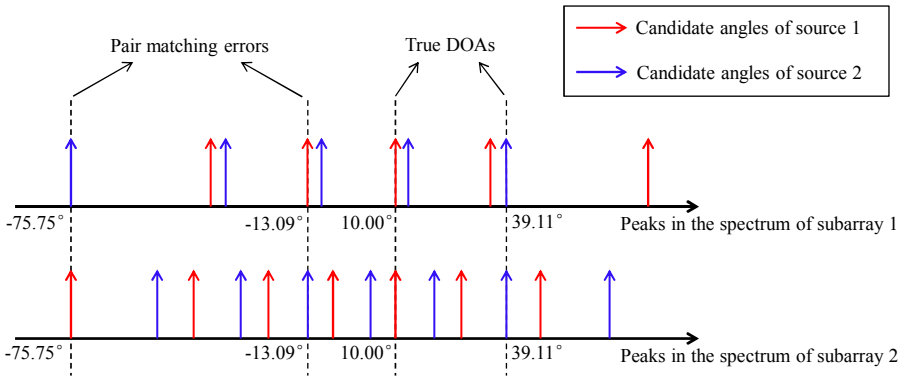

FIGURE 2.11 – Diagram of the generation of pair matching errors

2.3.3 Grating angles problem

Grating angles problem [60] is another problem of the subarray-based methods, which has been ignored by most of the open literature. In the situation of multiple incoming signals, because of the large inter-element spacing of the two subarrays, some signals may impinge from a set of angles which share an identical directional vector for one subarray. Consequently, the directional matrix of this subarray will be rank deficient, resulting in difficulties for the subsequent steps like noise subspace extraction and peak searching.

To provide a better understanding, let's consider a CLA with $N = 7$ and $M = 5$ senor elements in the two subarrays and three source signals impinging from $\theta_1 = 10.00°$, $\theta_2 = 27.35°$ and $\theta_3 = 35.01°$ respectively. It can be seen that $e^{jM\pi \sin\theta_1} \approx e^{jM\pi \sin\theta_3}$ and $e^{jN\pi \sin\theta_1} \approx e^{jN\pi \sin\theta_2}$. Then θ_1 and θ_3 are grating angles to each other for the 1^{st} subarray because they have the same directional vector. For the same reason, θ_1 and θ_2 are grating angles to each other for the 2^{nd} subarray. Then the directional matrices of the two subarrays are rank deficient, setting up a barrier to the DOA estimation.

For the CLA with $N = 7$ and $M = 5$, the grating angles problem also occurs in many other situations. As an example with three incoming signals, when $\{\theta_1, \theta_2, \theta_3\} = \{20.00°, 38.88°, 47.90°\}$, $\{\theta_1, \theta_2, \theta_3\} = \{30.00°, 51.79°, 64.16°\}$ and many other configurations, the phenomenon occurs. It is a real problem which cannot be ignored in real applications.

2.4 Conclusion

In this chapter, the configuration of CLAs is introduced. The two research orientations of DOA estimation with CLAs, namely difference coarray-based methods and subarray-based methods are discussed. The former exploits the difference coarray and tries to increase the number of consecutive lags in the virtual half-wavelength ULA such that the DOFs can be greatly increased. The latter treats the CLA as two sparse ULAs with large array aperture, and from each of them, high-precision but ambiguous DOA estimation is obtained, and then the ambiguities are eliminated according to the coprime property. In the following chapters, we focus on both the research directions. For the difference coarray-based methods, moving platform based CLAs are studied, and an improved configuration with much higher DOFs is proposed. Besides, to be more relevant to real applications, two dimensional coprime planar arrays are investigated. For the subarray-based methods, an ef-

ficient DOA estimation method is proposed, which can overcome the pair matching errors and grating angles problem successfully, achieving a reliable estimation performance.

CHAPITRE 3

MOVING PLATFORM BASED COPRIME LINEAR ARRAY CONFIGURATION

In the previous chapter, we have introduced the configuration of CLAs, as well as the two research orientations of DOA estimation in this domain. For the difference coarray-based methods, exhibiting more distinct lags, the difference coarray is usually applied for DOA estimation instead of the physical CLA to exploit higher DOFs. However, because of the existence of holes in the difference coarray and only the consecutive lags can be directly used to implement DOA estimation by high-resolution subspace based methods like MUSIC or ESPRIT, the achievable effective DOFs are not as high as expected. To solve this problem, many methods and configurations have been proposed to fill the holes and lengthen the consecutive part of the difference coarray. In [46], CLAs are generalized with two operations, by which two improved CLA configurations, namely coprime arrays with compressed inter-element spacing (CACIS) and coprime arrays with displaced subarrays (CADiS), are proposed. The CACIS configuration can be considered as a special case and forms a subset of the ECLAs introduced in Section 2.2.3, and CADiS can achieve a difference coarray with a much longer consecutive part by selecting appropriate parameters. In [47], the holes in the difference coarray are interpolated by nuclear norm minimization [89], allowing to use the remaining elements of the difference coarray and increase the number of detectable signals. In [51], an additional complementary subarray is added into an ECLA, resulting in a complete difference coarray without holes.

The above mentioned methods consider the CLAs based on fixed platform, and moving platform based CLAs have been studied in recent years [65–68]. It is shown that by shifting the CLA a half wavelength of incoming signals, where the source positions, incoming directions and signal temporal properties can be assumed to be constant, the majority or all holes in the difference coarray can be filled, generating then a difference coarray with more consecutive lags and increasing the effective DOFs. In this chapter, the moving platform base CLA configuration is introduced, and the resulting difference coarray is analyzed.

Then an improved CLA configuration for moving platform is proposed. By judiciously designing the sensor element positions, a difference coarray with much more consecutive lags and a higher effective DOFs can be obtained with the same number of sensors and the same length of array motion.

3.1 Signal model of moving coprime linear arrays

Consider a CLA composed of two subarrays having N and M sensor elements, with inter-element spacing Md and Nd respectively, where N and M are two coprime integers and $d = \frac{\lambda}{2}$. Without loss of generality, it is assumed that $M < N$. The sensor elements are located at positions $\{p_1 d, p_2 d, \cdots, p_L d\}$, where L is the total number of sensors, and because the first sensor is shared by the two subarrays and set as the reference point, there are $L = M + N - 1$ and $p_1 = 0$. The CLA is based on a platform moving along the array direction with a constant velocity v, and the DOAs of sources and signal temporal properties are assumed to be constant for a small array motion. FIGURE 3.1 shows the situation where $N = 5$ and $M = 4$.

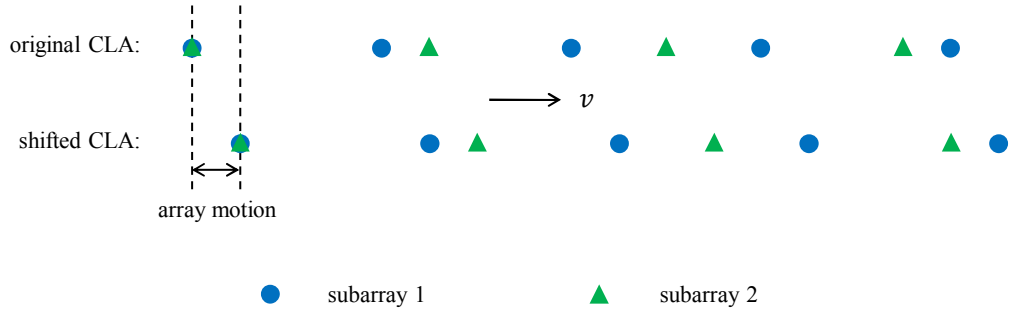

FIGURE 3.1 – Moving platform based CLA with $N = 5$ and $M = 4$

Suppose that there are K uncorrelated, far-field and narrowband signals impinging on the CLA from directions $\{\theta_1, \theta_2, \cdots, \theta_K\}$ respectively, with $-90^\circ < \theta_k < 90^\circ$ and $1 \leq k \leq K$. The observation of the CLA, at time t, can be expressed as

$$\mathbf{x}(t) = \mathbf{A}\mathbf{\Phi}\mathbf{s}(t) + \mathbf{n}(t) \tag{3.1}$$

where

$$\mathbf{A} = \begin{bmatrix} \mathbf{a}(\theta_1) & \mathbf{a}(\theta_2) & \cdots & \mathbf{a}(\theta_K) \end{bmatrix} \tag{3.2}$$

is the directional matrix of the CLA, with

$$\mathbf{a}\left(\theta_k\right) = \begin{bmatrix} 1 & e^{j2\pi \frac{p_2 d}{\lambda} \sin\theta_k} & \cdots & e^{j2\pi \frac{p_L d}{\lambda} \sin\theta_k} \end{bmatrix}^T \tag{3.3}$$

denoting the directional vector associated with the signal coming from θ_k. The movement of the array is indicated by

$$\mathbf{\Phi} = \mathrm{diag}\begin{bmatrix} e^{j2\pi \frac{vt}{\lambda} \sin\theta_1} & e^{j2\pi \frac{vt}{\lambda} \sin\theta_2} & \cdots & e^{j2\pi \frac{vt}{\lambda} \sin\theta_K} \end{bmatrix} \tag{3.4}$$

and

$$\mathbf{s}\left(t\right) = \begin{bmatrix} s_1\left(t\right) & s_2\left(t\right) & \cdots & s_K\left(t\right) \end{bmatrix}^T \tag{3.5}$$

represents the incoming signal vector with $s_k(t)$ the source signal coming from θ_k and received at the reference sensor. $\mathbf{n}(t)$, the white Gaussian noise vector with zero-mean and covariance matrix $\sigma^2\mathbf{I}_L$ with σ^2 the noise power, is supposed to be independent from the source signals.

At time $t+\tau$, the observation of the CLA becomes

$$\mathbf{x}\left(t+\tau\right) = \mathbf{B}\mathbf{\Phi}\mathbf{s}\left(t+\tau\right) + \mathbf{n}\left(t+\tau\right) \tag{3.6}$$

where

$$\mathbf{B} = \begin{bmatrix} \mathbf{b}\left(\theta_1\right) & \mathbf{b}\left(\theta_2\right) & \cdots & \mathbf{b}\left(\theta_K\right) \end{bmatrix} \tag{3.7}$$

and

$$\mathbf{b}\left(\theta_k\right) = \begin{bmatrix} e^{j2\pi \frac{v\tau}{\lambda} \sin\theta_k} & e^{j2\pi \frac{v\tau + p_2 d}{\lambda} \sin\theta_k} & \cdots & e^{j2\pi \frac{v\tau + p_L d}{\lambda} \sin\theta_k} \end{bmatrix}^T \tag{3.8}$$

denote the updated directional matrix and vector respectively. By setting $v\tau = d = \frac{\lambda}{2}$, there is

$$\mathbf{b}\left(\theta_k\right) = \begin{bmatrix} e^{j2\pi \frac{d}{\lambda} \sin\theta_k} & e^{j2\pi \frac{d + p_2 d}{\lambda} \sin\theta_k} & \cdots & e^{j2\pi \frac{d + p_L d}{\lambda} \sin\theta_k} \end{bmatrix}^T \tag{3.9}$$

For narrowband signals with carrier frequency f, there is

$$s_k\left(t+\tau\right) = e^{j2\pi f\tau} s_k\left(t\right) \tag{3.10}$$

and Equation (3.6) can be re-written as

$$\mathbf{x}\left(t+\tau\right) = e^{j2\pi f\tau}\mathbf{B}\mathbf{\Phi}\mathbf{s}\left(t\right) + \mathbf{n}\left(t+\tau\right) \tag{3.11}$$

Then using the phase factor compensating technique described in [90], we can get

$$\tilde{\mathbf{x}}(t+\tau) = e^{-j2\pi f\tau}\mathbf{x}(t+\tau) = \mathbf{B}\mathbf{\Phi}\mathbf{s}(t) + \tilde{\mathbf{n}}(t+\tau) \tag{3.12}$$

where

$$\tilde{\mathbf{n}}(t+\tau) = e^{-j2\pi f\tau}\mathbf{n}(t+\tau) \tag{3.13}$$

and by combining Equations (3.1) and (3.12), we can obtain the following equation

$$\mathbf{y}(t) = \begin{bmatrix} \mathbf{x}(t) \\ \tilde{\mathbf{x}}(t+\tau) \end{bmatrix} = \mathbf{A}_s\mathbf{s}_s(t) + \begin{bmatrix} \mathbf{n}(t) \\ \tilde{\mathbf{n}}(t+\tau) \end{bmatrix} \tag{3.14}$$

which can be regarded as the observation of the synthetic array composed of the original CLA and the shifted CLA after moving for a unit inter-element spacing d. $\mathbf{A}_s = \left[\mathbf{A}^T, \mathbf{B}^T\right]^T$ stands for the directional matrix of the synthetic array, and $\mathbf{s}_s(t) = \mathbf{\Phi}\mathbf{s}(t)$ is the equivalent incoming signal vector impinging on the synthetic array.

3.2 Difference coarray analysis

In this section, the difference coarray and the DOFs of the synthetic array are discussed. Taking d as unit, the sensor element positions of the original CLA and the shifted CLA can be given by

$$\mathbb{P}_o = \mathbb{P}_1 \cup \mathbb{P}_2 \tag{3.15}$$

$$\mathbb{P}_s = \mathbb{P}_{1'} \cup \mathbb{P}_{2'} \tag{3.16}$$

where

$$\mathbb{P}_1 = \{Mn \mid 0 \le n \le N-1\} \tag{3.17}$$

$$\mathbb{P}_2 = \{Nm \mid 0 \le m \le M-1\} \tag{3.18}$$

$$\mathbb{P}_{1'} = \{Mn+1 \mid 0 \le n \le N-1\} \tag{3.19}$$

$$\mathbb{P}_{2'} = \{Nm+1 \mid 0 \le m \le M-1\} \tag{3.20}$$

denote the positions of the sensor elements in each subarray, with subscripts 1 and 2 refer to the 1^{st} and 2^{nd} subarrays of the original CLA, and subscripts $1'$ and $2'$ refer to the 1^{st} and 2^{nd} subarrays of the shifted CLA respectively. And then the sensor positions of the synthetic

array can be expressed by

$$\mathbb{P}_{syn} = \mathbb{P}_o \cup \mathbb{P}_s \tag{3.21}$$

Based on the definition of the difference coarray shown in Equation (2.12), the difference coarray of the synthetic array is composed of the self-lags and cross-lags between all the subarrays of the original CLA and the shifted CLA. The set of self-lags is defined by

$$\mathbb{D}_{uu} = \{p - q \mid p, q \in \mathbb{P}_u\} \tag{3.22}$$

and the set of cross-lags is defined by

$$\mathbb{D}_{uv} = \mathbb{D}_{uv}^{+} \cup \mathbb{D}_{uv}^{-} \tag{3.23}$$

with

$$\mathbb{D}_{uv}^{+} = \{p - q \mid p \in \mathbb{P}_u, q \in \mathbb{P}_v\} \tag{3.24}$$

$$\mathbb{D}_{uv}^{-} = \{q - p \mid p \in \mathbb{P}_u, q \in \mathbb{P}_v\} \tag{3.25}$$

where $u, v \in \{1, 2, 1', 2'\}$ and $u \neq v$.

Because the sets of self-lags contain only the integer multiples of M or N, and the two subarrays of the original CLA or the shifted CLA share the first sensor, the self-lags can be considered as the cross-lags between every sensor of one subarray and the first sensor of the other subarray. Thus the self-lags form subsets of the cross-lags and do not affect the resulting difference coarray. Then the difference coarray of the synthetic array can be expressed as

$$\mathbb{D} = \mathbb{D}_{12} \cup \mathbb{D}_{11'} \cup \mathbb{D}_{12'} \cup \mathbb{D}_{21'} \cup \mathbb{D}_{22'} \cup \mathbb{D}_{1'2'} \tag{3.26}$$

with

$$\mathbb{D}_{12} = \{Mn - Nm\} \cup \{Nm - Mn\} \tag{3.27}$$

$$\mathbb{D}_{11'} = \{Mn - Mn' - 1\} \cup \{Mn' - Mn + 1\} \tag{3.28}$$

$$\mathbb{D}_{12'} = \{Mn - Nm' - 1\} \cup \{Nm' - Mn + 1\} \tag{3.29}$$

$$\mathbb{D}_{21'} = \{Nm - Mn' - 1\} \cup \{Mn' - Nm + 1\} \tag{3.30}$$

$$\mathbb{D}_{22'} = \{Nm - Nm' - 1\} \cup \{Nm' - Nm + 1\} \tag{3.31}$$

$$\mathbb{D}_{1'2'} = \{Mn' - Nm'\} \cup \{Nm' - Mn'\} \tag{3.32}$$

where m, n, m' and n' are four integers with $0 \leq m, m' \leq M-1$ and $0 \leq n, n' \leq N-1$.

From Equations (3.27) and (3.32), it can be seen that $\mathbb{D}_{12}$ and $\mathbb{D}_{1'2'}$ contain the same elements.

Then according to Equations (3.28) to (3.31), there are

$$\begin{aligned}\mathbb{D}_{11'} \cup \mathbb{D}_{22'} = &\{M(n-n')-1\} \cup \{M(n'-n)+1\} \cup \\ &\{N(m-m')-1\} \cup \{N(m'-m)+1\}\end{aligned} \tag{3.33}$$

$$\begin{aligned}\mathbb{D}_{12'} \cup \mathbb{D}_{21'} = &\{Mn-Nm'-1\} \cup \{Nm-Mn'-1\} \cup \\ &\{Nm'-Mn+1\} \cup \{Mn'-Nm+1\}\end{aligned} \tag{3.34}$$

When $m = m' = 0$, Equation (3.34) can be re-written as

$$\mathbb{D}_{12'} \cup \mathbb{D}_{21'} = \{Mn-1\} \cup \{-Mn'-1\} \cup \{-Mn+1\} \cup \{Mn'+1\} \tag{3.35}$$

Because $0 \leq n, n' \leq N-1$, there are

$$\{Mn-1\} \cup \{-Mn'-1\} = \{M(n-n')-1\} \tag{3.36}$$

$$\{-Mn+1\} \cup \{Mn'+1\} = \{M(n'-n)+1\} \tag{3.37}$$

and Equation (3.35) can be written as

$$\mathbb{D}_{12'} \cup \mathbb{D}_{21'} = \{M(n-n')-1\} \cup \{M(n'-n)+1\} \tag{3.38}$$

Similarly, when $n = n' = 0$, Equation (3.34) can be re-written as

$$\mathbb{D}_{12'} \cup \mathbb{D}_{21'} = \{-Nm'-1\} \cup \{Nm-1\} \cup \{Nm'+1\} \cup \{-Nm+1\} \tag{3.39}$$

and because $0 \leq m, m' \leq M-1$, there are

$$\{-Nm'-1\} \cup \{Nm-1\} = \{N(m-m')-1\} \tag{3.40}$$

$$\{Nm'+1\} \cup \{-Nm+1\} = \{N(m'-m)+1\} \tag{3.41}$$

and then Equation (3.35) can be written as

$$\mathbb{D}_{12'} \cup \mathbb{D}_{21'} = \{N(m-m')-1\} \cup \{N(m'-m)+1\} \tag{3.42}$$

Based on Equations (3.33), (3.38) and (3.42), it can be seen that $\mathbb{D}_{11'} \cup \mathbb{D}_{22'}$ forms a subset of $\mathbb{D}_{12'} \cup \mathbb{D}_{21'}$, and the difference coarray of the CLA after motion can be simplified as

$$\mathbb{D} = \mathbb{D}_{12} \cup \mathbb{D}_{12'} \cup \mathbb{D}_{21'} \tag{3.43}$$

According to Equations (3.29) and (3.30), it is easy to see that by exchanging the combinations of the subsets, $\mathbb{D}_{12'} \cup \mathbb{D}_{21'}$ can be transferred to $\mathbb{D}^{'}_{12'} \cup \mathbb{D}^{'}_{21'}$, where

$$\mathbb{D}^{'}_{12'} = \{Mn - Nm' - 1\} \cup \{Nm - Mn' - 1\} \tag{3.44}$$
$$\mathbb{D}^{'}_{21'} = \{Mn' - Nm + 1\} \cup \{Nm' - Mn + 1\} \tag{3.45}$$

According to the values of m, n, m' and n', $\mathbb{D}^{'}_{12'}$ and $\mathbb{D}^{'}_{21'}$ are equivalent to $\mathbb{D}^{L}_{12}$ and $\mathbb{D}^{R}_{12}$ respectively, with

$$\mathbb{D}^{L}_{12} = \{Mn - Nm - 1\} \cup \{Nm - Mn - 1\} \tag{3.46}$$
$$\mathbb{D}^{R}_{12} = \{Mn - Nm + 1\} \cup \{Nm - Mn + 1\} \tag{3.47}$$

which can be regarded as the difference coarray of the original CLA shifting one lag to the left and one lag to the right respectively.

Therefore the final difference coarray of the CLA after array motion can be given by

$$\mathbb{D} = \mathbb{D}_{12} \cup \mathbb{D}^{L}_{12} \cup \mathbb{D}^{R}_{12} \tag{3.48}$$

which can be regarded as the union of the difference coarray of the original CLA and its two shifted versions. Consequently, the neighboring holes of each lag in the difference coarray of the original CLA can be filled due to the array motion, lengthening the consecutive part and increasing the effective DOFs [65, 66].

Consider the moving platform based CLA shown in FIGURE 3.1, FIGURE 3.2 and FIGURE 3.3 show the difference coarrays of the CLA before and after motion respectively. It can be seen that thanks to the array motion, the holes are filled by their neighboring lags, resulting in a hole-free difference coarray, and also two additional lags are obtained at the two ends of the difference coarray.

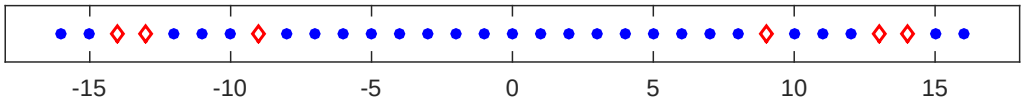

FIGURE 3.2 – Difference coarray of the CLA with $N = 5$ and $M = 4$ before array motion

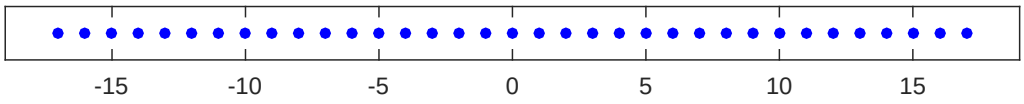

FIGURE 3.3 – Difference coarray of the CLA with $N = 5$ and $M = 4$ after array motion

Meanwhile, since the difference coarray of the original CLA shifts to the left or right for only one lag, if there are three or more consecutive holes in the difference coarray of the original CLA, only the holes having neighboring lags can be filled, and the others would be remained unfilled because such holes do not have lags at their neighboring positions. Consider a moving platform based CLA with $N = 6$ and $M = 5$, the difference coarrays of the CLA before and after array motion are shown in FIGURE 3.4 and FIGURE 3.5 respectively. It can be seen that there are two symmetric sets of three consecutive holes in the difference coarray of the original CLA $\{x \mid x = \pm 21, \pm 22, \pm 23\}$, leaving two holes unfilled in the difference coarray of the synthetic array $\{x \mid x = \pm 22\}$ after array motion.

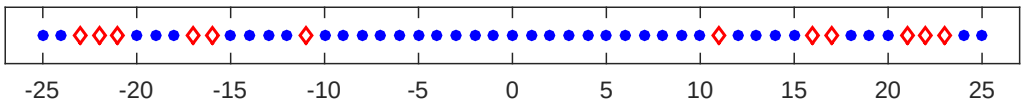

FIGURE 3.4 – Difference coarray of the CLA with $N = 6$ and $M = 5$ before array motion

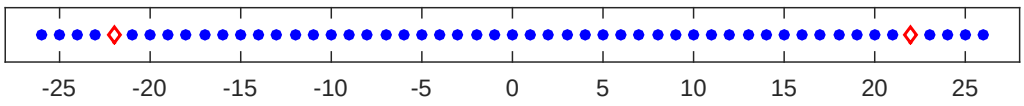

FIGURE 3.5 – Difference coarray of the CLA with $N = 6$ and $M = 5$ after array motion

Even if the resulting difference coarray of the synthetic array after motion is not always complete, the number of consecutive lags increases significantly with array motion, which is at most $2M(N-1)+3$ when the resulting difference coarray after motion is hole-free.

However, it can be noticed that only the lags which are neighbors of holes (e.g. $\{x \mid x = \pm 8, \pm 10, \pm 12, \pm 15\}$ in FIGURE 3.2) are used to fill the holes, For the consecutive lags without neighboring holes (e.g. $\{x \mid -7 \leq x \leq 7\}$ in FIGURE 3.2), the shifts of them generate lags which already exist in the difference coarray of the original CLA before array motion. Without generating new lags, such lags do not contribute to the increase of the DOFs by array motion.

In the next section, an improved configuration of moving platform based CLA is proposed, in which all the lags can be utilized to fill holes by array motion, such that more consecutive lags as well as higher effective DOFs can be obtained.

3.3 Improved coprime linear arrays for moving platform

3.3.1 Improved array configuration

Assume that M can be expressed as a product of two positive integers l and M' as

$$M = lM' \tag{3.49}$$

where $2 \leq l \leq M$. It is easy to see that M' and N are also coprime because M and N do not have common factors expect '1'. We compress the inter-element spacing of the subarray with N sensor elements from Md to $M'd$, then the resulting CLA turns out a CACIS in [46] with sensor numbers of the two subarrays N and M respectively with the compression factor l, or an ECLA of a prototype CLA with sensor numbers of the two subarrays N and M'. According to the discussion in Section 2.2.3, the difference coarray of the resulting CLA has a consecutive part with $2MN - 2\frac{M}{l}(N-1) - 1$ lags in the range of $[-MN + \frac{M}{l}(N-1) + 1, MN - \frac{M}{l}(N-1) - 1]$. Consider the CLA with $N = 5$ and $M = 4$ shown in FIGURE 3.1, by choosing $l = 2$, the resulting CLA configuration and the corresponding difference coarray after the inter-element spacing compression are shown in FIGURE 3.6 and FIGURE 3.7 respectively.

In order to use the lags in the consecutive part without neighboring holes by array motion, we lengthen the inter-element spacing of both the subarrays three times, from $M'd$ and Nd to $3M'd$ and $3Nd$ respectively. For the CLA shown in FIGURE 3.6, the redesigned CLA with lengthened inter-element spacing is shown in FIGURE 3.8.

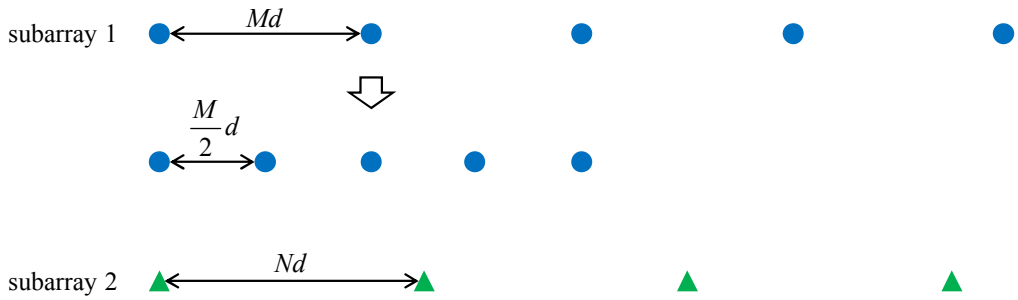

FIGURE 3.6 – Inter-element spacing compression of CLA with $N = 5$, $M = 4$ and $l = 2$

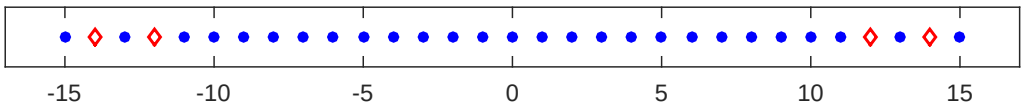

FIGURE 3.7 – Difference coarray of the inter-element spacing compressed CLA with $N = 5$, $M = 4$ and $l = 2$

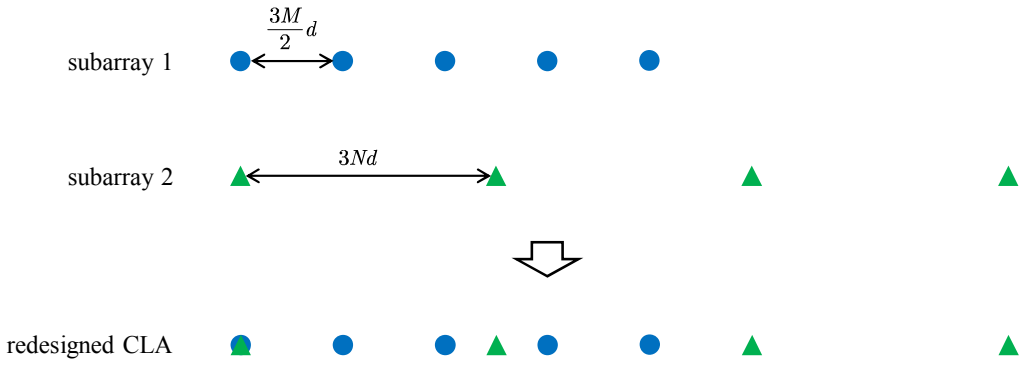

FIGURE 3.8 – Redesigned CLA with $N = 5$, $M = 4$ and $l = 2$

Consequently, according to the definition of the difference coarray shown in Equation (2.12), the positions of the lags in the new difference coarray are also enlarged three times, such that in the range of $[-3MN+\frac{3M}{l}(N-1)+3, 3MN-\frac{3M}{l}(N-1)-3]$, lags are uniformly distributed, and every two adjacent lags are exactly separated by two holes, which are generated by the lengthening of the inter-element spacing. Then for the lags in such range, the shifts of them with one lag to the left and one lag to the right generate new lags which do not exist in the difference coarray before array motion, filling their neighboring holes and generating a longer consecutive part. For the redesigned CLA shown in FIGURE 3.8, the corresponding difference coarrays before and after array motion are shown in FI-

GURE 3.9 and FIGURE 3.10 respectively. It can be seen that compared with the difference coarray associated with the original CLA configuration after array motion shown in FIGURE 3.3, by judiciously designing the sensor positions, a difference coarray with more consecutive lags can be obtained with the same number of sensors and the same length of array motion.

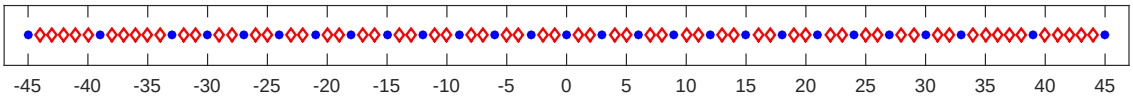

FIGURE 3.9 – Difference coarray of the redesigned CLA with $N = 5$, $M = 4$ and $l = 2$ before array motion

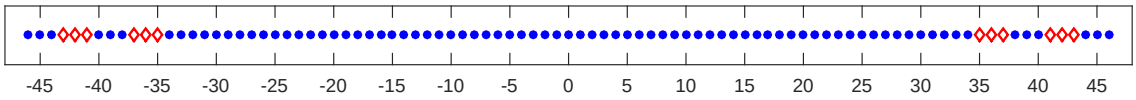

FIGURE 3.10 – Difference coarray of the redesigned CLA with $N = 5$, $M = 4$ and $l = 2$ after array motion

3.3.2 DOFs comparison

For the original moving platform based CLA configuration, we can obtain a difference coarray with at most $2M(N-1)+3$ consecutive lags after array motion. For the proposed configuration, although the final differencce coarray after array motion is not complete, it has a longer consecutive part in the range of $[-3MN + \frac{3M}{l}(N-1) + 2, 3MN - \frac{3M}{l}(N-1) - 2]$ with totally $6MN - \frac{6M}{l}(N-1) - 3$ consecutive lags, which gets the minimum when $l = 2$, being always larger than the number of the consecutive lags in the difference coarray of the original CLA configuration even when the latter is hole-free. Therefore, the proposed CLA configuration can significantly increase the effective DOFs with the same number of sensor elements and the same length of array motion. Table 3.1 shows the comparison of the numbers of the consecutive lags in the final difference coarrays of the original and proposed CLA configurations with different values of M and N.

TABLE 3.1 – Numbers of consecutive lags comparison

	(M, N)	l	consecutive lags numbers
original CLA configuration	$(4, 5)$		35
	$(5, 6)$		43
	$(4, 7)$		51
	$(5, 8)$		73
proposed CLA configuration	(M, N)	l	consecutive lags numbers
	$(4, 5)$	2	69
		4	93
	$(5, 6)$	5	147
	$(4, 7)$	2	93
		4	129
	$(5, 8)$	5	195

To show the benefit of the proposed moving platform based CLA configuration in terms of DOFs increasing, the MUSIC method is applied to perform DOA estimation on an original CLA with $N = 5$ and $M = 4$ shown in FIGURE 3.1, and a redesigned CLA with the same number of sensors and $l = 2$ shown in FIGURE 3.8 respectively. For the original CLA configuration, a difference coarray with 35 consecutive lags is obtained after the array motion with a length of $\frac{\lambda}{2}$. After the step of spatial smoothing, which is introduced in Section 2.2.2, a rank restored covariance matrix with dimension of 18×18 is obtained, and since at least one eigenvector spanning the noise subspace is needed such that MUSIC algorithm can be performed, up to 17 signals can be detected. FIGURE 3.11 depicts the DOA estimation result of the original configuration with 17 sources uniformly distributed from $-56°$ to $56°$, where SNR and the number of snapshots are 10dB and 2000 respectively. For the proposed CLA configuration, a difference coarray with 69 consecutive lags is obtained after the array motion with the same length, therefore a rank restored covariance matrix with dimension 35×35 is obtained, and up to 34 signals can be detected. With the same simulation conditions, FIGURE 3.12 depicts the DOA estimation result of the proposed configuration with 25 sources uniformly distributed from $-60°$ to $60°$. And the original

CLA configuration cannot work in such situation because the number of sources exceeds the number of DOFs.

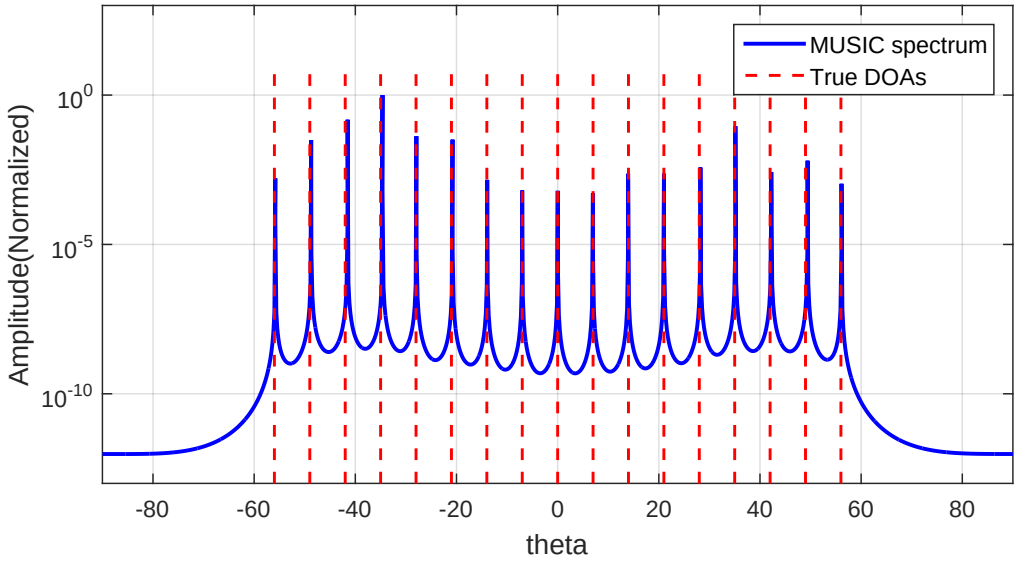

FIGURE 3.11 – MUSIC spectrum of the original CLA configuration

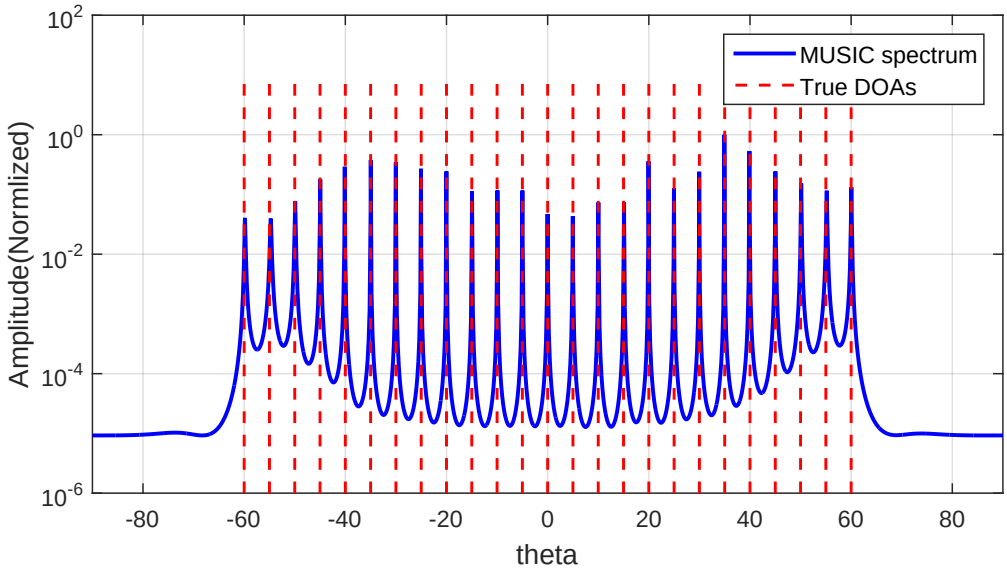

FIGURE 3.12 – MUSIC spectrum of the proposed CLA configuration

3.4 Conclusion

In this chapter, moving platform based CLA configuration is discussed. It is shown that due to such array motion, the resulting difference coarray can be regarded as the union of the difference coarray of the original CLA and its two shifted versions with one lag to the left and one lag to the right respectively, such that neighboring holes of each lag can be filled, generating then a difference coarray with more consecutive lags and increasing the effective DOFs. However, only the lags which are the neighbors of holes are utilized to fill the holes, but for the lags in the consecutive part without neighboring holes, the shifts of them generate lags already existing in the difference coarray of the original CLA, contributing negligibly to the resulting difference coarray and the DOFs. To address this issue, an improved CLA configuration for moving platform is proposed in this chapter. By judiciously designing the sensor element positions, a lengthened difference coarray with controlled hole positions is obtained, such that all lags can be utilized to fill the holes by array motion. Compared with the original CLAs, the proposed configuration can achieve a difference coarray with much more consecutive lags and higher DOFs with the same number of sensors and the same length of array motion. Contrary to [91], which discusses nested arrays, our proposition is dedicated to CLAs, being more suitable for practical applications because of the limited mutual coupling effect property.

CHAPITRE 4

DIFFERENCE COARRAY OF COPRIME PLANAR ARRAYS

CLAs have drawn lots of attention thanks to their high DOFs. However, since there are holes existing in the difference coarray, the effective DOFs are not as high as expected. The strategic point in filling the holes and increasing the effective DOFs is to find the exact expressions of the hole locations. Lots of effort have been made to address this issue, filling the holes in the difference coarray and increasing the DOFs.

Compared with one dimensional (1D) linear arrays, two dimensional (2D) planar arrays are more relevant to real applications. There are many research studies developed for 2D coprime planar arrays (CPAs). In [73] and [74], a CPA is treated as two uniform planar subarrays, which simplifies the system model, but leads to a significant loss of DOFs. In [75], the CPA geometry is generalized, resulting in higher DOFs than [73] and [74] with the same number of sensor elements. However, it also deals with the subarrays and the significant advantage in terms of DOFs is sacrificed. In order to exploit the high DOFs offered by the coprime geometry, the difference coarrays should be applied instead of the physical arrays. However, due to the existence of holes, the consecutiveness of the difference coarray of CPAs is highly limited, which significantly reduces the number of effective DOFs. Unfortunately, no closed-form expressions for the hole locations in the difference coarrays of CPAs have been found in the open literature, which rises the major challenge in holes-filling and DOFs-increasing for CPAs.

Compared with other existing 2D sparse array configurations [92–95], CPAs are more attractive because of their limited mutual coupling effect property. To offer a better understanding of CPAs and facilitate the future research in this field, in this chapter, CPAs are investigated from the perspective of difference coarrays. Closed-form expressions of the exact hole locations are derived, based on which an efficient method is proposed to fill the most critical holes, such that a difference coarray with more consecutive lags can be generated and higher effective DOFs can be obtained.

4.1 System model of coprime planar arrays

4.1.1 Signal model

A conventional CPA consists of two uniform sparse square subarrays. The 1^{st} subarray has $N \times N$ sensor elements with inter-element spacing Md, and the 2^{nd} subarray has $M \times M$ sensor elements with inter-element spacing Nd, where M, N are two coprime integers and $d = \frac{\lambda}{2}$. The locations of the sensor elements of the CPA can be expressed as :

$$\mathbb{P} = \mathbb{P}_1 \cup \mathbb{P}_2 \tag{4.1}$$

with

$$\mathbb{P}_1 = \{(n_1 Md, n_2 Md) \mid 0 \leq n_1, n_2 \leq N-1\} \tag{4.2}$$

$$\mathbb{P}_2 = \{(m_1 Nd, m_2 Nd) \mid 0 \leq m_1, m_2 \leq M-1\} \tag{4.3}$$

denoting the sensor element locations of the two subarrays respectively. Without loss of generality, it is assumed that $M < N$. FIGURE 4.1 shows a CPA located in $X - Z$ plane with $N = 5$ and $M = 3$. The sensor located at $(0, 0)$ is shared by the two subarrays and set as the reference point. The total number of sensor elements $L = N^2 + M^2 - 1$.

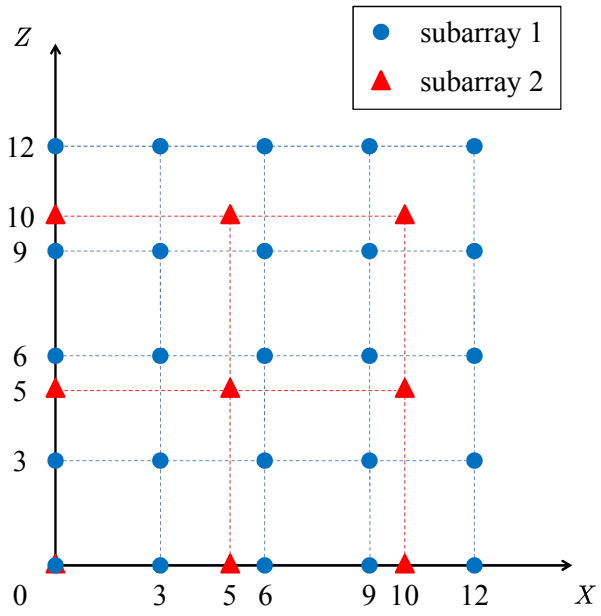

FIGURE 4.1 – Coprime planar array with $N = 5$ and $M = 3$

Suppose that there are K uncorrelated, far-field and narrowband signals impinging on the CPA from directions $\{(\theta_1, \varphi_1), (\theta_2, \varphi_2), \cdots, (\theta_K, \varphi_K)\}$, with θ_k and φ_k denoting the elevation and azimuth angles respectively of the k^{th} source and $1 \leq k \leq K$. The signal observed at the sensor element located at $\mathbf{p}_u$, where $\mathbf{p}_u = (p_{u,x}d, p_{u,z}d) \in \mathbb{P}$, can be expressed by

$$x_u(t) = \sum_{k=1}^{K} a_u(\theta_k, \varphi_k) s_k(t) + n_u(t) \tag{4.4}$$

where $s_k(t)$ denotes the impinging signal coming from (θ_k, φ_k) and received at the reference point, and $n_u(t)$ denotes the noise received at the sensor and it is assumed to be Gaussian white and independent from the source signals. $a_u(\theta_k, \varphi_k) = e^{j\pi(p_{u,x}\sin\theta_k\cos\varphi_k + p_{u,z}\cos\varphi_k)}$ represents the phase shift between the sensor elements located at $\mathbf{p}_u$ and the reference point associated with $s_k(t)$. Then the signal vector received by the CPA can be written as

$$\mathbf{x}(t) = \begin{bmatrix} x_1(t) & x_2(t) & \cdots & x_L(t) \end{bmatrix}^T \tag{4.5}$$

4.1.2 2D difference coarray

Similar with the definition given in Equation (2.12), the difference coarray of a CPA is defined as

$$\mathbb{D} = \{\mathbf{p}_u - \mathbf{p}_v \mid \mathbf{p}_u, \mathbf{p}_v \in \mathbb{P}\} \tag{4.6}$$

of which the elements are generated by all pairs of sensor elements in the CPA, and the observation of all the lags can be obtained from the covariance matrix of the signal received by the physical array.

The difference coarray of the CPA shown in FIGURE 4.1 is depicted in FIGURE 4.2, where the lags and holes are represented by blue dots and red rhombuses respectively as the previous chapters. It can be seen that the difference coarray exhibits a virtual planar array with much more distinct lags than the number of physical sensors in the CPA, possessing much higher DOFs. However, because of the necessity of the rank restoration for the implementation of DOA estimation with high-resolution subspace based methods, only the consecutive part in the difference coarray can be applied directly, and due to the existence of holes, the consecutiveness of the difference coarray is limited, and the achievable effective DOFs for subspace based DOA estimation methods like MUSIC are not as high as expected.

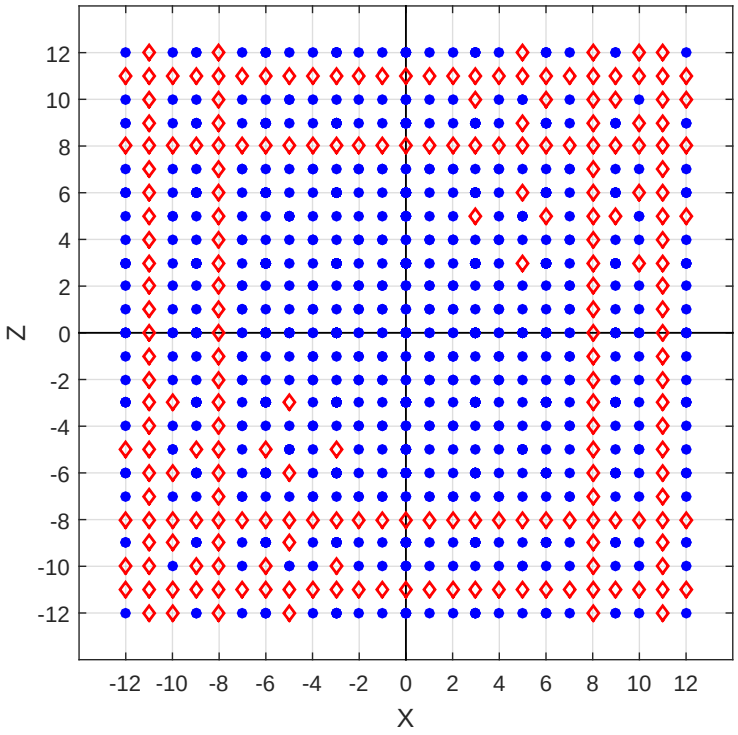

FIGURE 4.2 – Difference coarray of the CPA with $N = 5$ and $M = 3$

4.2 Holes locations in 2D difference coarray

According to the definition of the difference coarray shown in Equation (4.6), the difference coarray $\mathbb{D}$ of a CPA can be rewritten as

$$\mathbb{D} = \mathbb{D}_{12}^{+} \cup \mathbb{D}_{12}^{-} \cup \mathbb{D}_{11} \cup \mathbb{D}_{22} \tag{4.7}$$

where $\mathbb{D}_{12}^{+}$ and $\mathbb{D}_{12}^{-}$ denote the cross difference coarrays of the two subarrays with

$$\mathbb{D}_{12}^{+} = \{\mathbf{p}_u - \mathbf{p}_v \mid \mathbf{p}_u \in \mathbb{P}_1, \mathbf{p}_v \in \mathbb{P}_2\} \tag{4.8}$$

$$\mathbb{D}_{12}^{-} = \{\mathbf{p}_v - \mathbf{p}_u \mid \mathbf{p}_u \in \mathbb{P}_1, \mathbf{p}_v \in \mathbb{P}_2\} \tag{4.9}$$

and $\mathbb{D}_{11}$ and $\mathbb{D}_{22}$ denote the self difference coarrays of the two subarrays with

$$\mathbb{D}_{11} = \{\mathbf{p}_u - \mathbf{p}_v \mid \mathbf{p}_u, \mathbf{p}_v \in \mathbb{P}_1\} \tag{4.10}$$

$$\mathbb{D}_{22} = \{\mathbf{p}_u - \mathbf{p}_v \mid \mathbf{p}_u, \mathbf{p}_v \in \mathbb{P}_2\} \tag{4.11}$$

We first discuss the characteristics of the cross difference coarray $\mathbb{D}_{12}^{+}$. Taking d as the unit, $\mathbb{D}_{12}^{+}$ can be expressed as

$$\begin{aligned}\mathbb{D}_{12}^{+} =&\{(n_1M - m_1N, n_2M - m_2N) \mid \\ &0 \le n_1, n_2 \le N-1, 0 \le m_1, m_2 \le M-1\}\end{aligned} \tag{4.12}$$

According to the values of n_1, n_2, m_1 and m_2, it is easy to see that $\mathbb{D}_{12}^{+}$ is located in the range of $\{(x,z) \mid -(M-1)\,N \le x, z \le (N-1)\,M\}$.

In the following, the locations of the holes in $\mathbb{D}_{12}^{+}$ will be provided with detailed proof. Four general rules can be summarized as :

1) In $\{(x,z) \mid 0 \le x \le (N-1)\,M, -(M-1)\,N \le z \le (N-1)\,M\}$, the position (x,z) would be a hole for any z in such range if $x = aM + bN$ with $a \ge 0$, $b \ge 1$;
2) In $\{(x,z) \mid -(M-1)\,N \le x \le 0, -(M-1)\,N \le z \le (N-1)\,M\}$, the position (x,z) would be a hole for any z in such range if $x = aM + bN$ with $a \le -1$, $b \le 0$;
3) In $\{(x,z) \mid -(M-1)\,N \le x \le (N-1)\,M, 0 \le z \le (N-1)\,M\}$, the position (x,z) would be a hole for any x in such range if $z = aM + bN$ with $a \ge 0$, $b \ge 1$;
4) In $\{(x,z) \mid -(M-1)\,N \le x \le (N-1)\,M, -(M-1)\,N \le z \le 0\}$, the position (x,y) would be a hole for any x in such range if $z = aM + bN$ with $a \le -1$, $b \le 0$.

The proof of rule 1) is given in the following.

Based on [51], for any integer I in the range of $[0, (N-1)M]$, we can always find two integers a_0 and b_0, such that

$$I = a_0M + b_0N \tag{4.13}$$

Let $b' = b_0 \bmod M$, and there is

$$b_0 = tM + b' \tag{4.14}$$

where t is a non-negative integer and $b' \in [0, M-1]$. Then we can get

$$I = a'M + b'N \tag{4.15}$$

with $a' = a_0 + tN$, $b' = b_0 - tM$, and $\lceil -b'\frac{N}{M} \rceil \le a' \le N - 1 - \lceil -b'\frac{N}{M} \rceil$.

Then according to Equation (4.12), it can be seen that to prove rule 1), it is sufficient and necessary to prove that for any $I \in [0, (N-1)M]$ and in the form of $I = a'M + b'N$ with $a' \ge 0$ and $b' \ge 1$, there never exist n_1 and m_1, with $0 \le n_1 \le N-1$ and $0 \le m_1 \le M-1$,

satisfying

$$n_1 M - m_1 N = I = a'M + b'N \tag{4.16}$$

and for any $I \in [0, (N-1)M]$ and out of the form of $I = a'M + b'N$ with $a' \geq 0$ and $b' \geq 1$, there always exist n_1 and m_1, with $0 \leq n_1 \leq N-1$ and $0 \leq m_1 \leq M-1$, satisfying the above equation.

According to the values range of a' and b', the problem can be split into three cases :

i) $0 \leq a' \leq N-1, b' = 0$;

ii) $\lceil \frac{N}{M} \rceil - N \leq a' < 0, 0 < b' \leq M-1$;

iii) $0 \leq a' \leq N-1, 0 < b' \leq M-1$.

For i), Equation (4.16) can be written as

$$(n_1 - a')M = m_1 N \tag{4.17}$$

Since

$$\begin{cases} 0 \leq a' \leq N-1 \\ b' = 0 \end{cases} \tag{4.18}$$

and

$$\begin{cases} 0 \leq n_1 \leq N-1 \\ 0 \leq m_1 \leq M-1 \end{cases} \tag{4.19}$$

for any a' in this case, there always exist $n_1 = a'$ and $m_1 = 0$ satisfying Equation (4.17). Therefore, the positions corresponding to such a' and b' are not holes.

For ii), noticing that $m_1 + b' \geq 1$, Equation (4.16) can be written as

$$\frac{N}{M} = \frac{n_1 - a'}{m_1 + b'} \tag{4.20}$$

Since

$$\begin{cases} \lceil \frac{N}{M} \rceil - N \leq a' < 0 \\ 0 < b' \leq M-1 \end{cases} \tag{4.21}$$

and

$$\begin{cases} 0 \leq n_1 \leq N-1 \\ 0 \leq m_1 \leq M-1 \end{cases} \tag{4.22}$$

for any a' and b' in this case, there always exist n_1 and m_1, exhibiting

$$\begin{cases} n_1 - a' = N \\ m_1 + b' = M \end{cases} \tag{4.23}$$

and satisfying Equation (4.20). Therefore, the positions corresponding to such a' and b' are not holes.

For iii), similar with ii), Equation (4.16) can be written as Equation (4.20). Considering that M and N are two coprime integers, $(n_1 - a')$ and $(m_1 + b')$ should exactly equal to N and M respectively. Since

$$\begin{cases} 0 \leq a' \leq N-1 \\ 0 \leq n_1 \leq N-1 \end{cases} \tag{4.24}$$

for any a' in this case, we cannot find n_1 such that $n_1 - a' = N$. Therefore, the positions corresponding to such a' and b' are holes.

The proof of rule 1) ends, and the proof of the other three is similar and omitted here.

Then, we focus on the characteristics of the other cross difference coarray $\mathbb{D}_{12}^{-}$, which can be expressed as

$$\begin{aligned} \mathbb{D}_{12}^{-} = &\{(m_1 N - n_1 M, m_2 N - n_2 M) \mid \\ &0 \leq n_1, n_2 \leq N-1, 0 \leq m_1, m_2 \leq M-1\} \end{aligned} \tag{4.25}$$

and it is easy to see that $\mathbb{D}_{12}^{-}$ is located in the range of $\{(x,z) \mid -(N-1)M \leq x, z \leq (M-1)N\}$, and four similar general rules of the holes in $\mathbb{D}_{12}^{-}$ can be obtained as follows :

5) In $\{(x,z) \mid 0 \leq x \leq (M-1)N, -(N-1)M \leq z \leq (M-1)N\}$, the position (x,z) would be a hole for any z in such range if $x = aM + bN$ with $a \geq 1, b \geq 0$;

6) In $\{(x,z) \mid -(N-1)M \leq x \leq 0, -(N-1)M \leq z \leq (M-1)N\}$, the position (x,z) would be a hole for any z in such range if $x = aM + bN$ with $a \leq 0, b \leq -1$;

7) In $\{(x,z) \mid -(N-1)M \leq x \leq (M-1)N, 0 \leq z \leq (M-1)N\}$, the position (x,z) would be a hole for any x in such range if $z = aM + bN$ with $a \geq 1, b \geq 0$;

8) In $\{(x,z) \mid -(N-1)M \leq x \leq (M-1)N, -(N-1)M \leq z \leq 0\}$, the position (x,z) would be a hole for any x in such range if $z = aM + bN$ with $a \leq 0, b \leq -1$.

FIGURE 4.3 and FIGURE 4.4 depict the cross difference coarrays $\mathbb{D}_{12}^{+}$ and $\mathbb{D}_{12}^{-}$ of the CPA shown in FIGURE 4.1 respectively, supporting the above analysis.

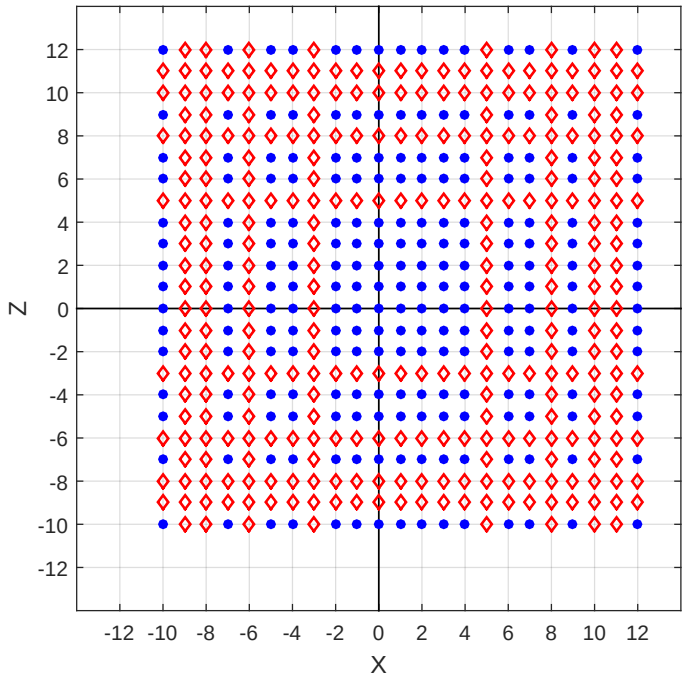

FIGURE 4.3 – Cross difference coarray $\mathbb{D}_{12}^{+}$ of the CPA with $N = 5$ and $M = 3$

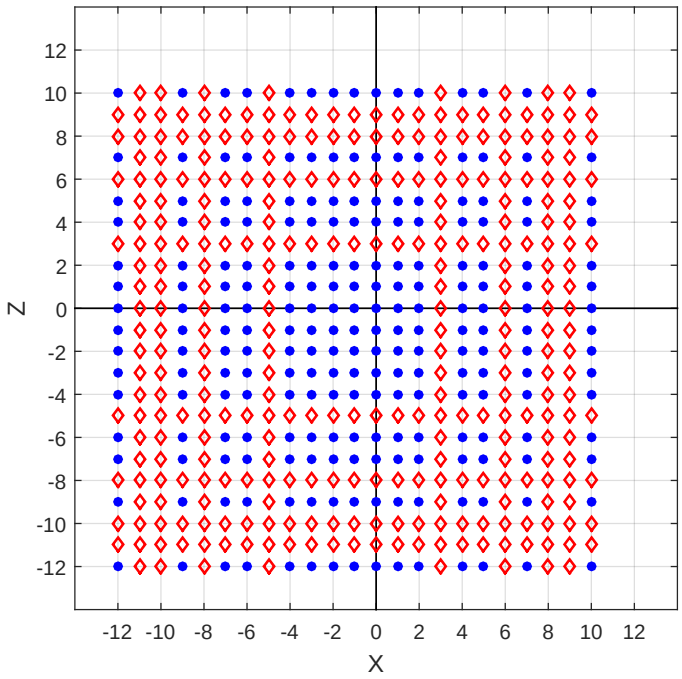

FIGURE 4.4 – Cross difference coarray $\mathbb{D}_{12}^{-}$ of the CPA with $N = 5$ and $M = 3$

Consider the two self difference coarrays $\mathbb{D}_{11}$ and $\mathbb{D}_{22}$, which according to Equations (4.10) and (4.11) can be expressed as

$$\begin{aligned}\mathbb{D}_{11} =&\{(n_{11}M - n_{12}M, n_{21}M - n_{22}M) \mid \\ &0 \leq n_{11}, n_{12}, n_{21}, n_{22} \leq N-1\}\end{aligned} \tag{4.26}$$

$$\begin{aligned}\mathbb{D}_{22} =&\{(m_{11}N - m_{12}N, m_{21}N - m_{22}N) \mid \\ &\leq m_{11}, m_{12}, m_{21}, m_{22} \leq M-1\}\end{aligned} \tag{4.27}$$

and be deduced as

$$\mathbb{D}_{11} = \{(aM, bM) \mid -(N-1) \leq a, b \leq (N-1)\} \tag{4.28}$$

$$\mathbb{D}_{22} = \{(aN, bN) \mid -(M-1) \leq a, b \leq (M-1)\} \tag{4.29}$$

The lags in the self difference coarrays $\mathbb{D}_{11}$ and $\mathbb{D}_{22}$ of the CPA shown in FIGURE 4.1 are depicted in FIGURE 4.5 and FIGURE 4.6 respectively.

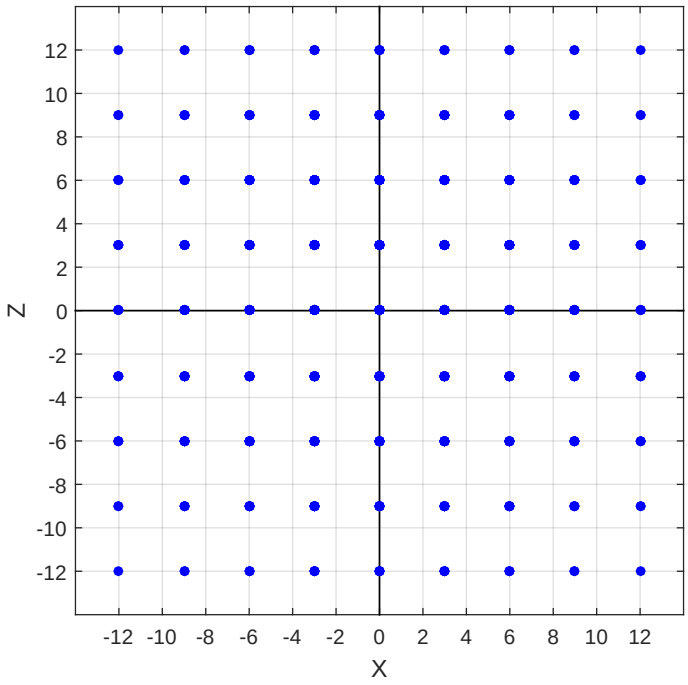

FIGURE 4.5 – Self difference coarray $\mathbb{D}_{11}$ of the CPA with $N = 5$ and $M = 3$

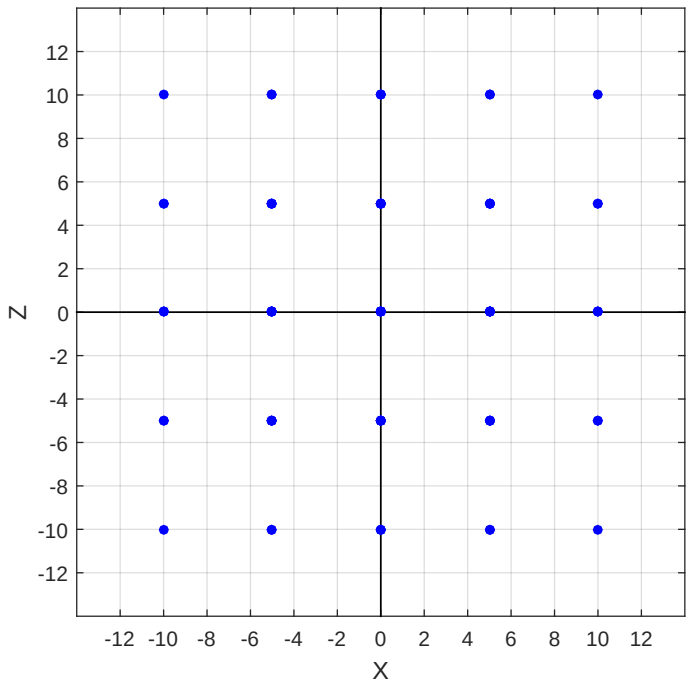

FIGURE 4.6 – Self difference coarray $\mathbb{D}_{22}$ of the CPA with $N = 5$ and $M = 3$

According to Equation (4.7), some holes in the cross difference coarrays $\mathbb{D}_{12}^{+}$ and $\mathbb{D}_{12}^{-}$ are filled by the lags in the self difference coarrays $\mathbb{D}_{11}$ and $\mathbb{D}_{22}$; and with rules 1) — 8), the precise expressions of the holes locations in the difference coarray $\mathbb{D}$ in the 1$^{\text{st}}$ quadrant $\mathbb{H}_1$ and 2$^{\text{nd}}$ quadrant $\mathbb{H}_2$ can be obtained as

$$\mathbb{H}_1 = \mathbb{H}_{11} \cup \mathbb{H}_{12} \cup \mathbb{H}_{13} \cup \mathbb{H}_{14} \tag{4.30}$$

$$\mathbb{H}_2 = \mathbb{H}_{21} \cup \mathbb{H}_{22} \tag{4.31}$$

with

$$\begin{aligned} \mathbb{H}_{11} = \{(x,z) \,|x = aM + bN, a \geq 1, b \geq 1, \\ 0 \leq x, z \leq (N-1)M\} \end{aligned} \tag{4.32}$$

$$\begin{aligned} \mathbb{H}_{12} = \{(x,z) \,|x = aN, z = bM, a \geq 1, b \geq 1, \\ 0 \leq x, z \leq (N-1)M\} \end{aligned} \tag{4.33}$$

$$\mathbb{H}_{13} = \{(x,z) \,|x = aM, z = bN, a \geq 1, b \geq 1, \\ 0 \leq x, z \leq (N-1)M\} \tag{4.34}$$

$$\mathbb{H}_{14} = \{(x,z) \,|z = aM + bN, a \geq 1, b \geq 1, \\ 0 \leq x, z \leq (N-1)M\} \tag{4.35}$$

and

$$\mathbb{H}_{21} = \{(x,z) \,|x = aM + bN, a \leq -1, b \leq -1, \\ -(N-1)M \leq x \leq 0, 0 \leq z \leq (N-1)M\} \tag{4.36}$$

$$\mathbb{H}_{22} = \{(x,z) \,|z = aM + bN, a \geq 1, b \geq 1, \\ -(N-1)M \leq x \leq 0, 0 \leq z \leq (N-1)M\} \tag{4.37}$$

According to the definition of $\mathbb{D}$, the holes locations in the 3^{rd} and 4^{th} quadrants are centrosymmetric to those in the 1^{st} and 2^{nd} quadrants. FIGURE 4.2 illustrates the analysis.

4.3 Holes-filling method

Based on the above analysis of the holes locations in the difference coarray, it can be seen that there exist some critical holes in the 1^{st} and 3^{rd} quadrants, which sparsely locate inside the range of $\{(x,z) \mid -(M+N) < x, z < (M+N)\}$ and break the consecutiveness of the difference coarray in such range. For the critical holes in the 1^{st} quadrant, which belong to $\mathbb{H}_{12}$ and $\mathbb{H}_{13}$, we propose a holes-filling method, by which such holes can be filled by adding few additional sensor elements, and because of the centrosymmetry of the difference coarray, the critical holes in the 3^{rd} quadrant will also be filled as long as the critical holes in the 1^{st} quadrant are filled.

We first focus on the elements of $\mathbb{H}_{12}$, which is given in Equation (4.33). Considering the assumption $M < N$, the most critical holes in the range $\{(x,z) \mid -(M+N) < x, z < (M+N)\}$ and belonging to $\mathbb{H}_{12}$ can be expressed as

$$\mathbb{H}_{12}^{'} = \left\{(N, kM) \mid 1 \leq k \leq K, K = \lfloor \frac{N}{M} \rfloor + 1\right\} \tag{4.38}$$

And such holes can be filled by adding an additional sensor element at position (N, KM). The proof is given in the following by two steps.

a) The position (N, KM) is not occupied by the sensor elements originally existing in

the CPA, which can be proved by contradiction :

If there exists a sensor element originally located at the position (N, KM), a lag would be generated by such sensor and the sensor located at $(0, 0)$, and would be found at the position (N, KM) in the difference coarray, which contradicts the above analysis of the holes locations given in Equation (4.33). The step a) is proved.

b) The holes $\mathbb{H}_{12}^{'}$ can be filled by the lags generated by the additional sensor element located (N, KM) and the sensor elements originally existing in the CPA and located at $(0, tM)$, where $0 \leq t \leq K-1$.

According to the sensor elements positions shown in Equation (4.2), there is

$$t \leq K-1 < \lfloor \frac{N}{M} \rfloor < \frac{N}{M} < N-1 \tag{4.39}$$

Therefore there is a sensor element originally existing in the CPA and located at the position $(0, tM)$. The lags generated by such sensor element and the added sensor element located at (N, KM) can be expressed as

$$\mathbb{C} = \{(N, gM) \mid g = K - t\} \tag{4.40}$$

It is easy to see that $\mathbb{C} = \mathbb{H}_{12}^{'}$, which means that the holes in $\mathbb{H}_{12}^{'}$ can be filled by the lags in $\mathbb{C}$, and the step b) is then proved.

From the above two steps, it has been proved that the critical holes in the range $\{(x, z) \mid -(M+N) < x, z < (M+N)\}$ and belonging to $\mathbb{H}_{12}$ can be filled by adding an additional sensor element at the position (N, KM). Then, for the critical holes in the range $\{(x, z) \mid -(M+N) < x, z < (M+N)\}$ and belonging to $\mathbb{H}_{13}$, which can be described as

$$\mathbb{H}_{13}^{'} = \left\{(kM, N) \mid 1 \leq k \leq K, K = \lfloor \frac{N}{M} \rfloor + 1\right\} \tag{4.41}$$

they can be filled by adding another additional sensor element at position (KM, N). The proof is similar as above and omitted here.

For the CPA shown in FIGURE 4.1 where $N = 5$ and $M = 3$, with the corresponding difference coarray shown in FIGURE 4.2, the most critical holes inside the range of $\{(x, z) \mid -8 < x, z < 8\}$ can be filled by adding two additional sensor elements at the positions $(5, 6)$ and $(6, 5)$. The CPA with the added sensor elements is shown in FIGURE 4.7 and the corresponding difference coarray with the filled holes is shown in FIGURE 4.8.

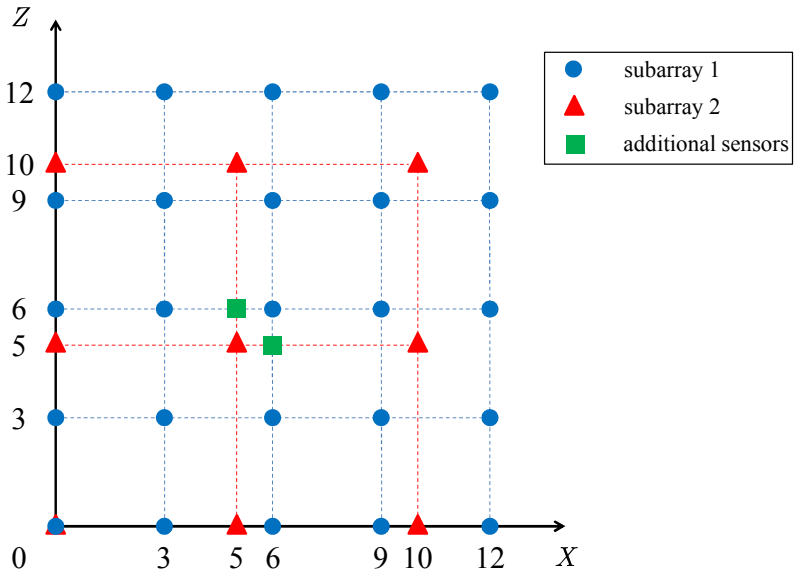

FIGURE 4.7 – Coprime planar array $N = 5$ and $M = 3$ with additional sensor elements

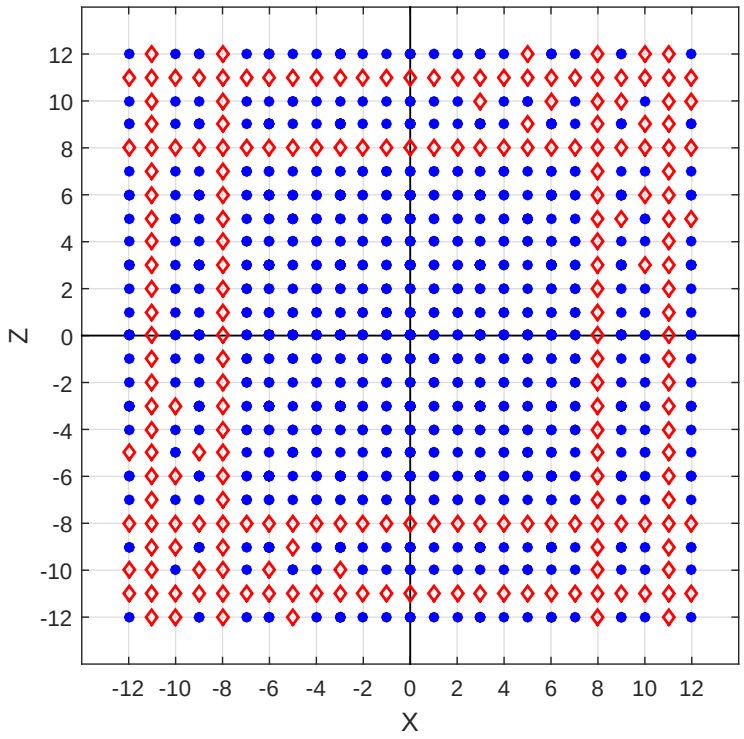

FIGURE 4.8 – Difference coarray of the CPA $N = 5$ and $M = 3$ after holes-filling

Thanks to the proposed holes-filling method, by judiciously adding two additional sensor elements, the critical holes inside the range $\{(x, z) \mid -(M + N) < x, z < (M + N)\}$ are filled, resulting in a difference coarray part containing the most consecutive lags located at $\{(x, z) \mid -(M + N - 1) < x, z < (M + N - 1)\}$, with the total number of consecutive lags being $(2M + 2N - 1)^2$. Compared with the difference coarray of the original CPA configuration, although the difference coarray of the CPA with the holes-filling method is not hole-free, it exhibits a much larger consecutive part with much more consecutive lags, greatly increasing the effective DOFs of the CPA.

4.4 Conclusion

In this chapter, 2D CPAs are studied from the perspective of difference coarray. Closed-form expressions of the holes locations are deduced with detailed proof, offering a better understanding of CPAs and facilitating the future research is this field. Then based on the knowledge of the holes locations, a holes-filling method is proposed. By judiciously adding two additional sensor elements, the most critical holes which highly threaten the consecutiveness of the difference coarray can be filled. Consequently, the consecutive part of the difference coarray can be enlarged, which significantly increases the effective DOFs of the array.

CHAPITRE 5

AN EFFICIENT DOA ESTIMATION METHOD FOR COPRIME LINEAR SUBARRAYS

In the previous chapters, coprime arrays are investigated from the perspective of difference coarray-based methods, which try to increase the number of consecutive lags in a virtual half-wavelength spacing uniform coarray to increase the effective DOFs. In this chapter, we focus on the subarray-based methods, where a CLA is treated as two sparse uniform linear subarrays. From each of them, high-precision but ambiguous DOA estimation is obtained, and the ambiguities caused by the large inter-element spacing are eliminated according to the coprime property. Compared with difference coarray-based methods, separately dealing with two uniform linear subarrays, the subarray-based methods sacrifice the DOFs, but they simplify the system model and can directly and efficiently exploit the uniform property of each subarrays. Consequently, the DOA estimation can be accomplished with low-complexity methods, which is more practical in some real applications.

Many DOA estimation methods have been proposed in this research orientation. A MUSIC-based method is proposed in [56]. By dividing a CLA into two sparse ULAs, and finding the common peaks of their MUSIC-spectrums, the DOAs can be uniquely obtained and the ambiguities caused by the large inter-element spacing can be eliminated based on the coprime property. But the complexity caused by the step of peak-searching is high. Another method is proposed in [57], which can reduce the computational complexity by limiting the peak-searching region. However, since it also involves the step of peak-searching, the computational burden is still heavy. Besides, the methods in [56] and [57] suffer from the problem of pair matching errors when the number of incoming signals is greater than one. A low complexity method based on ESPRIT is proposed in [58]. Without spectral searching, the complexity is significantly reduced. The matching errors are eliminated by beamforming-based techniques, and true DOAs are estimated uniquely. Similarly,

another method for fixing the pair matching errors problem is proposed in [59]. Based on Root-MUSIC [96, 97], it has low complexity. By exploiting the relationship between the directional matrices of the two subarrays, the pair matching of the estimated angles can be achieved automatically, and the ambiguities can be mitigated one by one. However, the grating angles problem is not considered. Because of the large inter-element spacing, some signals may impinge from a set of grating angles which share an identical directional vector for one subarray. Consequently, the directional matrix of this subarray will be rank deficient, it is then a challenge to find the true DOAs for all the above mentioned methods. The grating angles problem is firstly discussed in [60], where a joint singular value decomposition (JSVD) [98] based method is proposed. Thanks to the JSVD algorithm, the grating angles can be differentiated and the pair matching can be accomplished. Nevertheless, since a "beamforming-like“ method with spectral searching is involved, the performance of this method is limited by the length of searching step and high complexity.

In this chapter, an efficient DOA estimation method is proposed. For each subarray, the true DOAs are mapped into equivalent DOAs corresponding to a virtual traditional half-wavelength spacing ULA. From the perspective of accuracy and efficiency, after estimating the number of the equivalent signals, the ESPRIT method is performed and two sets of equivalent DOAs can be estimated from the two subarrays respectively. Then the associated equivalent signals can be recovered. By analyzing the cross-correlations between the equivalent signals recovered from the two subarrays, the pair matching of the equivalent DOAs is accomplished. Consequently, based on the relationship between a DOA and its equivalent DOAs, two sets of candidate DOAs are recovered for each pair of matched equivalent angles, and the corresponding true DOA is uniquely determined by finding the common element. Compared with other existing methods, the proposed method is able to achieve a better estimation performance in all situations, in terms of accuracy and complexity. Simulation results are provided to show the performance of the proposed method.

5.1 Mapped system model

Firstly, let's recall the signal model of coprime subarrays. Consider a CLA composed of two sparse uniform linear subarrays, having M_1 and M_2 sensor elements with inter-element spacing $d_1 = M_2\frac{\lambda}{2}$ and $d_2 = M_1\frac{\lambda}{2}$ respectively. Suppose that there are K uncorrelated, far-field and narrowband signals impinging on the CLA from directions $\{\theta_1, \theta_2, \cdots, \theta_K\}$ respectively, with $-90^\circ < \theta_k < 90^\circ$ and $1 \leq k \leq K$, where K is supposed to be known

and $K < \min\{M_1, M_2\}$. The signal received by the i^{th} subarray can be expressed as

$$\mathbf{x}_i(t) = \sum_{k=1}^{K} \mathbf{a}_i(\theta_k) s_k(t) + \mathbf{n}_i(t) = \mathbf{A}_i \mathbf{s}(t) + \mathbf{n}_i(t) \tag{5.1}$$

where

$$\mathbf{A}_i = \begin{bmatrix} \mathbf{a}_i(\theta_1) & \mathbf{a}_i(\theta_2) & \cdots & \mathbf{a}_i(\theta_K) \end{bmatrix} \tag{5.2}$$

denotes the directional matrix of the i^{th} subarray with

$$\mathbf{a}_i(\theta_k) = \begin{bmatrix} 1 & e^{jM_{\tilde{i}}\pi \sin\theta_k} & \cdots & e^{j(M_i-1)M_{\tilde{i}}\pi \sin\theta_k} \end{bmatrix}^T \tag{5.3}$$

where $i, \tilde{i} \in \{1, 2\}$ and $i \neq \tilde{i}$;

$$\mathbf{s}(t) = \begin{bmatrix} s_1(t) & s_2(t) & \cdots & s_K(t) \end{bmatrix}^T \tag{5.4}$$

denotes the source signals vector with $s_k(t)$ the signal transmitted by the k^{th} source and received at the reference sensor element shared by the two subarrays. $\mathbf{n}_i(t)$, which is assumed to be independent from the source signals, is a white Gaussian noise vector with zero-mean and covariance matrix $\sigma^2 \mathbf{I}_{M_i}$, with σ^2 the noise power.

To offer a better understanding of the signal model of the coprime subarrays as well as the potential problems in DOA estimation introduced in Section 2.3, a mapped system model based on traditional half-wavelength spacing ULAs is introduced. Due to the property of the sinusoid function, for the signal coming from θ_k and impinging on the i^{th} subarray, there exists a unique angle denoted as $\theta_{i,k}^{map}$ with $-90^\circ < \theta_{i,k}^{map} < 90^\circ$, satisfying

$$\sin\theta_{i,k}^{map} = M_{\tilde{i}} \sin\theta_k + 2n_{i,k} \tag{5.5}$$

where $n_{i,k}$ is an integer with $-\frac{M_{\tilde{i}}+1}{2} < n_{i,k} < \frac{M_{\tilde{i}}-1}{2}$.

Because of the property of the complex exponential function, the directional vector associated with this signal in Equation (5.3) can be re-written as

$$\mathbf{a}_i^{map}\left(\theta_{i,k}^{map}\right) = \begin{bmatrix} 1 & e^{j\pi \sin\theta_{i,k}^{map}} & \cdots & e^{j(M_i-1)\pi \sin\theta_{i,k}^{map}} \end{bmatrix}^T \tag{5.6}$$

Therefore, it can be considered that the signal with the true DOA θ_k impinging on the i^{th} subarray is mapped into a virtual signal with the mapped DOA $\theta_{i,k}^{map}$ impinging on a virtual half-wavelength spacing ULA with M_i sensor elements. The mapped system model of the

i^{th} subarray is shown in FIGURE 5.1.

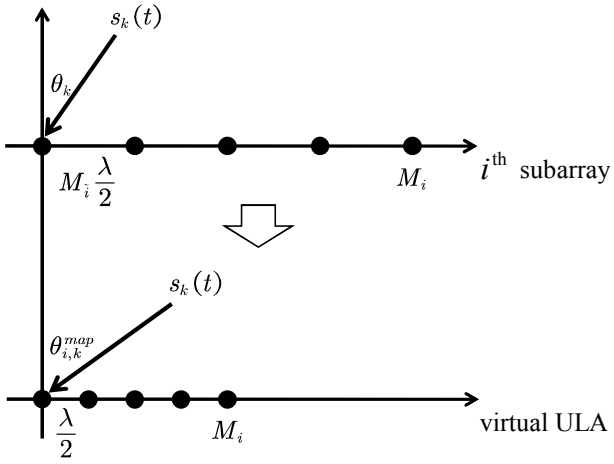

FIGURE 5.1 – Mapped system model

Accordingly, for multiple incoming signals, the received signal model of the i^{th} subarray can be regarded as K signals coming from K mapped DOAs $\{\theta_{i,1}^{map}, \theta_{i,2}^{map}, \cdots, \theta_{i,K}^{map}\}$ impinging on a virtual half-wavelength spacing ULA with M_i sensor elements. Equation (5.1) can then be re-written as

$$\mathbf{x}_i(t) = \sum_{k=1}^{K} \mathbf{a}_i^{map}\left(\theta_{i,k}^{map}\right) s_k(t) + \mathbf{n}_i(t) = \mathbf{A}_i^{map}\mathbf{s}(t) + \mathbf{n}_i(t) \tag{5.7}$$

where

$$\mathbf{A}_i^{map} = \left[\mathbf{a}_i^{map}\left(\theta_{i,1}^{map}\right) \quad \mathbf{a}_i^{map}\left(\theta_{i,2}^{map}\right) \quad \cdots \quad \mathbf{a}_i^{map}\left(\theta_{i,K}^{map}\right)\right] \tag{5.8}$$

denotes the mapped directional matrix of the i^{th} subarray, and the set of the K mapped DOAs associated with the K true DOAs is defined as $\mathbf{\Theta}_i^{map} = \{\theta_{i,1}^{map}, \theta_{i,2}^{map}, \cdots, \theta_{i,K}^{map}\}$.

To address the potential problems in DOA estimation with coprime subarrays introduced in Section 2.3, instead of the original system, the DOA estimation will be implemented on the traditional half-wavelength spacing ULAs based mapped system. For the signal coming from θ_k and impinging on the i^{th} subarray, its mapped DOA $\theta_{i,k}^{map}$ rather than the true DOA θ_k can be directly obtained from the mapped system. According to Equation (5.5), each mapped DOA $\theta_{i,k}^{map}$ corresponds to $M_{\tilde{i}}$ candidate angles, and the m^{th} candidate angle $\theta_{i,k}^{cand,m}$ can be recovered by

$$\theta_{i,k}^{cand,m} = \arcsin\left(\frac{1}{M_{\tilde{i}}}\left(\sin\theta_{i,k}^{map} - 2n_{i,k}^{m}\right)\right) \tag{5.9}$$

with $n_{i,k}^{m}$ the value of $n_{i,k}$ associated with the m^{th} candidate angle $\theta_{i,k}^{cand,m}$. One of the candidate angles recovered by Equation (5.9) is the true DOA θ_k, and the others are ambiguities. According to Section 2.3, the true DOA θ_k can be uniquely determined by finding the common angle in the two sets of candidates angles recovered from the mapped angles $\theta_{1,k}^{map}$ and $\theta_{2,k}^{map}$, which are obtained from the two subarrays respectively.

Considering the pair matching errors introduced in Section 2.3.2 from the perspective of the equivalent system model, the problem occurs when there exist other common angles in the candidate angles recovered from the mapped DOAs of difference sources in different subarrays. Therefore, the mapped DOAs estimated from the two subarrays associated with a common source should be pair matched, such that for each of the K pairs of matched DOAs, two sets of candidate angles can be recovered, and the associated true DOA can be obtained by finding the common element among them without pair matching errors.

And considering the grating angles problem introduced in Section 2.3.3 from the perspective of the equivalent system model, the problem occurs when some signals come from a set of distinct angles belonging to a common candidate angles set and sharing a common mapped DOA. Consequently, their associated directional vectors will be identical and the directional matrix of this subarray will be rank deficient. It will result in difficulties for the subsequent steps like DOA estimation and ambiguities elimination.

5.2 Proposed DOA estimation method

Considering the grating angles problem or the rank deficiency of the directional matrices, in this section, an equivalent system model is introduced. Then an efficient DOA estimation method is proposed, which remains robust in any situations with higher accuracy and lower complexity.

5.2.1 Equivalent system model

When some signals come from a set of angles, which are grating angles to each other for one subarray, the mapped DOAs of them are the same, or in other word, these signals seem to come from a "same" direction to the virtual half-wavelength spacing ULA. In this situation, the received signal model of the i^{th} subarray can be regraded as K_i equivalent signals $s_{i,l}^{eqv}(t)$ coming from K_i different equivalent DOAs $\theta_{i,l}^{eqv}$ impinging on a virtual half-wavelength spacing ULA, with $1 \leq K_i \leq K$ and $1 \leq l \leq K_i$. The set of the K_i equivalent

DOAs of the K_i equivalent signals is defined as $\mathbf{\Theta}_i^{eqv}$ with $\mathbf{\Theta}_i^{eqv} = \left\{\theta_{i,1}^{eqv}, \theta_{i,2}^{eqv}, \cdots, \theta_{i,K_i}^{eqv}\right\}$. Note that $\mathbf{\Theta}_i^{eqv} \subseteq \mathbf{\Theta}_i^{map}$, and without grating angles problem, we have $K_i = K$ and $\mathbf{\Theta}_i^{eqv} = \mathbf{\Theta}_i^{map}$, and the equivalent system model is identical to the mapped system model introduced in Section 5.1. In practice, the number of equivalent signals K_i can be estimated by Akaike Information Criterion (AIC) or Minimum Description Length (MDL) method [99–101]. When the grating angles problem occurs, some of the equivalent signals $s_{i,l}^{eqv}(t)$ should be a combination of some original signals $s_k(t)$, as shown in FIGURE 5.2.

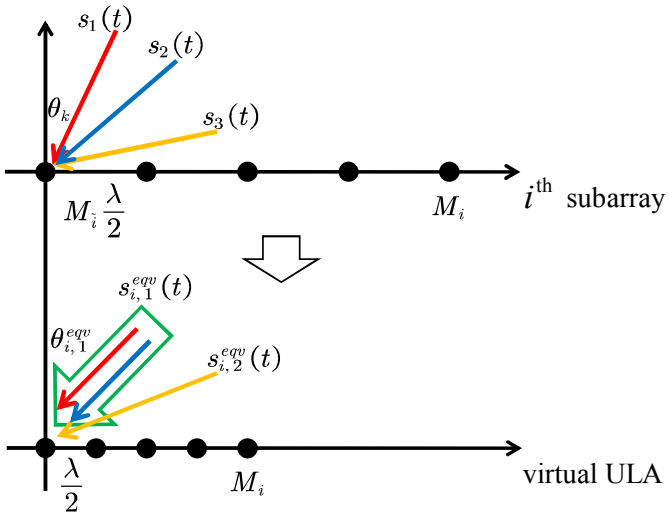

FIGURE 5.2 – Equivalent system model when grating angles problem occurs

Based on the equivalent system model, the signals observed at the i^{th} subarray can be re-written as

$$\mathbf{x}_i(t) = \sum_{l=1}^{K_i} \mathbf{a}_i^{map}\left(\theta_{i,l}^{eqv}\right) s_{i,l}^{eqv}(t) + \mathbf{n}_i(t) = \mathbf{A}_i^{eqv}\mathbf{s}_i^{eqv}(t) + \mathbf{n}_i(t) \tag{5.10}$$

where

$$\mathbf{A}_i^{eqv} = \left[\mathbf{a}_i^{map}\left(\theta_{i,1}^{eqv}\right) \quad \mathbf{a}_i^{map}\left(\theta_{i,2}^{eqv}\right) \quad \cdots \quad \mathbf{a}_i^{map}\left(\theta_{i,K_i}^{eqv}\right)\right] \tag{5.11}$$

denotes the equivalent directional matrix, and

$$\mathbf{s}_i^{eqv}(t) = \left[s_{i,1}^{eqv}(t) \quad s_{i,2}^{eqv}(t) \quad \cdots \quad s_{i,K_i}^{eqv}(t)\right]^T \tag{5.12}$$

denotes the equivalent source signal vector of the i^{th} subarray.

5.2.2 DOA estimation

After estimating the number of the equivalent source signals K_i, the ESPRIT method introduced in Section 1.3.4 can be performed on the signals received by the two subarrays, and two sets of equivalent DOAs can be obtained from them respectively, denoted as

$$\hat{\mathbf{\Theta}}_1^{eqv} = \left\{ \hat{\theta}_{1,1}^{eqv}, \hat{\theta}_{1,2}^{eqv}, \cdots, \hat{\theta}_{1,K_1}^{eqv} \right\} \tag{5.13}$$

$$\hat{\mathbf{\Theta}}_2^{eqv} = \left\{ \hat{\theta}_{2,1}^{eqv}, \hat{\theta}_{2,2}^{eqv}, \cdots, \hat{\theta}_{2,K_2}^{eqv} \right\} \tag{5.14}$$

To achieve the pair matching of the equivalent DOAs, the equivalent source signals vector of the two subarrays $\mathbf{s}_1^{eqv}(t)$ and $\mathbf{s}_2^{eqv}(t)$ should be recovered, and the pair matching of the equivalent DOAs can be achieved by exploring the cross-correlations between their associated equivalent signals.

Based on the equivalent DOAs estimated previously, an estimated equivalent directional matrix can be constructed for each subarray as follows

$$\hat{\mathbf{A}}_i^{eqv} = \left[\mathbf{a}_i^{map}\left(\hat{\theta}_{i,1}^{eqv}\right) \quad \mathbf{a}_i^{map}\left(\hat{\theta}_{i,2}^{eqv}\right) \quad \cdots \quad \mathbf{a}_i^{map}\left(\hat{\theta}_{i,K_i}^{eqv}\right) \right] \tag{5.15}$$

with the estimated mapped directional vector

$$\mathbf{a}_i^{map}\left(\hat{\theta}_{i,l}^{eqv}\right) = \left[1 \quad e^{j\pi \sin \hat{\theta}_{i,l}^{eqv}} \quad \cdots \quad e^{j(M_i-1)\pi \sin \hat{\theta}_{i,l}^{eqv}} \right]^T \tag{5.16}$$

Then the equivalent source signals of the i^{th} subarray can be recovered by

$$\hat{\mathbf{s}}_i^{eqv}(t) = \left(\hat{\mathbf{A}}_i^{eqv}\right)^{+} \mathbf{x}_i(t) \tag{5.17}$$

where

$$\hat{\mathbf{s}}_i^{eqv}(t) = \left[\hat{s}_{i,1}^{eqv}(t) \quad \hat{s}_{i,2}^{eqv}(t) \quad \cdots \quad \hat{s}_{i,K_i}^{eqv}(t) \right]^T \tag{5.18}$$

of which the elements denote the equivalent signals respect to the K_i equivalent DOAs.

In order to study the cross-correlations between the equivalent source signals of the two subarrays got by Equation (5.17), $K_1 \times K_2$ cross-correlations can be estimated by

$$\hat{r}_{p,q} = \frac{1}{J} \sum_{t=1}^{J} \hat{s}_{1,p}^{eqv}(t) \left(\hat{s}_{2,q}^{eqv}(t) \right)^* \tag{5.19}$$

where $1 \le p \le K_1$, $1 \le q \le K_2$ and J is the number of snapshots.

Since an equivalent signal may be a combination of some original signals, if a common original signal is contained in two equivalent signals of the two subarrays $\hat{s}_{1,p}^{eqv}(t)$ and $\hat{s}_{2,q}^{eqv}(t)$, the modulus of the cross-correlation between them $|\hat{r}_{p,q}|$ would be a large value. Otherwise, it would be a small value. One the other hand, it has been proved in [79] that thanks to the coprimality between M_1 and M_2, for two distinct DOAs having the same directional vector for one subarray, their directional vectors for the other subarray are necessarily different. In other words, two distinct DOAs with same mapped DOA for one subarray have necessarily different mapped DOAs for the other one. Therefore, in the $K_1 \times K_2$ cross-correlations, there exist K cross-correlations with large modulus corresponding to the K original sources. By finding the K cross-correlations with largest modulus, the K pairs of matched equivalent DOAs can be found. Similarly to Equation (5.9), for each pair of matched equivalent DOAs, two sets of candidate DOAs can be recovered as follows

$$\hat{\mathbf{\Theta}}_{1,k}^{cand} = \left\{ \hat{\theta}_{1,k}^{cand,1} \quad \hat{\theta}_{1,k}^{cand,2} \quad \cdots \quad \hat{\theta}_{1,k}^{cand,M_2} \right\} \tag{5.20}$$

$$\hat{\mathbf{\Theta}}_{2,k}^{cand} = \left\{ \hat{\theta}_{2,k}^{cand,1} \quad \hat{\theta}_{2,k}^{cand,2} \quad \cdots \quad \hat{\theta}_{2,k}^{cand,M_1} \right\} \tag{5.21}$$

by

$$\hat{\theta}_{i,k}^{cand,m} = \arcsin\left(\frac{1}{M_{\tilde{i}}} \left(\sin \hat{\theta}_{i,k}^{eqv} - 2n_{i,k}^{m} \right) \right) \tag{5.22}$$

and the estimation of the true DOA $\hat{\theta}_k$ can be determined by finding the common angle among them.

As a matter of illustration of this principle, the processing flow charts of the proposed method for a normal situation and a grating angles problem situation are depicted in FIGURE 5.3 and FIGURE 5.4 respectively, where "L" stands for a large value and "S" stands for a small value. It is assumed that three signals impinge on a coprime linear array from $\{\theta_1, \theta_2, \theta_3\}$; in the grating angles problem situation shown in FIGURE 5.4, θ_1 and θ_3 are grating angles for the 1^{st} subarray, and θ_1 and θ_2 are grating angles for the 2^{nd} subarray. It can be seen that thanks to the equivalent system model, the proposed method can overcome the rank deficiency caused by the grating angles problem, and the estimation results can be pair matched automatically. Finally, two sets of candidate DOAs can be recovered from each pair of matched equivalent DOAs, and the common element among them can be found to obtain the estimation of the true DOAs. The main steps of the proposed method can be summarized in TABLE 5.1.

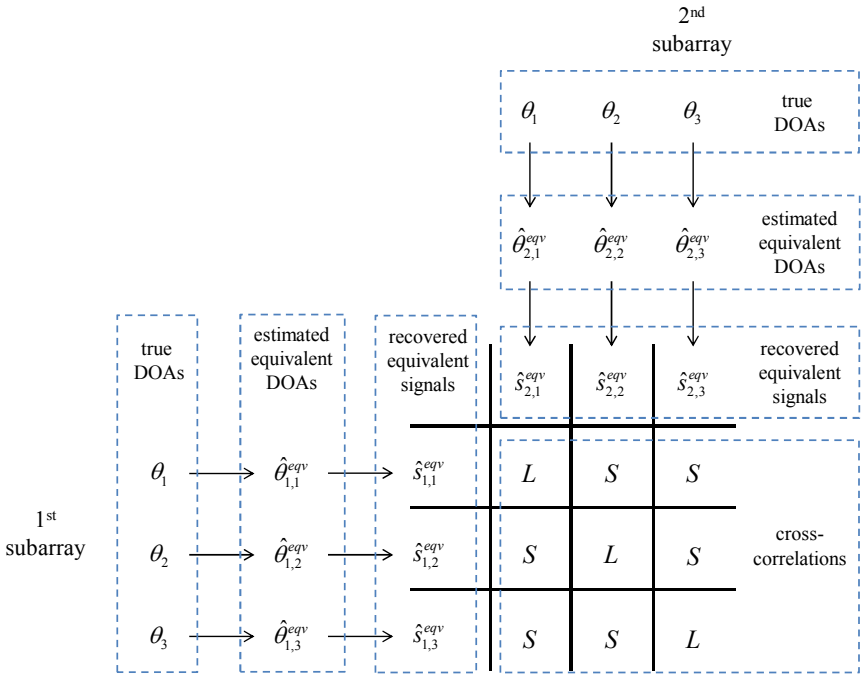

FIGURE 5.3 – Processing flow chart for a normal situation

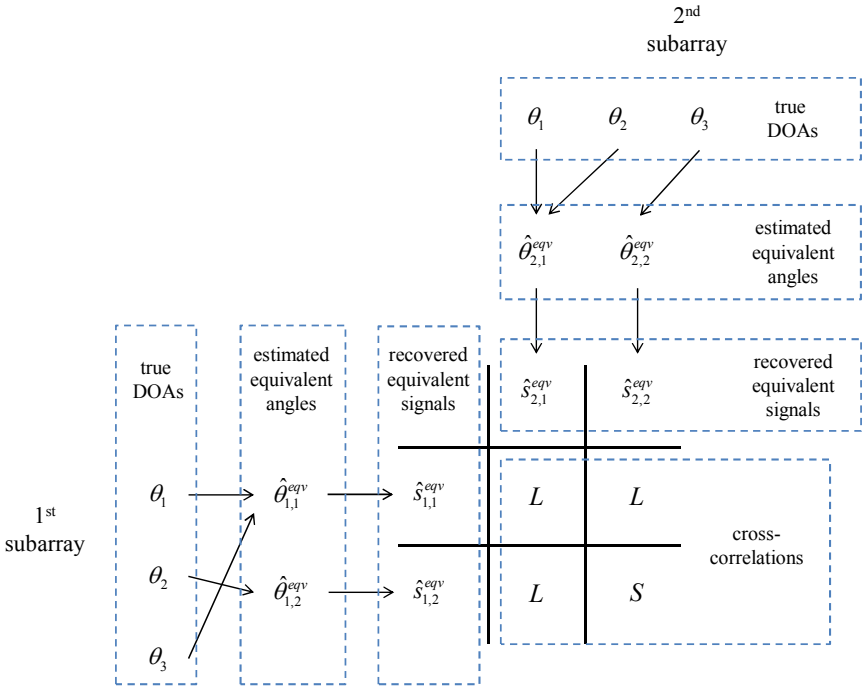

FIGURE 5.4 – Processing flow chart for a grating angles problem situation

TABLE 5.1 – Main steps of the proposed method

step 1	Estimate the numbers of the equivalent source signals received by the two subarrays K_1 and K_2.
step 2	Perform the ESPRIT method to estimate the two sets of the equivalent DOAs $\hat{\mathbf{\Theta}}_1^{eqv}$ and $\hat{\mathbf{\Theta}}_2^{eqv}$ from the signals received by the two subarrays $\mathbf{x}_1(t)$ and $\mathbf{x}_2(t)$ respectively.
step 3	Construct the two equivalent directional matrices of the two subarrays $\hat{\mathbf{A}}_1^{eqv}$ and $\hat{\mathbf{A}}_2^{eqv}$ with the two sets of estimated equivalent DOAs $\hat{\mathbf{\Theta}}_1^{eqv}$ and $\hat{\mathbf{\Theta}}_2^{eqv}$ respectively (Equation (5.15)).
step 4	Recover the equivalent source signals $\hat{\mathbf{s}}_1^{eqv}(t)$ and $\hat{\mathbf{s}}_2^{eqv}(t)$ impinging on the two subarrays (Equation (5.17)).
step 5	Calculate the cross-correlations between $\hat{\mathbf{s}}_1^{eqv}(t)$ and $\hat{\mathbf{s}}_2^{eqv}(t)$ (Equation (5.19)), and achieve the pair matching of the estimated equivalent DOAs by finding the K cross-correlations with the largest modulus.
step 6	For each of the K pairs of the matched equivalent DOAs, generate two sets of candidate DOAs $\hat{\mathbf{\Theta}}_{1,k}^{cand}$ and $\hat{\mathbf{\Theta}}_{1,k}^{cand}$ (Equation (5.22)). The estimate of the true DOA $\hat{\theta}_k$ ($k = 1, 2, \cdots, K$) is given by the unique common angle among them.

5.3 Simulation and analysis

To assess the performance of the proposed method, firstly, the proposed method is compared with Zhou's method in [56] in a pair matching errors situation. Then in a grating angles problem situation, it is compared with the Sun's method in [58] and Zhang's method in [59], which solve the pair matching errors. Finally, in order to assess the accuracy and complexity performance of the proposed method, it is compared with Yang's method in [60], which also considers the pair matching errors and grating angles problem.

5.3.1 Reliability comparison

To show the superiority of the proposed method in pair matching errors situations, consider the situation mentioned Section 2.3.2, where a CLA is composed of two coprime

subarrays with the numbers of sensor elements $M_1 = 7$, $M_2 = 5$, and two incoming signals impinging on the CLA from $\theta_1 = 10.00°$ and $\theta_2 = 39.11°$ respectively. The reliability comparison of the proposed method and Zhou's method is shown in FIGURE 5.5 with 10 independent simulation runs, in which the SNR is 0dB and the number of snapshots is 200. It can be seen that because Zhou's method only finds out the common peaks in the MUSIC spectrums obtained from the two subarrays without pair matching, the estimation results may be ambiguous. In contrast, thanks to the equivalent system model, the proposed method can achieve the pair matching of the equivalent DOAs associated with the same source in different subarrays by analyzing the cross-correlations between the equivalent signals, and the performance remains remarkable and stable.

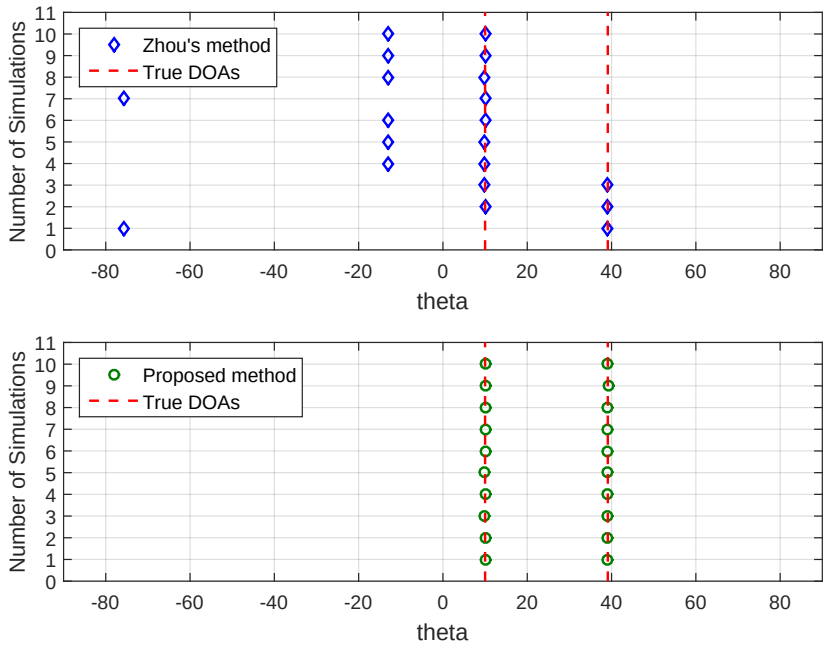

FIGURE 5.5 – Reliability comparison in the pair matching errors situation

To emphasize the superiority of the proposed method in grating angles problem situations, consider the situation mentioned Section 2.3.3, where a CLA is composed of two coprime subarrays with the numbers of sensor elements $M_1 = 7$, $M_2 = 5$, and three incoming signals impinging on the CLA from $\theta_1 = 10.00°$, $\theta_2 = 27.35°$ and $\theta_3 = 35.01°$ respectively. The reliability comparison of the proposed method with Sun's method in [58] and Zhang's method in [59] is shown in FIGURE 5.6 with 10 independent simulation runs, in which the SNR is 0dB and the number of snapshots is 200. It is obvious that although the two existing methods can overcome the pair matching errors with beamforming-based

methods and the relationship between the directional matrices of the two subarrays, they ignore the fact that the directional matrices would be rank deficient due to the grating angles problem, and their performance cannot remain stable. In contrast, thanks to the equivalent system model, the equivalent directional matrices are full rank, and the correctly matched equivalent DOA pairs can be found by studying the cross-correlations between the equivalent signals. Thus it can work correctly in such situations.

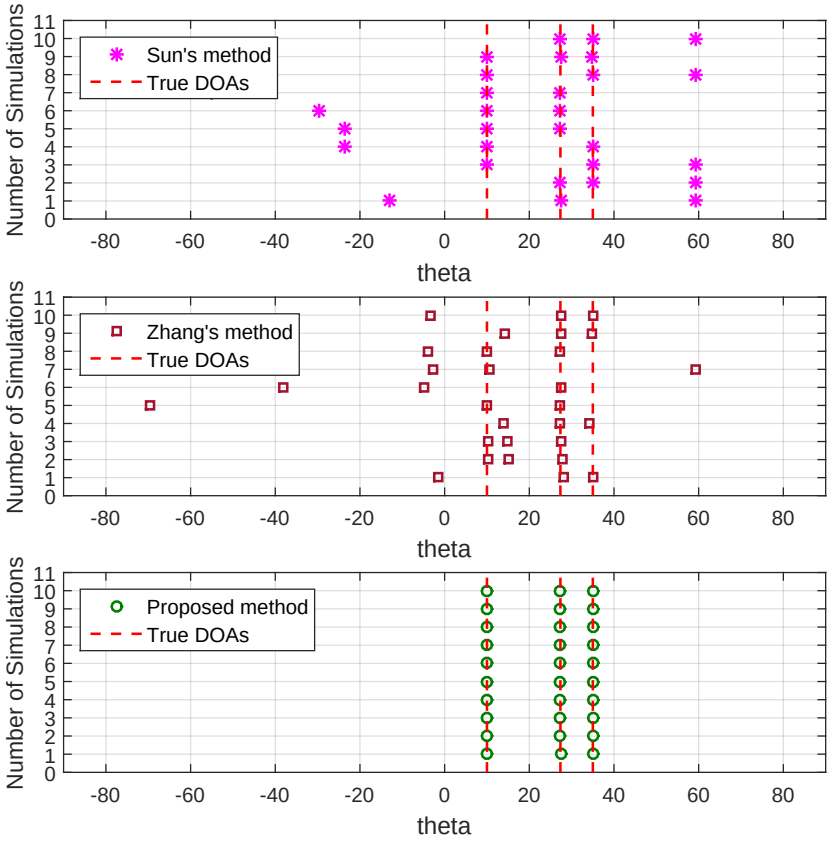

FIGURE 5.6 – Reliability comparison in the grating angles problem situation

5.3.2 Accuracy comparison

To assess the DOA estimation performance of the proposed method, the root mean square error (RMSE) is used as performance measurement, which is defined as

$$\text{RMSE} = \sqrt{\frac{1}{KQ}\sum_{k=1}^{K}\sum_{q=1}^{Q}\left(\hat{\theta}_{q,k}-\theta_k\right)^2} \tag{5.23}$$

with K the number of incoming signals, Q the number of Monte Carlo trials, and $\hat{\theta}_{q,k}$ the estimate of the true DOA θ_k at the q^{th} Monte Carlo trial. $Q = 500$ is used, and a CLA with $M_1 = 7$ and $M_2 = 5$ is considered. The Cramér-Rao lower bound (CRB) for this CLA geometry is also given as a benchmark [102–104].

The RMSE performance of the proposed method and Yang's method in [60] is compared in a normal situation, where two signals are assumed to impinge on the CLA from $\theta_1 = 10.00°$ and $\theta_2 = 40.00°$, and a grating angles problem situation, where three signal are assumed to impinge on the CLA from $\theta_1 = 10.00°$, $\theta_2 = 27.35°$ and $\theta_3 = 35.01°$, versus SNR (snapshots number is 200) and snapshots number (SNR is 10dB). FIGURE 5.7 — FIGURE 5.10 illustrate the obtained results. Because the peak-searching in Yang's method is performed in the sine domain, the searching step is chosen as 0.001 to obtain a precise estimation. It can be seen that both methods can achieve a remarkable performance in grating angles problem situations, but since a "beamforming-like" method is utilized, the accuracy of the method in [60] is limited. On the contrary, based on the ESPRIT method, the proposed method can achieve a better estimation result, and its RMSE curves are closer to the CRB.

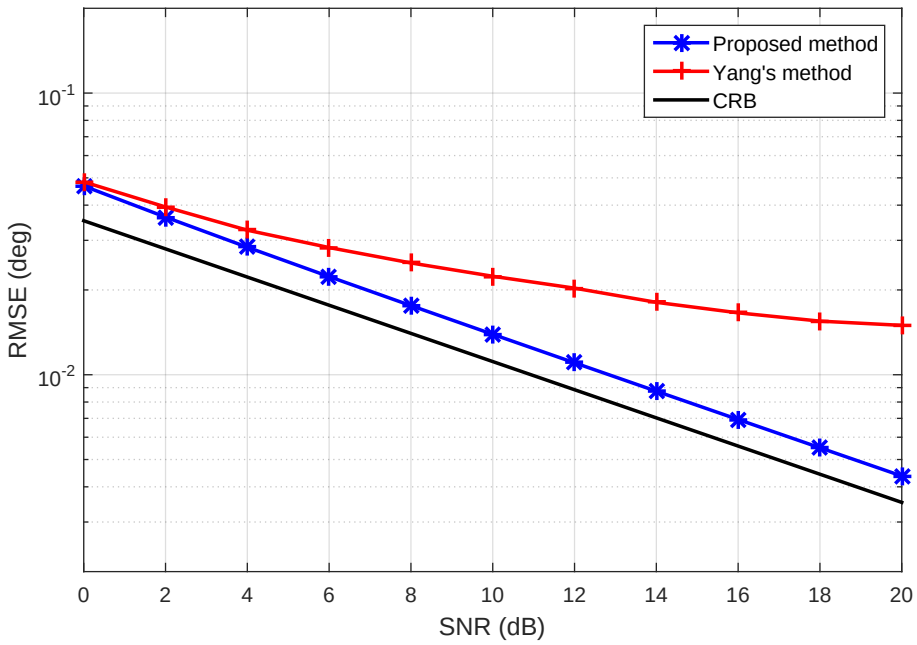

FIGURE 5.7 – RMSE comparison versus SNR in the normal situation

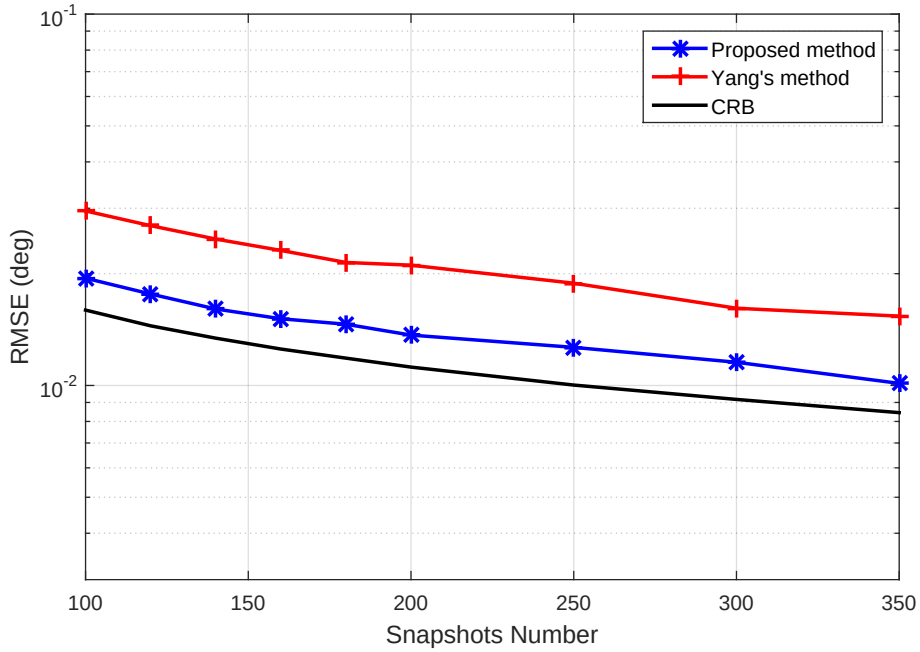

FIGURE 5.8 – RMSE comparison versus snapshots number in the normal situation

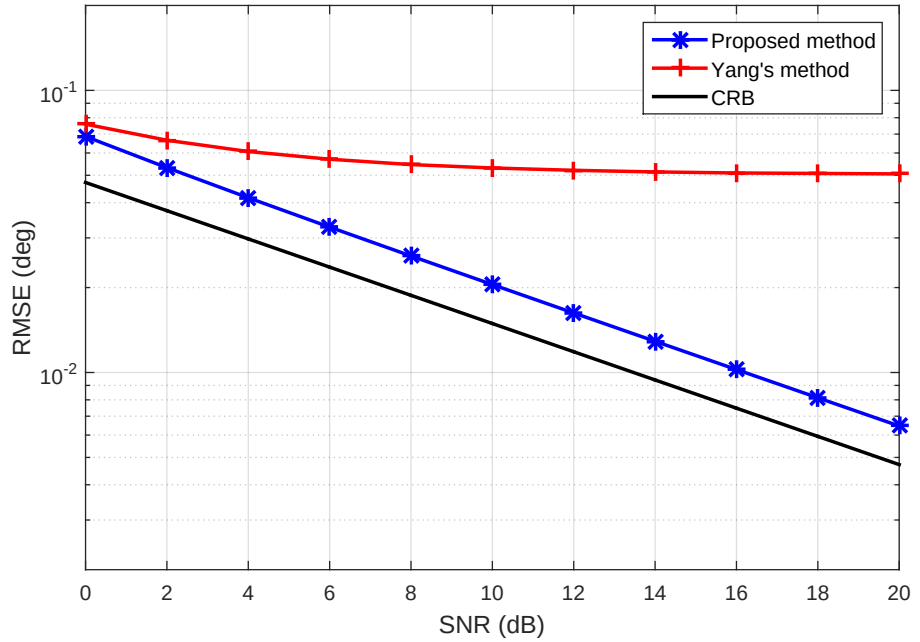

FIGURE 5.9 – RMSE comparison versus SNR in the grating angles problem situation

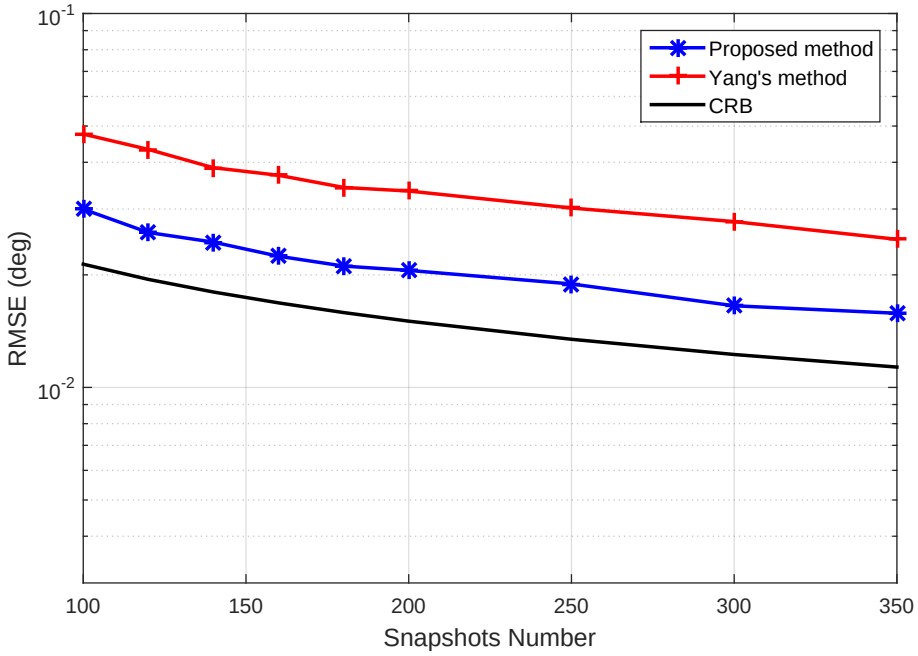

FIGURE 5.10 – RMSE comparison versus snapshots number in the grating angles problem situation

5.3.3 Complexity comparison

According to TABLE 5.1, the proposed method requires the covariance matrices estimation, eigenvalue decomposition of the covariance matrices, equivalent signals recovery and cross-correlation computation. The resulted complexity is given by

$$\mathcal{O}\left(\left(M_1^2+M_2^2\right)J+M_1^3+M_2^3+5K^2\left(M_1+M_2\right)+6K^3+\left(M_1+M_2\right)KJ+K^2J\right) \tag{5.24}$$

And for Yang's method in [60], it requires the cross-covariance matrix estimation, singular value decomposition of the cross-covariance matrix and peak-searching with the order of complexity given as

$$\mathcal{O}\left(M_1M_2J+4M_1M_2^2+M_2^3+3M_1K^2+2K^3+\frac{2M_1K}{M_2\times sch}\right) \tag{5.25}$$

where J is the number of snapshots and sch is the searching step length. The complexity comparison versus total number of sensors (M_1+M_2-1) is given in FIGURE 5.11, with $K=2$, $J=200$, and the grating angles problem is assumed to be not existing. The sear-

ching step length is set as 0.0001 to achieve a similar RMSE performance between the two algorithms. It can be observed that without peak-searching, the proposed method has lower computational complexity. When grating angles problem exists, some K in Equation (5.24) will be replaced by K_1 or K_2 with $K_1, K_2 < K$, and the corresponding computational complexity will be lower than Equation (5.24). Therefore, with the proposed method, the DOA estimation can be accomplished more efficiently.

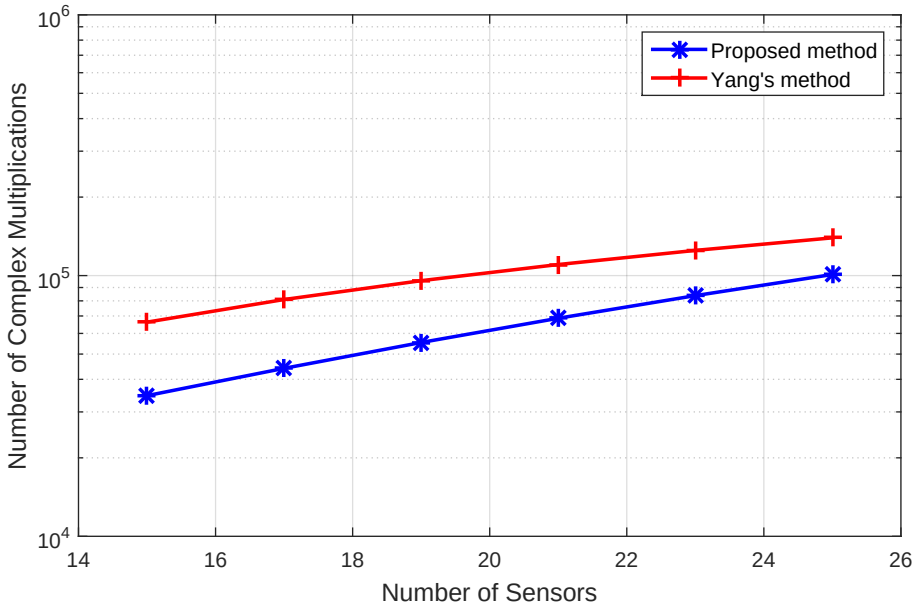

FIGURE 5.11 – Complexity comparison versus sensors number

For the other compared methods in [56, 58, 59], their practicability is limited by the pair matching errors or grating angles problem. Therefore, their performance in terms of accuracy and complexity is less significant in the case of real applications.

5.4 Conclusion

In this chapter, an efficient DOA estimation method with coprime linear subarrays is proposed. Considering the rank deficiency of the directional matrices caused by the grating angles problem, a traditional half-wavelength spacing ULA based equivalent system model is introduced, where the true DOAs are mapped into their corresponding equivalent DOAs and the equivalent directional matrices are full rank. After the estimation of the equivalent DOAs, the corresponding equivalent signals can be recovered from the received signals,

the pair matching of the equivalent DOAs can then be achieved by analyzing the cross-correlations between the equivalent signals. Compared with other existing research works, the proposed method remains robust in any situations with a better estimation performance in terms of accuracy and complexity.

CHAPITRE 6

DOA ESTIMATION WITH UNFOLDED COPRIME LINEAR ARRAYS

In the previous chapter, the DOA estimation with coprime linear subarrays is discussed. It is shown that by considering a CLA as two sparse ULAs and performing DOA estimation on both of them separately, high-precision but ambiguous DOA estimation can be obtained, and the ambiguities caused by the large inter-element spacing can be eliminated according to the coprime property. Besides, methods have been proposed to successfully solve the potential problems like pair matching errors and grating angles problem. However, separately handling the two subarrays causes the following problems :

i) the final DOFs are determined by the smallest DOFs of the two subarrays, which are much less than the total number of sensor elements ;

ii) only the self information of the two subarrays is utilized, which results in a sub-optimal estimation performance ;

iii) further processes are required to eliminate the ambiguities caused by the large inter-element spacing, leading to computational burden in practical applications.

To tackle these problems, an antenna geometry named unfolded coprime linear array (UCLA) is proposed in [79]. By unfolding the two subarrays of a general CLA in two opposite directions, the array aperture can be extended. Furthermore, instead of treating the two subarrays separately, the MUSIC method is performed with the received signal of the whole array. This technique, having been extended to the scenarios of noncircular signals in [81] and 2D DOA estimation in [82, 83], enjoys the advantages that both self and mutual information can be exploited and full DOFs can be obtained. Besides, it has been admitted that the ambiguities caused by the large inter-element spacing can be suppressed thanks to the coprime property. However, it is not always true. When there are two different DOAs having the same directional vectors with the directional vector of a given DOA for the two subarrays respectively, there would still be ambiguous angles of which the corresponding

directional vectors can be represented as linear combinations of the directional vectors of true DOAs. As a consequence, the directional vectors of these ambiguous angles are also orthogonal to the noise subspace, which means that some peaks associated with these ambiguous angles will also be found in the MUSIC spectrum.

In this chapter, the DOA estimation with UCLAs is introduced. For the ignored ambiguity problem, the principle of its generation is investigated and a modified DOA estimation method with ambiguity-eliminating is proposed. Firstly, a decision variable is defined to determine the existence of the ambiguity problem. Then all the angles associated with the highest spectral peaks, including the true DOAs and the ambiguous angles, are selected out and the Classical Beamforming (CBF) approach is utilized to distinguish them. Simulation results are provided to show the efficiency of the proposed method.

6.1 System model and DOA estimation

A UCLA consists of two sparse ULAs arranged along two opposite directions, having M_1 and M_2 sensor elements with inter-element spacing $d_1 = M_2\frac{\lambda}{2}$ and $d_2 = M_1\frac{\lambda}{2}$, respectively, where M_1 and M_2 are two coprime integers. FIGURE 6.1 shows the case of $M_1 = 7$ and $M_2 = 5$. The element shared by the two subarrasy is set as the reference point, and the total number of sensor elements is $N = M_1 + M_2 - 1$.

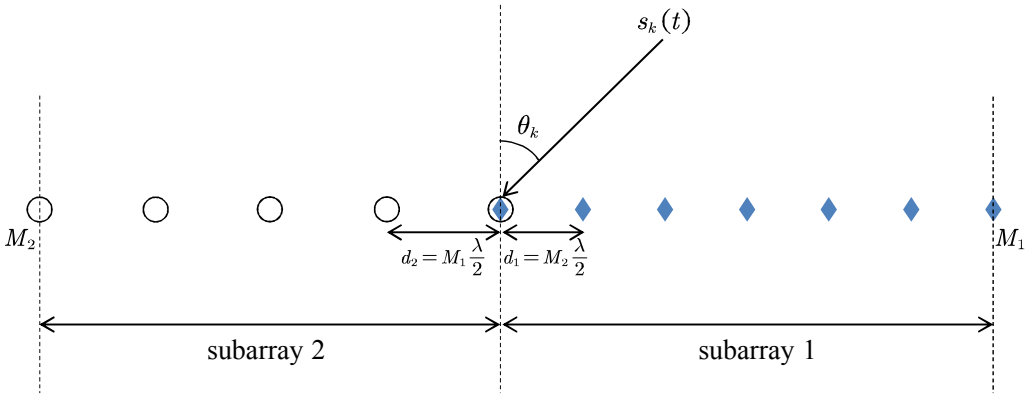

FIGURE 6.1 – Unfolded coprime linear array with $M_1 = 7$ and $M_2 = 5$

Assume that there are K (K is supposed to be known and $K < N$) uncorrelated, far-field and narrowband source signals coming from directions $\{\theta_1, \theta_2, \cdots, \theta_K\}$, with $-90° < \theta_k < 90°$ and $1 \leq k \leq K$, respectively. The received signal of the UCLA can be presented

as

$$\mathbf{x}(t) = \mathbf{A}\mathbf{s}(t) + \mathbf{n}(t) \tag{6.1}$$

where

$$\mathbf{A} = \begin{bmatrix} \mathbf{a}(\theta_1) & \mathbf{a}(\theta_2) & \cdots & \mathbf{a}(\theta_K) \end{bmatrix} \tag{6.2}$$

denotes the directional matrix and

$$\mathbf{a}(\theta_k) = \begin{bmatrix} \mathbf{a}_1^T(\theta_k) & \mathbf{a}_2^T(\theta_k) \end{bmatrix}^T \tag{6.3}$$

denotes the directional vector of the UCLA, with

$$\mathbf{a}_1(\theta_k) = \begin{bmatrix} 1 & e^{jM_2\pi\sin\theta_k} & \cdots & e^{j(M_1-1)M_2\pi\sin\theta_k} \end{bmatrix}^T \tag{6.4}$$

$$\mathbf{a}_2(\theta_k) = \begin{bmatrix} e^{-j(M_2-1)M_1\pi\sin\theta_k} & e^{-j(M_2-2)M_1\pi\sin\theta_k} & \cdots & e^{-jM_1\pi\sin\theta_k} \end{bmatrix}^T \tag{6.5}$$

the directional vectors of the two subarrays respectively ;

$$\mathbf{s}(t) = \begin{bmatrix} s_1(t) & s_2(t) & \cdots & s_K(t) \end{bmatrix}^T \tag{6.6}$$

denotes the source signal vector with $s_k(t)$ the signal transmitted by the signal coming from θ_k and received at the reference sensor, and $\mathbf{n}(t)$ is the white Gaussian noise vector with zero-mean and covariance matrix $\sigma^2\mathbf{I}_N$, and supposed to be independent from the source signals.

Instead of estimating the DOAs with the two subarrays separately, the MUSIC method is performed on the whole array, and the covariance matrix of the received signal can be estimated with L snapshots by

$$\hat{\mathbf{R}} = \frac{1}{L}\sum_{t=1}^{L}\mathbf{x}(t)\,\mathbf{x}^H(t) = \begin{bmatrix} \hat{\mathbf{R}}_{11} & \hat{\mathbf{R}}_{12} \\ \hat{\mathbf{R}}_{21} & \hat{\mathbf{R}}_{22} \end{bmatrix} \tag{6.7}$$

where $\hat{\mathbf{R}}_{11}$ and $\hat{\mathbf{R}}_{22}$ are the auto-covariance matrices and $\hat{\mathbf{R}}_{12}$ and $\hat{\mathbf{R}}_{21}$ are the cross-covariance matrices of the signals received by the two subarrays respectively. It can be seen that except the self-information of the two subarrays $\hat{\mathbf{R}}_{11}$ and $\hat{\mathbf{R}}_{22}$, which is only used in subarrays-based methods, the mutual information $\hat{\mathbf{R}}_{12}$ and $\hat{\mathbf{R}}_{21}$ is also used by UCLAs, contributing to the improvement of the estimation performance.

The eigenvalue decomposition of the covariance matrix $\hat{\mathbf{R}}$ can be written as

$$\hat{\mathbf{R}} = \mathbf{U}_s \mathbf{\Lambda}_s \mathbf{U}_s^H + \mathbf{U}_n \mathbf{\Lambda}_n \mathbf{U}_n^H \tag{6.8}$$

where $\mathbf{U}_s$ and $\mathbf{U}_n$ are composed by the eigenvectors spanning the signal subspace and noise subspace respectively, and $\mathbf{\Lambda}_s$ and $\mathbf{\Lambda}_n$ are the eigenvalue matrices corresponding to $\mathbf{U}_s$ and $\mathbf{U}_n$ respectively. The pseudo-spectrum of MUSIC can be represented by

$$P_{MUSIC}(\theta) = \frac{1}{\mathbf{a}^H(\theta)\,\mathbf{U}_n \mathbf{U}_n^H \mathbf{a}(\theta)} \tag{6.9}$$

Then according to the orthogonality between signal and noise subspaces, the DOAs can be determined by peak-searching of $P_{MUSIC}(\theta)$ over $(-90°, 90°)$. Specifically, unlike the spectrums of the subarrays, for a given DOA, only the spectral peak related to the real DOA estimate arise without ambiguities, of which the proof is given in the following.

Suppose that for a given DOA θ_k, except its real estimate $\hat{\theta}_k$, there exists another estimate, denoted as $\hat{\theta}_k^{amb} \neq \hat{\theta}_k$, presenting an ambiguous peak in the MUSIC spectrum, which means that the ambiguous estimate $\hat{\theta}_k$ has the same directional vector for the UCLA with the real estimate θ_k. Then we have

$$\mathbf{a}\left(\hat{\theta}_k\right) = \mathbf{a}\left(\hat{\theta}_k^{amb}\right) \tag{6.10}$$

and according to Equations (6.3) — (6.5), there are

$$\mathbf{a}_1\left(\hat{\theta}_k\right) = \mathbf{a}_1\left(\hat{\theta}_k^{amb}\right) \tag{6.11}$$

$$\mathbf{a}_2\left(\hat{\theta}_k\right) = \mathbf{a}_2\left(\hat{\theta}_k^{amb}\right) \tag{6.12}$$

and

$$M_2 \pi \sin\hat{\theta}_k = M_2 \pi \sin\hat{\theta}_k^{amb} + 2k_1\pi \tag{6.13}$$

$$M_1 \pi \sin\hat{\theta}_k = M_1 \pi \sin\hat{\theta}_k^{amb} + 2k_2\pi \tag{6.14}$$

where k_1 and k_2 are two non-zero with $k_1 \in [-M_2+1, -1] \cup [1, M_2-1]$ and $k_2 \in [-M_1+1, -1] \cup [1, M_1-1]$ respectively.

Then it can be deduced that

$$\sin\hat{\theta}_k - \sin\hat{\theta}_k^{amb} = \frac{2k_1}{M_2} \tag{6.15}$$

$$\sin\hat{\theta}_k - \sin\hat{\theta}_k^{amb} = \frac{2k_2}{M_1} \tag{6.16}$$

and

$$\frac{2k_1}{M_2} = \frac{2k_2}{M_1} \tag{6.17}$$

Due to the coprime property between M_1 and M_2, we cannot find such k_1 and k_2 satisfying Equation (6.17). Therefore, except $\hat{\theta}_k$, there is no $\hat{\theta}_k^{amb}$ satisfying Equation (6.10) and exhibiting a peak in the MUSIC spectrum. FIGURE 6.2 depicts the DOA estimation result of the situation where an incoming signal impinges on a UCLA with the sensor element numbers of the two subarrays $M_1 = 7$ and $M_2 = 5$ from direction $\theta = 10°$. The number of snapshots is set to 200 with SNR $= 10$dB. Compared with the traditional CLA with subarrays-based methods, of which the DOA estimation result is shown in FIGURE 2.9, it can be seen that the ambiguities caused by the large inter-element spacing are suppressed thanks to the coprime property, then the following step to eliminate the ambiguities by searching for the overlapped peaks is no more needed.

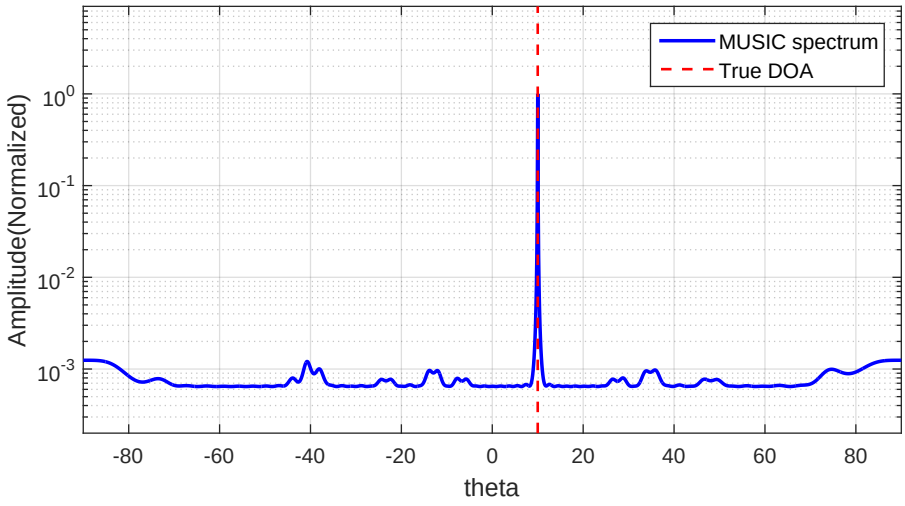

FIGURE 6.2 – DOA estimation result of the UCLA with $M_1 = 7$ and $M_2 = 5$

Although it has been admitted that for a single incoming signal, no ambiguities exist in the MUSIC spectrum of the whole UCLA, it is not always true for the scene of multiple incoming signals. When there are two different DOAs having the same directional vectors

with the directional vector of a given DOA for the two subarrays respectively, there would still be ambiguous angles, of which the proof is given in the following section.

6.2 Ambiguity problem

Because of the large inter-element spacing of each subarray, for a given DOA with its associated directional vector, there exist several other angles having the same directional vector for either subarray. Consider that there are three distinct DOAs θ_1, θ_2 and θ_3, of which the directional vectors satisfy that

$$\mathbf{a}_1(\theta_1) = \mathbf{a}_1(\theta_3) \tag{6.18}$$

$$\mathbf{a}_2(\theta_1) = \mathbf{a}_2(\theta_2) \tag{6.19}$$

Then the relationship between θ_1, θ_2 and θ_3 can be written as

$$M_2\pi\sin\theta_1 = M_2\pi\sin\theta_3 + 2k_1\pi \tag{6.20}$$

$$M_1\pi\sin\theta_1 = M_1\pi\sin\theta_2 + 2k_2\pi \tag{6.21}$$

where k_1 and k_2 are two non-zero integers with $k_1 \in [-M_2+1, -1] \cup [1, M_2-1]$ and $k_2 \in [-M_1+1, -1] \cup [1, M_1-1]$ respectively.

From Equations (6.20) and (6.21), it can be deduced that

$$\sin\theta_2 - \sin\theta_3 = \frac{2k_1}{M_2} - \frac{2k_2}{M_1} \tag{6.22}$$

which can be re-written as

$$\sin\theta_2 + \frac{2}{M_2}(-k_1) = \sin\theta_3 + \frac{2}{M_1}(-k_2) \tag{6.23}$$

Defining the term $\sin\theta_4$ and expressing Equation (6.23) in the two following equations as

$$\sin\theta_4 = \sin\theta_2 + \frac{2}{M_2}(-k_1) \tag{6.24}$$

$$\sin\theta_4 = \sin\theta_3 + \frac{2}{M_1}(-k_2) \tag{6.25}$$

then it comes that

$$M_2\pi \sin\theta_4 = M_2\pi \sin\theta_2 + 2\left(-k_1\right)\pi \tag{6.26}$$

$$M_1\pi \sin\theta_4 = M_1\pi \sin\theta_3 + 2\left(-k_2\right)\pi \tag{6.27}$$

Then the following equations are obtained

$$\mathbf{a}_1\left(\theta_4\right) = \mathbf{a}_1\left(\theta_2\right) \tag{6.28}$$

$$\mathbf{a}_2\left(\theta_4\right) = \mathbf{a}_2\left(\theta_3\right) \tag{6.29}$$

and according to Equations (6.18), (6.19) and Equations (6.28) and (6.29), there is the relationship between the directional vectors of θ_1, θ_2, θ_3 and θ_4 as

$$\left[\begin{array}{c}\mathbf{a}_1\left(\theta_1\right)\\ \mathbf{a}_2\left(\theta_1\right)\end{array}\right] - \left[\begin{array}{c}\mathbf{a}_1\left(\theta_2\right)\\ \mathbf{a}_2\left(\theta_2\right)\end{array}\right] - \left[\begin{array}{c}\mathbf{a}_1\left(\theta_3\right)\\ \mathbf{a}_2\left(\theta_3\right)\end{array}\right] + \left[\begin{array}{c}\mathbf{a}_1\left(\theta_4\right)\\ \mathbf{a}_2\left(\theta_4\right)\end{array}\right] = 0 \tag{6.30}$$

It can be seen that the directional vector of θ_4 can be represented as a linear combination of the directional vectors of the other three angles, and when there are three signals coming from any three of the four angles, the directional vector of the remaining one would lie in the signal subspace and be also orthogonal to the noise subspace, resulting in an ambiguous peak in the MUSIC spectrum. Generally, for an arbitrary number of incoming signals (at least three), if the DOAs of three of them meet the conditions given by Equations (6.18) and (6.19), then the ambiguity problem occurs.

Consider a UCLA with $M_1 = 7$, $M_2 = 5$, and three incoming signals impinge on the UCLA from $\theta_1 = 10.00°$, $\theta_2 = 27.35°$ and $\theta_3 = 35.01°$ respectively, satisfying Equations (6.18) and (6.19). The simulation result is shown in FIGURE 6.3, in which SNR $= 10$dB and the number of snapshots is 200. It is clear that apart from the three correct estimates, there is another angle $\theta_4 = 59.25°$, satisfying Equations (6.28) — (6.30) and giving an ambiguous peak in the MUSIC spectrum. For such UCLA configuration, the ambiguity problem also occurs in the cases of $\{\theta_1, \theta_2, \theta_3\} = \{20.00°, 38.88°, 47.90°\}$, $\{30.00°, 12.37°, 64.16°\}$ and others satisfying Equations (6.18) and (6.19), which is a real problem in the applications of UCLAs.

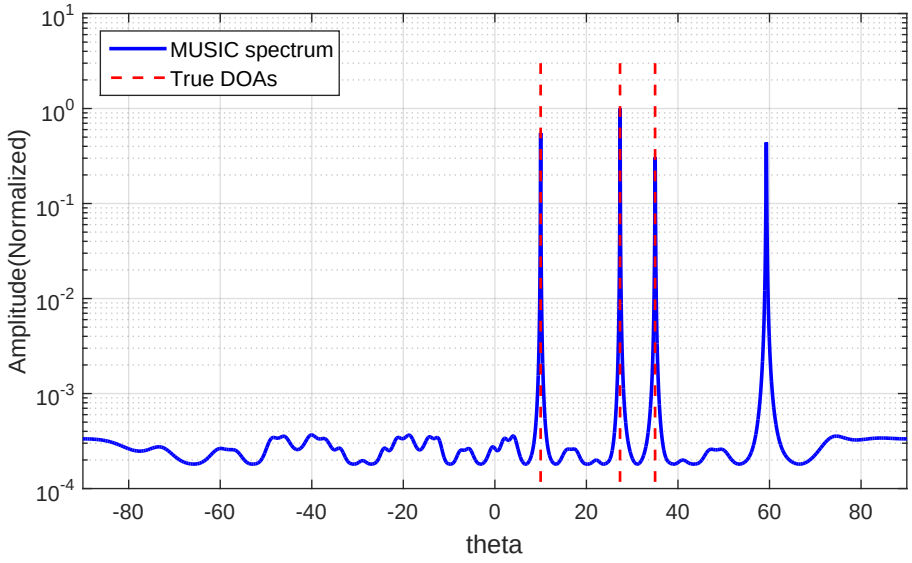

FIGURE 6.3 – Ambiguity problem of UCLAs

6.3 Proposed ambiguity-eliminating method

In order to solve the ambiguity problem, we propose an eliminating method. Firstly, it is required to determine if the problem exists or not. The MUSIC spectrum is expected to exhibit K high peaks associated with the K true DOAs. However, when some ambiguous peaks exist, more than K high peaks will be found. Suppose that there are totally Q peaks in the MUSIC spectrum, of which the locations and amplitudes are denoted as $(\hat{\theta}_p, y_p)$ with $p = 1, 2, \cdots, Q$. Sorting y_p in descending order, we have

$$y_1 > y_2 > \cdots > y_Q \tag{6.31}$$

Define a decision variable as

$$D(n) = \frac{y_n - y_{n+1}}{y_{n+1}} \tag{6.32}$$

where $n = 1, 2, \cdots, Q-1$. It can be noticed that when both y_n and y_{n+1} are two amplitudes of high peaks or low peaks, the decision variable $D(n)$ is small. If y_n is the amplitude of a high peak and y_{n+1} is the amplitude of a low peak, the decision variable $D(n)$ becomes much larger. Thus the number of high peaks can be decided by

$$J = \arg\max_n D(n) \tag{6.33}$$

and when $J > K$, the ambiguity problem is considered as existing.

To distinguish the true DOAs and the ambiguous angles, the Classical Beamforming (CBF) approach can be utilized. The J angles associated with the J highest peaks $\hat{\theta}_q$ with $q = 1, 2, \cdot, J$ are selected out as candidate DOAs, then J candidate directional vectors can be constructed with these candidate DOAs by

$$\mathbf{a}\left(\hat{\theta}_q\right) = \begin{bmatrix} \mathbf{a}_1\left(\hat{\theta}_q\right) \\ \mathbf{a}_2\left(\hat{\theta}_q\right) \end{bmatrix} \tag{6.34}$$

Then according to Section 1.3.1, the CBF powers of the J candidate directional vectors can be calculated by

$$P_{CBF,q} = \frac{\mathbf{a}^H\left(\hat{\theta}_q\right)\hat{\mathbf{R}}\mathbf{a}\left(\hat{\theta}_q\right)}{N^2} \tag{6.35}$$

Signals come from the true DOAs and there is no physical signal coming from ambiguous angles. Therefore the CBF power at the true DOAs is greater than that at the ambiguous angles. By finding the K greatest results in Equation (6.35), the true DOAs can be obtained.

6.4 Simulations and analysis

6.4.1 Reliability comparison

To illustrate the effectiveness of the proposed ambiguity-eliminating method, consider the ambiguity problem case of which the simulation result is shown in FIGURE 6.3. Select out the locations and amplitudes of all the peaks in the MUSIC spectrum and calculate the decision variable $D(n)$ with Equation (6.32). The obtained results are shown in TABLE 6.1. According to the maximum of $D(n)$, there are $J = 4$ peaks obviously higher than the others, corresponding to the three true DOAs and one ambiguous angle. Select out the $J = 4$ candidate angles and calculate their corresponding CBF powers $P_{CBF,q}$ with Equation (6.35). The obtained results are shown in TABLE 6.2. It is clear that the CBF powers at the three true DOAs are greater than that at the ambiguous angle. Therefore, the true DOAs can be distinguished among the candidate angles, and the ambiguity problem is solved successfully.

TABLE 6.1 – Decision variable

n	1	2	3	4	5	$6-29$
$D(n)$	0.8098	0.2572	0.4372	833.58	0.0046	<0.3

TABLE 6.2 – CBF powers and test results

$\hat{\theta}_q$	10.00°	35.02°	27.36°	59.31°
$P_{CBF,q}$	1.4465	1.2200	1.1740	0.4997
true or ambiguous	true	true	true	ambiguous

The ambiguity problem does not affect the estimation accuracy, but invalidates the estimation by introducing non-existing DOAs. The proposed method can achieve the same estimation performance as the existing method when there is no ambiguity problem, and is still robust and reliable when the problem occurs. To reveal the reliability of the proposed ambiguity-eliminating method in ambiguity problem cases, the comparison of the proposed method and the original method in [79] is shown in Figure 6.4, with 20 independent simulations, in which SNR is 10dB and the number of snapshots is 200. The three estimated angles with the highest peak amplitudes and the greatest CBF powers are chosen as the final estimation results for the original method in [79] and the proposed method respectively. It can be seen that the estimation results of the original method are ambiguous and the unsolved ambiguity problem reduces the rate of success of DOA estimation. In contrast, the proposed ambiguity-eliminating method can solve the ambiguity problem successfully, and the performance remains stable and remarkable.

6.4.2 Complexity comparison

According to the principle of the proposed ambiguity-eliminating method, the computational complexity will be different, depending on the existence of the ambiguity problem. When the ambiguity problem does not exist, the computational complexity of the proposed method is

$$\mathcal{O}\left(N^2L + N^3 + TN\left(N-K\right)\right) \tag{6.36}$$

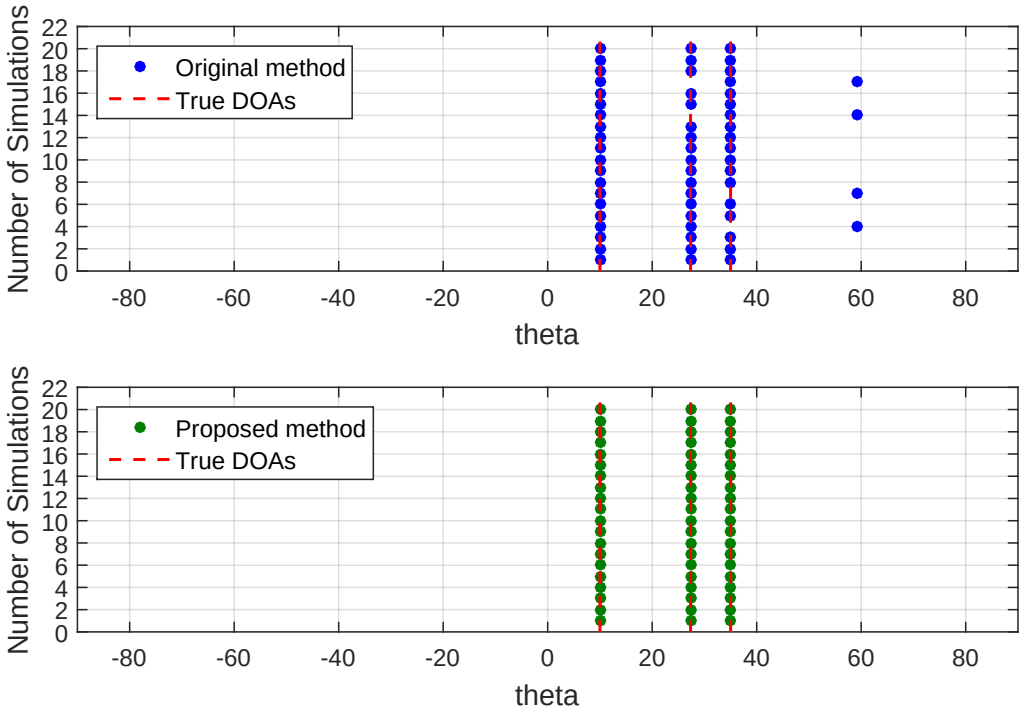

FIGURE 6.4 – Reliability comparison

which is the same as the original method in [79], where T is the number of spectral peak-searching. When the problem exists, the computational complexity of the proposed method turns out to be

$$\mathcal{O}\left(N^2L + N^3 + TN\left(N-K\right) + JN^2\right) \tag{6.37}$$

which slightly exceeds that of the original method.

6.5 Conclusion

In this chapter, the DOA estimation with UCLAs is discussed and an ignored ambiguity problem is investigated. We show that there would be ambiguous peaks in the MUSIC spectrum when there are two different DOAs having the same directional vectors with the directional vector of a given DOA for the two subarrays respectively. To address this issue, an ambiguity-eliminating method is proposed. Firstly, a decision variable is defined to determine the existence of the problem, and then the true DOAs are distinguished based on the CBF technique. Simulation results show that the proposed method can successfully solve the ambiguity problem with a slight additional computational complexity burden,

achieving a wider range of applications.

CHAPITRE 7

CONCLUSION AND PERSPECTIVES

7.1 Conclusion of contributions

In this thesis, the DOA estimation with coprime arrays is considered. Both the two research orientations, which are difference-coarray based methods and subarray-based methods, are investigated, and array configurations and DOA estimation methods are improved for better performance in terms of DOFs and reliability. The main contribution are summarized as follows.

For difference-coarray based methods, moving platforms based CLAs with their corresponding difference coarrays are studied, and the problem that the lags in the consecutive difference coarray part contribute negligibly to the increase of the DOFs after array motion is pointed out. To address this issue, an improved CLA configuration for moving platform is proposed. By judiciously redesigning the sensor element positions, the lags in the consecutive part of the original difference coarray can be used to fill holes after array motion, lengthening the consecutive part of the difference coarray and increasing the effective DOFs.

Then, to be more relevant to real applications, the structure of the difference coarrays of 2D CPAs is investigated. Closed-form expressions of the exact hole locations are deduced, offering a better understanding of CPAs and providing a basis for the future research in this domain. Besides, a holes-filling method is proposed, by which the most critical holes can be filled, such that a difference coarray with more consecutive lags can be generated and higher effective DOFs can be obtained.

For subarray-based methods, the existing problems associated with this class of methods, including ambiguity, pair matching errors and grating angles problem, are discussed. Considering the possible rank deficiency of the directional matrices, an equivalent system model is introduced, and a reliable and efficient DOA estimation method is proposed, which can work correctly in all situations and has a better performance in terms of estimation accuracy and computational complexity.

Finally, for the UCLAs which enjoy the advantages of full DOFs and better estimation performance compared to CLAs with subarrays based methods, the ambiguity problem ignored by the existing works is revealed, and an appropriate fixing method is proposed, by which such problem can be solved successfully and efficiently.

7.2 Perspectives of future work

For the future work, the following lists several suggestions based on the proposition presented in the thesis.

For the moving platform based CLAs, the CLAs are assumed to be air-borne, vehicle-attached or ship-based, which is proposed for practical applications. Considering that the motion of the platform is controllable and not necessarily along the array direction, moving the CLA in another direction to generate a 2D difference coarray aiming to solve 2D DOA estimation problems is more relevant and efficient to practical applications, and is recommended to investigate in the future.

For the CPAs with the proposed holes-filling method, although the effective DOFs can be significantly increased, the resulting difference coarray is not complete, and there still exist unfilled holes. With the knowledge of the deduced hole locations, the filling of such remaining holes would be one of the future research orientations.

For the CLAs with subarray-based methods, the proposed DOA estimation and ambiguity-solving methods assume the sources to be far-field, narrowband and uncorrelated, which may not be valid in practical situations. Hence, the improvement of such theory for more general assumptions would be another topic of the future research.

BIBLIOGRAPHIE

[1] J. G. Andrews, S. Buzzi, W. Choi, S. V. Hanly, A. Lozano, A. C. Soong, and J. C. Zhang, "What will 5G be ?," *IEEE Journal on selected areas in communications*, vol. 32, no. 6, pp. 1065–1082, 2014.

[2] L. Lu, G. Y. Li, A. L. Swindlehurst, A. Ashikhmin, and R. Zhang, "An overview of massive MIMO : Benefits and challenges," *IEEE journal of selected topics in signal processing*, vol. 8, no. 5, pp. 742–758, 2014.

[3] E. G. Larsson, O. Edfors, F. Tufvesson, and T. L. Marzetta, "Massive MIMO for next generation wireless systems," *IEEE communications magazine*, vol. 52, no. 2, pp. 186–195, 2014.

[4] J. Li and P. Stoica, *MIMO radar signal processing*. John Wiley & Sons, 2008.

[5] J. U. Quistgaard, "Signal acquisition and processing in medical diagnostic ultrasound," *IEEE Signal Processing Magazine*, vol. 14, no. 1, pp. 67–74, 1997.

[6] J. F. Synnevag, A. Austeng, and S. Holm, "Adaptive beamforming applied to medical ultrasound imaging," *IEEE transactions on ultrasonics, ferroelectrics, and frequency control*, vol. 54, no. 8, pp. 1606–1613, 2007.

[7] D. Tarchi, F. Oliveri, and P. F. Sammartino, "MIMO radar and ground-based SAR imaging systems : Equivalent approaches for remote sensing," *IEEE Transactions on Geoscience and Remote Sensing*, vol. 51, no. 1, pp. 425–435, 2012.

[8] W. Wang, "Applications of MIMO technique for aerospace remote sensing," in *2007 IEEE Aerospace Conference*, pp. 1–10, IEEE, 2007.

[9] E. G. Williams, J. D. Maynard, and E. Skudrzyk, "Sound source reconstructions using a microphone array," *The Journal of the Acoustical Society of America*, vol. 68, no. 1, pp. 340–344, 1980.

[10] R. N. Bracewell, "Radio astronomy techniques," in *Astrophysik V : Verschiedenes/Astrophysics V : Miscellaneous*, pp. 42–129, Springer, 1962.

[11] H. Krim and M. Viberg, "Two decades of array signal processing research : the parametric approach," *IEEE signal processing magazine*, vol. 13, no. 4, pp. 67–94, 1996.

[12] R. W. Heath, N. Gonzalez-Prelcic, S. Rangan, W. Roh, and A. M. Sayeed, "An overview of signal processing techniques for millimeter wave MIMO systems," *IEEE journal of selected topics in signal processing*, vol. 10, no. 3, pp. 436–453, 2016.

[13] A. L. Swindlehurst and P. Stoica, "Maximum likelihood methods in radar array signal processing," *Proceedings of the IEEE*, vol. 86, no. 2, pp. 421–441, 1998.

[14] J. Benesty, J. Chen, and Y. Huang, *Microphone array signal processing*, vol. 1. Springer Science & Business Media, 2008.

[15] S. Haykin, J. Litva, T. J. Shepherd, *et al.*, *Radar array processing*. Springer, 1993.

[16] M. Jin, G. Liao, and J. Li, "Joint DOD and DOA estimation for bistatic MIMO radar," *Signal Processing*, vol. 89, no. 2, pp. 244–251, 2009.

[17] M. L. Bencheikh and Y. Wang, "Joint DOD-DOA estimation using combined ESPRIT-MUSIC approach in MIMO radar," *Electronics letters*, vol. 46, no. 15, pp. 1081–1083, 2010.

[18] R. Rajagopal and P. Rao, "Generalised algorithm for DOA estimation in a passive sonar," in *IEE Proceedings F (Radar and Signal Processing)*, vol. 140, pp. 12–20, IET, 1993.

[19] J. Li, Q. Lin, C. Kang, K. Wang, and X. Yang, "DOA estimation for underwater wideband weak targets based on coherent signal subspace and compressed sensing," *Sensors*, vol. 18, no. 3, p. 902, 2018.

[20] H. Cox, R. Zeskind, and M. Owen, "Robust adaptive beamforming," *IEEE Transactions on Acoustics, Speech, and Signal Processing*, vol. 35, no. 10, pp. 1365–1376, 1987.

[21] W. Roh, J.-Y. Seol, J. Park, B. Lee, J. Lee, Y. Kim, J. Cho, K. Cheun, and F. Aryanfar, "Millimeter-wave beamforming as an enabling technology for 5G cellular communications : Theoretical feasibility and prototype results," *IEEE communications magazine*, vol. 52, no. 2, pp. 106–113, 2014.

[22] L. C. Godara, "Application of antenna arrays to mobile communications. II. beamforming and direction-of-arrival considerations," *Proceedings of the IEEE*, vol. 85, no. 8, pp. 1195–1245, 1997.

[23] T. B. Lavate, V. Kokate, and A. Sapkal, "Performance analysis of MUSIC and ESPRIT DOA estimation algorithms for adaptive array smart antenna in mobile communication," in *2010 Second International Conference on Computer and Network Technology*, pp. 308–311, IEEE, 2010.

[24] C.-T. Chiang and A.-C. Chang, "DOA estimation in the asynchronous DS-CDMA system," *IEEE Transactions on antennas and propagation*, vol. 51, no. 1, pp. 40–47, 2003.

[25] J. Capon, "High-resolution frequency-wavenumber spectrum analysis," *Proceedings of the IEEE*, vol. 57, no. 8, pp. 1408–1418, 1969.

[26] G. Bienvenu and L. Kopp, "Optimality of high resolution array processing using the eigensystem approach," *IEEE Transactions on acoustics, speech, and signal processing*, vol. 31, no. 5, pp. 1235–1248, 1983.

[27] R. Schmidt, "Multiple emitter location and signal parameter estimation," *IEEE transactions on antennas and propagation*, vol. 34, no. 3, pp. 276–280, 1986.

[28] R. Roy and T. Kailath, "Esprit-estimation of signal parameters via rotational invariance techniques," *IEEE Transactions on acoustics, speech, and signal processing*, vol. 37, no. 7, pp. 984–995, 1989.

[29] D. H. Johnson and D. E. Dudgeon, *Array signal processing : concepts and techniques*. Simon & Schuster, Inc., 1992.

[30] H. L. Van Trees, *Optimum array processing : Part IV of detection, estimation, and modulation theory*. John Wiley & Sons, 2004.

[31] B. Yao, Z. Dong, W. Zhang, W. Wang, and Q. Wu, "Degree-of-freedom strengthened cascade array for DOD-DOA estimation in MIMO array systems," *Sensors*, vol. 18, no. 5, p. 1557, 2018.

[32] M. Yangg, A. M. Haimovich, B. Chen, and X. Yuan, "A new array geometry for DOA estimation with enhanced degrees of freedom," in *2016 IEEE international conference on acoustics, speech and signal processing (ICASSP)*, pp. 3041–3045, IEEE, 2016.

[33] J. Shi, G. Hu, X. Zhang, F. Sun, W. Zheng, and Y. Xiao, "Generalized co-prime MIMO radar for DOA estimation with enhanced degrees of freedom," *IEEE Sensors Journal*, vol. 18, no. 3, pp. 1203–1212, 2017.

[34] A. Moffet, "Minimum-redundancy linear arrays," *IEEE Transactions on antennas and propagation*, vol. 16, no. 2, pp. 172–175, 1968.

[35] C.-Y. Chen and P. P. Vaidyanathan, "Minimum redundancy MIMO radars," in *2008 IEEE International Symposium on Circuits and Systems*, pp. 45–48, IEEE, 2008.

[36] P. Pal and P. P. Vaidyanathan, "Nested arrays : A novel approach to array processing with enhanced degrees of freedom," *IEEE Transactions on Signal Processing*, vol. 58, no. 8, pp. 4167–4181, 2010.

[37] P. Pal and P. Vaidyanathan, "Nested arrays in two dimensions, part II : Application in two dimensional array processing," *IEEE Transactions on Signal Processing*, vol. 60, no. 9, pp. 4706–4718, 2012.

[38] C.-L. Liu and P. Vaidyanathan, "High order super nested arrays," in *2016 IEEE Sensor Array and Multichannel Signal Processing Workshop (SAM)*, pp. 1–5, IEEE, 2016.

[39] C. S. Ruf, "Numerical annealing of low-redundancy linear arrays," *IEEE Transactions on Antennas and Propagation*, vol. 41, no. 1, pp. 85–90, 1993.

[40] B. Friedlander and A. J. Weiss, "Direction finding in the presence of mutual coupling," *IEEE transactions on antennas and propagation*, vol. 39, no. 3, pp. 273–284, 1991.

[41] I. Gupta and A. Ksienski, "Effect of mutual coupling on the performance of adaptive arrays," *IEEE Transactions on Antennas and Propagation*, vol. 31, no. 5, pp. 785–791, 1983.

[42] H. Singh, H. Sneha, and R. Jha, "Mutual coupling in phased arrays : A review," *International Journal of Antennas and Propagation*, vol. 2013, 2013.

[43] P. P. Vaidyanathan and P. Pal, "Sparse sensing with co-prime samplers and arrays," *IEEE Transactions on Signal Processing*, vol. 59, no. 2, pp. 573–586, 2010.

[44] P. Pal and P. P. Vaidyanathan, "Coprime sampling and the MUSIC algorithm," in *2011 Digital Signal Processing and Signal Processing Education Meeting (DSP/SPE)*, pp. 289–294, IEEE, 2011.

[45] P. Vaidyanathan and P. Pal, "Theory of sparse coprime sensing in multiple dimensions," *IEEE Transactions on Signal Processing*, vol. 59, no. 8, pp. 3592–3608, 2011.

[46] S. Qin, Y. D. Zhang, and M. G. Amin, "Generalized coprime array configurations for direction-of-arrival estimation," *IEEE Transactions on Signal Processing*, vol. 63, no. 6, pp. 1377–1390, 2015.

[47] C.-L. Liu, P. Vaidyanathan, and P. Pal, "Coprime coarray interpolation for DOA estimation via nuclear norm minimization," in *2016 IEEE International Symposium on Circuits and Systems (ISCAS)*, pp. 2639–2642, IEEE, 2016.

[48] C. Zhou, Y. Gu, X. Fan, Z. Shi, G. Mao, and Y. D. Zhang, "Direction-of-arrival estimation for coprime array via virtual array interpolation," *IEEE Transactions on Signal Processing*, vol. 66, no. 22, pp. 5956–5971, 2018.

[49] E. BouDaher, Y. Jia, F. Ahmad, and M. G. Amin, "Direction-of-arrival estimation using multi-frequency co-prime arrays," in *2014 22nd European Signal Processing Conference (EUSIPCO)*, pp. 1034–1038, IEEE, 2014.

[50] C. Zhou and J. Zhou, "Direction-of-arrival estimation with coarray ESPRIT for co-prime array," *Sensors*, vol. 17, no. 8, p. 1779, 2017.

[51] X. Wang and X. Wang, "Hole identification and filling in k-times extended co-prime arrays for highly efficient DOA estimation," *IEEE Transactions on Signal Processing*, vol. 67, no. 10, pp. 2693–2706, 2019.

[52] A. Raza, W. Liu, and Q. Shen, "Thinned coprime arrays for DOA estimation," in *2017 25th European Signal Processing Conference (EUSIPCO)*, pp. 395–399, IEEE, 2017.

[53] C. Zhou, Y. Gu, Y. D. Zhang, Z. Shi, T. Jin, and X. Wu, "Compressive sensing-based coprime array direction-of-arrival estimation," *IET Communications*, vol. 11, no. 11, pp. 1719–1724, 2017.

[54] Z. Shi, C. Zhou, Y. Gu, N. A. Goodman, and F. Qu, "Source estimation using coprime array : A sparse reconstruction perspective," *IEEE Sensors Journal*, vol. 17, no. 3, pp. 755–765, 2016.

[55] Q. Shen, W. Liu, W. Cui, and S. Wu, "Extension of co-prime arrays based on the fourth-order difference co-array concept," *IEEE Signal Processing Letters*, vol. 23, no. 5, pp. 615–619, 2016.

[56] C. Zhou, Z. Shi, Y. Gu, and X. Shen, "DECOM : DOA estimation with combined MUSIC for coprime array," in *2013 International Conference on Wireless Communications and Signal Processing*, pp. 1–5, IEEE, 2013.

[57] F. Sun, P. Lan, and B. Gao, "Partial spectral search-based DOA estimation method for co-prime linear arrays," *Electronics Letters*, vol. 51, no. 24, pp. 2053–2055, 2015.

[58] F. Sun, B. Gao, L. Chen, and P. Lan, "A low-complexity ESPRIT-based DOA estimation method for co-prime linear arrays," *Sensors*, vol. 16, no. 9, p. 1367, 2016.

[59] D. Zhang, Y. Zhang, G. Zheng, C. Feng, and J. Tang, "Improved DOA estimation algorithm for co-prime linear arrays using root-MUSIC algorithm," *Electronics Letters*, vol. 53, no. 18, pp. 1277–1279, 2017.

[60] X. Yang, X. Wu, S. Li, and T. K. Sarkar, "A fast and robust DOA estimation method based on JSVD for co-prime array," *IEEE Access*, vol. 6, pp. 41697–41705, 2018.

[61] Z. Weng and P. M. Djurić, "A search-free DOA estimation algorithm for coprime arrays," *Digital Signal Processing*, vol. 24, pp. 27–33, 2014.

[62] J. Li, D. Jiang, and X. Zhang, "DOA estimation based on combined unitary ESPRIT for coprime MIMO radar," *IEEE Communications Letters*, vol. 21, no. 1, pp. 96–99, 2016.

[63] B. Hu, W. Lv, and X. Zhang, "2d-doa estimation for co-prime l-shaped arrays with propagator method," in *2015 4th National Conference on Electrical, Electronics and Computer Engineering*, Atlantis Press, 2015.

[64] J. Li, F. Wang, and D. Jiang, "DOA estimation based on real-valued cross correlation matrix of coprime arrays," *Sensors*, vol. 17, no. 3, p. 638, 2017.

[65] G. Qin, M. G. Amin, and Y. D. Zhang, "DOA estimation exploiting sparse array motions," *IEEE Transactions on Signal Processing*, vol. 67, no. 11, pp. 3013–3027, 2019.

[66] G. Qin, M. G. Amin, and Y. D. Zhang, "Analysis of coprime arrays on moving platform," in *ICASSP 2019-2019 IEEE International Conference on Acoustics, Speech and Signal Processing (ICASSP)*, pp. 4205–4209, IEEE, 2019.

[67] A. M. Elbir, "Two-dimensional DOA estimation via shifted sparse arrays with higher degrees of freedom," *Circuits, Systems, and Signal Processing*, vol. 38, no. 12, pp. 5549–5575, 2019.

[68] S. Li and X.-P. Zhang, "A novel moving sparse array geometry with increased degrees of freedom," in *ICASSP 2020-2020 IEEE International Conference on Acoustics, Speech and Signal Processing (ICASSP)*, pp. 4767–4771, IEEE, 2020.

[69] X. Yang, L. Liu, and Y. Wang, "A new low complexity DOA estimation algorithm for massive MIMO systems," in *2016 IEEE international conference on consumer electronics-china (ICCE-china)*, pp. 1–4, IEEE, 2016.

[70] P. Heidenreich, A. M. Zoubir, and M. Rubsamen, "Joint 2-D DOA estimation and phase calibration for uniform rectangular arrays," *IEEE Transactions on Signal Processing*, vol. 60, no. 9, pp. 4683–4693, 2012.

[71] Z. Zheng, W.-Q. Wang, H. Meng, H. C. So, and H. Zhang, "Efficient beamspace-based algorithm for two-dimensional DOA estimation of incoherently distributed

sources in massive MIMO systems," *IEEE Transactions on Vehicular Technology*, vol. 67, no. 12, pp. 11776–11789, 2018.

[72] H. Wu, C. Hou, H. Chen, W. Liu, and Q. Wang, "Direction finding and mutual coupling estimation for uniform rectangular arrays," *Signal Processing*, vol. 117, pp. 61–68, 2015.

[73] Q. Wu, F. Sun, P. Lan, G. Ding, and X. Zhang, "Two-dimensional direction-of-arrival estimation for co-prime planar arrays : A partial spectral search approach," *IEEE Sensors Journal*, vol. 16, no. 14, pp. 5660–5670, 2016.

[74] D. Zhang, Y. Zhang, G. Zheng, B. Deng, C. Feng, and J. Tang, "Two-dimensional direction of arrival estimation for coprime planar arrays via polynomial root finding technique," *IEEE Access*, vol. 6, pp. 19540–19549, 2018.

[75] W. Zheng, X. Zhang, and H. Zhai, "Generalized coprime planar array geometry for 2-D DOA estimation," *IEEE Communications Letters*, vol. 21, no. 5, pp. 1075–1078, 2017.

[76] H. Xu, Y. Zhang, B. Ba, D. Wang, and X. Li, "Two-dimensional direction-of-arrival fast estimation of multiple signals with matrix completion theory in coprime planar array," *Sensors*, vol. 18, no. 6, p. 1741, 2018.

[77] G. Wang, Z. Fei, S. Ren, and X. Li, "Improved 2D coprime array structure with the difference and sum coarray concept," *Electronics*, vol. 9, no. 2, p. 273, 2020.

[78] H. Xu, D. Wang, B. Ba, W. Cui, and Y. Zhang, "Direction-of-arrival estimation for both uncorrelated and coherent signals in coprime array," *IEEE Access*, vol. 7, pp. 18590–18600, 2019.

[79] W. Zheng, X. Zhang, P. Gong, and H. Zhai, "DOA estimation for coprime linear arrays : An ambiguity-free method involving full DOFs," *IEEE Communications Letters*, vol. 22, no. 3, pp. 562–565, 2017.

[80] J. Li and X. Zhang, "Direction of arrival estimation of quasi-stationary signals using unfolded coprime array," *IEEE access*, vol. 5, pp. 6538–6545, 2017.

[81] H. Zhai, X. Zhang, W. Zheng, and P. Gong, "DOA estimation of noncircular signals for unfolded coprime linear array : Identifiability, DOF and algorithm (may 2018)," *IEEE Access*, vol. 6, pp. 29382–29390, 2018.

[82] P. Gong, X. Zhang, and W. Zheng, "Unfolded coprime L-shaped arrays for two-dimensional direction of arrival estimation," *International Journal of Electronics*, vol. 105, no. 9, pp. 1501–1519, 2018.

[83] J. Li, Y. Li, and X. Zhang, "Two-dimensional off-grid DOA estimation using unfolded parallel coprime array," *IEEE Communications Letters*, vol. 22, no. 12, pp. 2495–2498, 2018.

[84] T.-J. Shan, M. Wax, and T. Kailath, "On spatial smoothing for direction-of-arrival estimation of coherent signals," *IEEE Transactions on Acoustics, Speech, and Signal Processing*, vol. 33, no. 4, pp. 806–811, 1985.

[85] W. Du and R. L. Kirlin, "Improved spatial smoothing techniques for DOA estimation of coherent signals," *IEEE Transactions on signal processing*, vol. 39, no. 5, pp. 1208–1210, 1991.

[86] C.-L. Liu and P. Vaidyanathan, "Remarks on the spatial smoothing step in coarray MUSIC," *IEEE Signal Processing Letters*, vol. 22, no. 9, pp. 1438–1442, 2015.

[87] Q. Xie, X. Pan, and S. Xiao, "Enhance degrees of freedom for coprime array using optspace algorithm," *IEEE Access*, vol. 7, pp. 32672–32680, 2019.

[88] W. Zheng, Z. Xiaofei, Y. Wang, J. Shen, and B. Champagne, "Padded coprime arrays for improved DOA estimation : Exploiting hole representation and filling strategies," *IEEE Transactions on Signal Processing*, 2020.

[89] B. Recht, M. Fazel, and P. A. Parrilo, "Guaranteed minimum-rank solutions of linear matrix equations via nuclear norm minimization," *SIAM review*, vol. 52, no. 3, pp. 471–501, 2010.

[90] S. Stergiopoulos and E. J. Sullivan, "Extended towed array processing by an overlap correlator," *The Journal of the Acoustical Society of America*, vol. 86, no. 1, pp. 158–171, 1989.

[91] G. Qin, Y. D. Zhang, and M. G. Amin, "DOA estimation exploiting moving dilated nested arrays," *IEEE Signal Processing Letters*, vol. 26, no. 3, pp. 490–494, 2019.

[92] C. R. Greene and R. C. Wood, "Sparse array performance," *The Journal of the Acoustical Society of America*, vol. 63, no. 6, pp. 1866–1872, 1978.

[93] P. Pal and P. Vaidyanathan, "Nested arrays in two dimensions, part I : Geometrical considerations," *IEEE Transactions on Signal Processing*, vol. 60, no. 9, pp. 4694–4705, 2012.

[94] C.-L. Liu and P. P. Vaidyanathan, "Hourglass arrays and other novel 2-D sparse arrays with reduced mutual coupling," *IEEE Transactions on Signal Processing*, vol. 65, no. 13, pp. 3369–3383, 2017.

[95] C.-L. Liu and P. Vaidyanathan, "Two-dimensional sparse arrays with hole-free co-array and reduced mutual coupling," in *2016 50th Asilomar Conference on Signals, Systems and Computers*, pp. 1508–1512, IEEE, 2016.

[96] A. Barabell, "Improving the resolution performance of eigenstructure-based direction-finding algorithms," in *ICASSP'83. IEEE International Conference on Acoustics, Speech, and Signal Processing*, vol. 8, pp. 336–339, IEEE, 1983.

[97] B. D. Rao and K. S. Hari, "Performance analysis of root-MUSIC," *IEEE Transactions on Acoustics, Speech, and Signal Processing*, vol. 37, no. 12, pp. 1939–1949, 1989.

[98] J.-F. Gu and P. Wei, "Joint SVD of two cross-correlation matrices to achieve automatic pairing in 2-D angle estimation problems," *IEEE Antennas and Wireless Propagation Letters*, vol. 6, pp. 553–556, 2007.

[99] H. Akaikei, "Information theory and an extension of maximum likelihood principle," in *Proc. 2nd Int. Symp. on Information Theory*, pp. 267–281, 1973.

[100] J. Rissanen, "A universal prior for integers and estimation by minimum description length," *The Annals of statistics*, pp. 416–431, 1983.

[101] M. Wax and T. Kailath, "Detection of signals by information theoretic criteria," *IEEE Transactions on acoustics, speech, and signal processing*, vol. 33, no. 2, pp. 387–392, 1985.

[102] P. Stoica and A. Nehorai, "MUSIC, maximum likelihood, and Cramer-Rao bound," *IEEE Transactions on Acoustics, speech, and signal processing*, vol. 37, no. 5, pp. 720–741, 1989.

[103] P. Stoica and A. Nehorai, "Performance study of conditional and unconditional direction-of-arrival estimation," *IEEE Transactions on Acoustics, Speech, and Signal Processing*, vol. 38, no. 10, pp. 1783–1795, 1990.

[104] P. Stoica, E. G. Larsson, and A. B. Gershman, "The stochastic CRB for array processing : A textbook derivation," *IEEE Signal Processing Letters*, vol. 8, no. 5, pp. 148–150, 2001.

DOCTORAT BRETAGNE LOIRE MATHSTIC

UNIVERSITÉ DE NANTES

Titre : **Estimation de la Direction d'Arrivée avec les Réseaux Coprimes**

Mots clés : réseaux coprimes, estimation de DOA, difference coarray, sous- réseaux, ambiguïté

Résumé: L'estimation de la direction d'arrivée (DOA) des sources avec les réseaux coprimes a été beaucoup étudiée grâce à leurs degrés de liberté (DOFs) élévés et leurs meilleures performances d'estimation. La recherche existante dans ce domaine évolue vers deux orientations, qui sont les méthodes basées sur le difference coarray, qui tentent d'augmenter les DOFs effectifs, et les méthodes basées sur les sous-réseaux, qui tentent d'obtenir une estimation de DOA avec haute précision et faible complexité. Dans cette thèse, les deux orientations de recherche sont toutes les deux investies. Du point de vue des méthodes basées sur le difference coarray, les réseaux linéaires coprimes basés sur une plate-forme mobile sont étudiés, et les positions des capteurs sont judicieusement redéfinies, de sorte que les DOFs effectifs sont considérablement augmentés. Ensuite, la structure des difference coarrays des réseaux planaires coprimes est explorée, et les expressions des emplacements des trous dans les difference coarrays sont déduites, fournissant une base pour la recherche future. Du point de vue des méthodes basées sur les sous-réseaux, les problèmes potentiels associés à cette classe de méthodes sont mis en évidence, et une méthode d'estimation de DOA fiable et efficace est proposée. En outre, la configuration des réseaux linéaires coprimes dépliés est étudiée. Un problème d'ambiguïté ignoré par la recherche existante est discuté, et une méthode de levée des ambiguités est proposée, par laquelle le problème peut être résolu efficacement.

Title : **Direction of Arrival Estimation with Coprime Arrays**

Keywords : coprime arrays, DOA estimation, difference coarray, subarrays, ambiguity

Abstract : Direction of arrival (DOA) estimation with coprime arrays has been investigated a lot thanks to the higher degrees of freedom (DOFs) and better estimation performance. The existing research in this domain develops towards two orientations, which are difference coarray-based methods, trying to increase the effective DOFs, and subarray-based methods, aiming to obtain high precision DOA estimation with low complexity. In this dissertation, the two research orientations are both investigated. From the perspective of difference coarray-based methods, moving platform based coprime linear arrays are investigated, and the sensor element positions are judiciously redesigned, such that the effective DOFs are significantly increased. Then the structure of the difference coarrays of coprime planar arrays is explored, and closed-form expressions of the hole locations in the difference coarrays are deduced, providing a basis for the future research. From the perspective of subarray-based methods, the potential problems associated with this class of methods are discussed, and a reliable and efficient DOA estimation method is proposed. Besides, the configuration of unfolded coprime linear arrays is investigated. An ambiguity problem ignored by the existing research is discussed, and an ambiguity-eliminating method is proposed, by which the problem can be solved efficiently.